Joint PhD Programme in Integrated Management of Water, Soil and Waste

Faculty of Environmental Sciences
Technische Universität Dresden

and

Institute for Integrated Management of Material Fluxes and of Resources
United Nations University

Temporal changes in the soil pore size distribution and variability of soil hydraulic properties under long-term conventional and conservation tillage

A dissertation submitted on 21 November 2019 in partial fulfillment of the requirements for the degree of

Doctor of Philosophy (Ph.D.)

by

Janis Leonhard Kreiselmeier, M.Sc.

born on 12 September 1988 in Schwäbisch Hall, Germany

Day of defense: 26 June 2020

Reviewers:

Prof. Dr. Karl-Heinz Feger (supervisor)
Institute of Soil Science and Site Ecology, Technische Universität Dresden

Dr. habil. Kai Schwärzel (supervisor)
Thünen Institute of Forest Ecosystems, formerly UNU-FLORES

Prof. em. Dr. Gerd Wessolek
formerly Institute for Ecology, Technische Universität Berlin

Digging up and up and up again

Like the eldermen and fathers before then

Songs of Soil - Fire Away

Declaration of conformity

I hereby confirm that this copy conforms with the original dissertation on the topic:
"Temporal changes in the soil pore size distribution and variability of soil hydraulic properties under long-term conventional and conservation tillage"

Dresden, 26 June 2020

Janis Leonhard Kreiselmeier

Acknowledgements

First and foremost, I would like to thank my supervisors Kai Schwärzel and Karl-Heinz Feger for giving me the opportunity to work on their project and develop my thesis under their guidance. Kai, thank you for giving "a long leash" most of the times but occasionally "tightening the reins". I could always rely on your help. Karl-Heinz, thank you for your constant support in administrative and technical matters. Your constructive feedback was always appreciated.

This dissertation was developed in the frame of the DFG-funded project 'Development of models to predict land-use-induced soil pore-space changes and their hydrological impacts' (Soil Pore Dynamics). Project partners were from the Institute of Soil Science and Site Ecology (grant number FE 504/11-1) of TU Dresden and the Institute for Soil Physics and Rural Water Management (FWF grant number I-2122-B16) of the University of Natural Resources and Life Science in Vienna, Austria. The funding of the PhD work was received from grant number SCHW 1448/6-1 at UNU-FLORES which I gratefully acknowledge. A big thank you is due to the whole Soil Pore Dynamics project team. The Austrian side with Andreas Schwen and Thomas Weninger helped in the planning of field campaigns, WP4C measurements, data analysis and paper writing. Thank you, Thomas, for looking at things with a fresh mind and your support in R. I am also grateful to Stefan Julich for his ideas and constructive feedback. Last but not least in this row of team members is Parvathy Chandrasekhar. My partner in crime for four straight years. We sat back to back in the office, and finally reached the end of this PhD journey together. I appreciate your company, even though you would not use my data.

A lot of the work in the field and the lab would not have been possible without the help of a number of people. Birgit Ziegelmayer assisted in administrative matters. Gisela Ciesielski with her cheerful attitude and stride introduced me to all the machinery and procedures in the lab. Together with Manuela Unger she processed numerous samples for this project. Thank you all for that. In the field, I was supported by Gabriela Fontenla Razzetto through pouring rain and sweltering heat. I made you work long hours in Lüttewitz. Thank you for bearing with me and fighting to get the HYPROPs to work. I would also like to express my sincere gratitude to all the other people assisting me in the field and lab over the last years. Access to the tillage site was made possible by Südzucker AG. Here, I am especially grateful to Daniel Kunzendorf who let me work on his fields even on short notice and who must have provided thousands of liters of water for my experiments.

This work was done within the Joint PhD Programme in Integrated Management of Water, Soil and Waste of UNU-FLORES and TU Dresden. I would like to thank the awesome gang of PhD students of this programme that is Agossou, Andrea, Anika, Mahesh, Parvathy, Sekela, Solomon, Sridhar and Thuy. You made this an unforgettable experience and I can say to have gained some true friends. The PhD coordinators Hiroshan Hettiarachchi and Stephan Hülsmann did their best to get this programme running. I think we all appreciated your commitment. Thanks are also due to all the other colleagues at UNU-FLORES who helped in administrative matters, editorial work or simply in exchanging ideas and delicious food from all over the world. It was a pleasure working with and among you.

I would also like to extend my gratitude to my fellow PhD students and staff at the Institute of Soil Science and Site Ecology of TU Dresden in Tharandt. There always seemed to be cake when I visited. You truly are amazing confectioners and great company.

Last but not least, I would like to thank my family and friends for their support and patience in the past years. Isabella, you brightened up the final months of this journey. I am looking forward to new beginnings and adventures with you.

Table of Contents

List of Figures

List of Tables

Nomenclature

SDG	Sustainable Development Goal
CA	conservation agriculture
FAO	Food and Agriculture Organization of the United Nations
NT	no tillage
CT	conventional tillage
SOC	soil organic carbon
⌀	diameter
SHP	soil hydraulic properties
PSD	soil pore size distribution
WRC	water retention characteristic
θ	volumetric water content
h	(supply) pressure head or soil water tension
r	soil pore radius
K	hydraulic conductivity
HCC	hydraulic conductivity characteristic
ϱ_b	soil bulk density
K_s	saturated hydraulic conductivity
RT	reduced mulch tillage
Φ	total porosity
SPQ	soil physical quality
WRB	World Reference Base for Soil Resources
K_{slab}	saturated hydraulic conductivity measured in the lab
HI	hood infiltrometer
TI	tension infiltrometer
BP	soil bubbling pressure
K_{2cm}	hydraulic conductivity at h = -2cm
r_{BP}	threshold pore radius
R^2	coefficient of determination
S_e	effective saturation
θ_s	saturated water content
θ_r	residual water content
w	weighting factor
h_m	median pressure head
r_m	median pore radius
σ	standard deviation of the lognormal pore size distribution
pF	base 10 logarithm of the soil water tension in cm
$k_{pF2.0}$	hydraulic conductivity at pF 2.0
$k_{pF2.5}$	hydraulic conductivity at pF 2.5
$k_{pF3.0}$	hydraulic conductivity at pF 3.0
Φ_{mac}	macroporosity
Φ_{mes}	mesoporosity
RFC	relative field capacity

AC	air capacity
GM	geometric mean
GCV	geometric coefficient of variation
AM	arithmetic mean
SD	standard deviation
ANOVA	analysis of variance
LSD	least significant difference
ϱ	Spearman's rank correlation coefficient
RMSE	root mean square error
$\Phi_{mac+mes}$	sum of macro-and mesoporosity

Abstract

Conservation tillage systems are increasingly adapted replacing conventional turnover moldboard plowing practices worldwide. This is part of a sustainable intensification of agriculture to meet future global food demand while at the same time sustaining environmental resources. The choice of tillage system affects soil structure and thereby also soil hydraulic properties (SHP) such as the water retention characteristic (WRC) and the hydraulic conductivity characteristic (HCC). Effects of agricultural management on SHP have been widely studied in the past decades. Thereby, temporal variations were identified as a major source of variability in the quantification of soil pore space and SHP. Such variability is introduced by tillage creating a loose soil matrix that eventually settles due to gravity, wetting-drying cycles and temperature fluctuations but also variable soil organic matter distributions in the soil and biological activity.

Past efforts to model soil water dynamics showed that consideration of time-variable SHP may significantly improve simulation results. This involves both the seasonal variability as well as long-term land-use changes from conventionally to untilled soil. A prerequisite for such an approach is the periodic quantification of the WRC and HCC in the field and laboratory. In addition to the direct provision of modeling parameters, the quantification of WRC and HCC over time yields information on soil structural changes in the shape of a soil pore size distribution (PSD). The evolution of derived PSDs can be modeled and with that, the evolution of SHP might be predicted. However, there is little data available and the processes happening over one cropping season or between land-use changes need to be better understood.

The aim of this dissertation was to shed light on soil pore space and associated hydraulic property changes on a long-term (23 years) tillage experiment in Eastern Germany. Three treatments with varying tillage intensity were investigated: conventional tillage with a turnover moldboard plow (CT), reduced mulch tillage with a cultivator (RT) and no tillage with direct sowing (NT). The soil was a Haplic Luvisol with silt loam texture. Objectives were twofold:

- Objective 1) was to quantify the temporal variability in PSD over one winter wheat cropping season by frequently measuring SHP. Soil physical quality of the three treatments was assessed using this data.

- Objective 2) was to characterize the soil structural differences between the treatments by relating hydraulic conductivity over a wide soil moisture range to other soil physical and chemical properties.

For Objective 1), undisturbed soil cores (250 cm^3) were taken over one winter wheat cropping cycle on five occasions from December 2015 to after the harvest in August 2016. Those soil cores were used to determine the saturated hydraulic and the WRC as well as the HCC in the laboratory. The data was parametrized with the bimodal Kosugi and Mualem model. Soil physical quality was assessed by the relative field capacity and air capacity as suggested in recent literature.

Results showed that tilled soil, *i.e.* CT and RT, exhibited a distinct bimodal PSD with a structural and a textural mode. However, this structural mode was temporally instable and diminished after the winter and throughout the early growing season. Likely processes behind those changes were wetting-drying cycles, rainfall impact and freeze-thaw cycles. Shortly before and after the harvest some of the structural mode was restored which was probably induced by decomposing organic matter mixed into the topsoil from the previous winter wheat harvest during stubble breaking. Described changes were evident in decreases of transmission pores (⌀ 50 - 500 µm) during winter and increases during summer. Untilled soil, *i.e.* NT, tended towards a unimodal PSD with less transmission but more storage (⌀ 0.5 - 50 µm) pores. Temporally this soil was rather inert. This was attributed to natural compaction in absence of annual tillage for more than 20 years. Soil physical quality varied with the changes in PSD. Water availability was not an issue. Overall, the soil physical quality indicators for soil aeration were outside of an optimal range for indicators for most of the time.

For Objective 2), field infiltration measurements were conducted with a hood (tension) infiltrometer to obtain (near-) saturated hydraulic conductivity. Soil cores were taken to quantify unsaturated hydraulic conductivity. Other properties for correlation and multiple regression analysis were bulk density, the bubbling pressure, organic C, as well as macro- and mesoporosity. X-ray µCT imaging on undisturbed soil cores from CT and NT treatments gave additional information on soil pore metrics.

Results pointed towards a distinctly different soil structure between tilled and untilled soil. Near-saturated hydraulic conductivity of tilled soil was negatively correlated with bulk density as well as macro- and mesoporosity. None of the properties was meaningful for untilled soil. Imaging results confirmed the hypothesis, that (near-) saturated hydraulic conductivity on NT is governed by few well-connected large pores, while the soil matrix is

comparably dense conducting only small amounts of infiltrating water. On tilled soil, the overall porosity is relevant for water transmission. Large continuous pore systems, however, get destroyed by annual tillage.

In summary, the study showed distinct differences in soil structure and inherently also SHP between conservation and conventional tillage treatments. Differences in SHP, both in (near-) saturated hydraulic conductivity as well as WRC and HCC were large between some occasions. Therefore, this study confirmed the notion that on arable soils one-off measurements of SHP are not enough for their proper quantification. This was especially true for tilled soil. Modeling tasks over one cropping period, *i.e.* for example for irrigation schedules, will make periodic measurements necessary, *i.e.* unless an accurate modeling of the PSD becomes feasible. Current restraints are that most PSD models only consider a short-term post-tillage loss of porosity while a restored macropore system is not accounted for. In contrast to CT and RT, NT soil was temporally stable. While water retention was improved, (near-) saturated hydraulic conductivity was overall lower than on tilled soil. Correlation and regression analysis in combination with X-ray μCT explained some of the differences observed by tension infiltration measurements. Results highlighted that for arable soil, tillage treatments and probably other agricultural management practices, need to be considered when developing pedotransfer functions for an accurate estimation of SHP.

Zusammenfassung

Die Weltbevölkerung wird vorraussichtlich bis Ende des Jahrhunderts weiter wachsen. Dies geht mit einem steigenden Bedarf an Nahrungsmitteln einher. Gleichzeitig nehmen Umweltprobleme durch die steigende Nahrungsmittelproduktion zu. Als Teil einer nachhaltigen Intensivierung der Landwirtschaft, ersetzt konservierende Bodenbearbeitung zunehmend die noch weit verbreitete konventionelle Bodenbearbeitung mit dem Scharpflug. Je nach Verfahren wird die Bodenstruktur beim Pflügen unterschiedlich beeinflusst. Dies hat einen direkten Effekt auf bodenhydraulische Kennfunktionen wie die Wasserretentionskurve (*water retention characteristic*, WRC) und die hydraulische Leitfähigkeitskurve (*hydraulic conductivity characteristic*, HCC). In den letzten Jahrzehnten wurden Bewirtschaftungseffekte auf hydraulische Bodeneigenschaften eingehend erforscht. Dabei stellte sich heraus, dass zeitliche Veränderungen im Bodenporenraum die Hauptursache für die Variabilität von im Feld und Labor bestimmten hydraulischen Bodeneigenschaften (*soil hydraulic properties,* SHP) sind. Dafür gibt es mehrere Gründe. Pflugbearbeitung lockert die Bodenmatrix. Es bilden sich vermehrt Makroporen. Mit der Zeit setzt sich diese lockere Struktur aber wieder. Faktoren wie Schwerkraft, Regen und Temperaturfluktuationen, aber auch biologische Aktivität sowie die Verfügbarkeit organischer Bodenbestandteile, sorgen für kontinuierliche Änderungen im Bodenporenraum.

In Studien zur Modellierung des Bodenwasserhaushalts hat sich gezeigt, dass sich durch die Berücksichtigung solcher zeitlichen Veränderungen der SHP die Vorhersagen maßgeblich verbessern lassen. Das betrifft sowohl saisonale Dynamiken als auch langfristige Änderungen in der Landnutzung, z.B. von konventionell gepflügtem zu ungepflügtem Boden. Solche Modellierungen setzen fundierte Kenntnisse über die zeitliche Entwicklung der hydraulischen Kennfunktionen voraus, was meist mit regelmäßigen und aufwendigen Feld- und Labormessungen verbunden ist. Über die Kapillartheorie lassen sich aus der WRC und der HCC Porengrößenverteilungen (*pore size distribution*, PSD) ableiten. Die zeitliche Entwicklung solcher PSD lässt sich modellieren und könnte damit einen Teil der Feld- und Labormessungen zukünftig obsolet machen. Allerdings ist die Datengrundlage hierfür noch zu klein und viele Prozesse, die zur Entwicklung der Bodenstruktur über eine Wachstumsperiode oder bei Landnutzungsänderungen beitragen, müssen noch besser untersucht und beschrieben werden.

Die vorliegende Dissertation verfolgte die Absicht, die Porenraumveränderungen auf dem Langzeitpflugversuch (23 Jahre) Lüttewitz im Mittelsächsischen Lösshügelland zu quantifizieren und die damit verbundenen SHP zu charakterisieren. Dabei wurden drei

Varianten mit unterschiedlicher Pflugintensität untersucht. Die konventionelle wendende Bodenbearbeitung mit dem Scharpflug bis zu 30 cm Tiefe (*conventional tillage*, CT) stellte die intensivste Variante dar, gefolgt von der nicht-wendenden Variante Mulch mit dem Grubber bis zu 15 cm Tiefe (*reduced tillage*, RT). Die geringsten Störungen der Bodenstruktur der vorherrschenden schluffreichen Parabraunerden waren auf der Variante mit Direktsaat (*no tillage*, NT) zu erwarten. Die Ziele waren zweierlei:

- Ziel 1) bestand in der Quantifizierung der zeitlichen Variabilität der PSD während einer Winterweizensaison. Dies wurde durch regelmäßige Bestimmung der SHP durch Messungen im Feld und Labor erreicht. Hierbei wurde auch die Veränderungen des Bodens hinsichtlich bodenphysikalischer Eigenschaften (*soil physical quality*, SPQ) der drei Varianten untersucht.
- Ziel 2) war die Unterschiede in der Bodenstruktur der drei Varianten zu charakterisieren. Hierzu wurde versucht, die hydraulischen Leitfähigkeiten über einen weiten Feuchtebereich mit anderen physikalischen und chemischen Bodeneigenschaften zu verknüpfen und vorherzusagen.

Um die Fragestellung von Ziel 1 zu beantworten, wurden an fünf Zeitpunkten während einer Winterweizensaison von Dezember 2015 bis nach der Ernte im August 2016 ungestörte Bodenproben (250 cm^3) genommen. Damit wurden im Labor die WRC und HCC sowie die gesättigte Leitfähigkeit bestimmt. Die so gewonnenen Daten wurde mit dem bimodalen Retentions- und Leitfähigkeitsmodellen von Kosugi und Mualem parametrisiert. Wie in der aktuellen Literatur vorgeschlagen, wurde die SPQ anhand der Indikatoren relative Feldkapazität und Luftkapazität bewertet.

Die Ergebnisse zeigten eine ausgeprägte bimodale PSD des Bodens unter Pflugbearbeitung (CT und RT). Ein Modus ist dabei von der Textur, der andere von der Struktur des Bodens geprägt. Allerdings war der strukturelle Modus instabil und verschwand schon früh in der Wachstumsperiode über den Winter und Frühling. Wahrscheinliche Einflussfaktoren waren abwechselnde Benetzungs- und Austrocknungszyklen (*wetting-drying cycles*), die kinetische Energie von Niederschlag auf die vergleichsweise ungeschützte Bodenoberfläche und zyklischem Wechsel von Gefrieren und Auftauen (*freeze-thaw cycles*). Kurz vor und nach der Ernte konnte eine teilweise Wiederherstelling der strukturellen Bodenporen beobachtet werden. Wahrscheinliche Faktoren hierfür sind die Zersetzung der organischen Erntereste, die durch die Stoppelbearbeitung nach der vorherigen Ernte mit einem Grubber in den Oberboden eingearbeitet wurden. Die beschriebenen Veränderungen im strukturellen Modus spiegelten sich vor allem in der Variabilität von Poren, die

hauptsächlich Wasser transportieren (⌀ 50 - 500 µm, *transmission pores*), wider. Während des Winters nahm deren Anteil am Gesamtporenvolumen ab, im Sommer wieder zu. Der ungepflügte NT-Boden hingegen wies insgesamt eine eher unimodale PSD auf und war vergleichsweise zeitlich stabil. Die Wasserretention war hier durch einen größeren Anteil an Poren mit ⌀ 0,5 - 50 µm (*storage pores*) und weniger Poren die zum Wassertransport beitragen verbessert. Dies ist wahrscheinlich auf die kontinuierliche Verdichtung nach mehr als 20 Jahren ohne maschinelle Lockerung zurückzuführen. Die Qualität des Bodens hinsichtlich seiner physikalischen Eigenschaften änderte sich zusammen mit den Änderungen in der PSD. Wasserverfügbarkeit war auf allen Varianten generell unproblematisch. Die Indikatoren für die Bodenbelüftung hingegen lagen meist außerhalb des Optimalbereichs.

Um die Fragestellungen für Ziel 2 zu beantworten, wurden Infiltrationsmessungen mit dem Haubeninfiltrometer gemacht. Damit wurde die hydraulische Leitfähigkeit bei und nahe Sättigung bestimmt. Ungestörte Bodenproben wurden zur Bestimmung der hydraulischen Leitfähigkeit im ungesättigten Bereich verwendet. Für Korrelationsanalysen und multiple lineare Regressionen wurde die Trockenrohdichte, der Luftdurchtrittspunkt, organische Kohlenstoffkonzentrationen sowie Makro- und Mesoporosität bestimmt. Mithilfe von Röntgentomographie an ungestörten Bodenproben der Varianten CT und NT konnten zusätzlich Porenkennzahlen zur Validierung der Ergebnisse und zur Charakterisierung der Bodenhydraulik herangezogen werden.

Die Ergebnisse deuten auf einen klaren Unterschied der Bodenstruktur zwischen gepfügtem (CT, RT) und ungepflügtem Boden (NT) hin. Nah-gesättigte Leitfähigkeit auf gepflügtem Boden zeigte eine negative Korrelation mit der Trockenrohdichte sowie Makro- und Mesoporosität. Keine dieser Parameter konnte die Leitfähigkeit unter NT erklären. Das bildgebende Verfahren unterstützte die Hypothese, dass (nah-)gesättigte Leitfähigkeit unter NT von wenigen, gut miteinander verbundenen, großen Poren reguliert wird. Die Bodenmatrix ist hier vergleichsweise dicht gelagert und trägt nur wenig zum Wassertransport bei. Auf gepflügtem Boden hingegen ist die Porosität der entscheidende Faktor für den Wassertransport. Makroporensysteme können sich hier nicht dauerhaft etablieren, da sie jedes Jahr durch die maschinelle Bodenbearbeitung zerstört werden.

Zusammenfassend lässt sich sagen, dass die Struktur des Bodens, und damit auch dessen hydraulische Eigenschaften, sich klar zwischen konservierender und konventioneller Bodenbearbeitung unterscheiden. Auch die Variabilität der SHP zwischen einzelnen Kampagnen war groß. Damit bestätigt diese Arbeit die Hypothese, dass einmalige Messungen, sogenannte *Snapshots*, auf landwirtschaftlichen Böden nicht geeignet sind, die SHP ausreichend

zu erfassen. Dies gilt vor allem für gepflügten Boden. Eine Simulation des Bodenwasserhaushalts über eine Anbausaison hinweg, z.B. für die Bewässerungsplanung, machen mehrere Messungen notwendig, es sei denn, die PSD lässt sich ausreichend gut modellieren. Solche Modelle berücksichtigen allerdings bislang nur den kurzfristigen Verlust von Porosität, während zum Beispiel ein Aufbau von Makroporen nicht abgebildet werden kann. Im Gegensatz zu CT und RT, war der Boden unter NT zeitlich stabil. Die Wasserretention war hier verbessert, während die (nah-)gesättigte Leitfähigkeit ingesamt verringert war. Korrelations- und Regressionsanalysen in Verbindung mit Röntgentomographie konnten einige Unterschiede in der Bodenstruktur, die durch Tensionsinfiltrometrie beobachtet wurden, erklären. Die Ergebnisse zeigten, dass bei der Entwicklung von Pedotransferfunktionen zur einfacheren Ableitung von SHP die Bodenbearbeitung, sowie potentiell andere landwirtschaftliche Maßnahmen berücksichtigt werden sollten.

1 Introduction

1.1 The sustainable development agenda and conservation tillage

With the passage of the Sustainable Development Goals (SDG) by the United Nations General Assembly in 2015, the world community committed to a list of 17 goals that aim to tackle global challenges related to poverty, inequality, climate, environmental degradation, prosperity, peace and justice by 2030 (United Nations General Assembly, 2015). Among those goals is SDG 2 'Zero Hunger', which in particular aims to end hunger and malnutrition while at the same time ensuring sustainable food production systems and implementing resilient agricultural systems (United Nations, 2019). By 2019, 820 million people were still suffering from hunger while another 2 billion people are suffering from moderate to severe malnutrition. With this outlook, the achievement of SDG 2 by 2030 is at risk (FAO *et al.*, 2019). The global population will continue to grow, albeit at a continued decreasing rate with a likely population between 9.4 and 12.7 billion in 2100 (United Nations *et al.*, 2019). Therefore, agricultural food production systems will need to further adapt to meet the increasing demand while sustaining environmental resources already under threat from climate change and land degradation (Godfray *et al.*, 2010). If global agriculture were to continue the current trends of intensification in developed countries and clearing of land in developing countries to meet global food demands until 2050, an estimated additional 1 billion ha of land would be used for food production and large amounts of greenhouse gases be released (Tilman *et al.*, 2011). In order to keep further impacts on environmental resources at a minimum, the sustainable intensification of agriculture may be the way forward (Godfray and Garnett, 2014), reducing land transformation, greenhouse gas emissions and fertilizer use (Tilman *et al.*, 2011).

Conservation agriculture (CA), as promoted by the Food and Agriculture Organization of the United Nations (FAO) (FAO, 2019), is part of sustainable intensification of agricultural production systems (Godfray and Garnett, 2014). The globally largest areas under CA, as defined by the FAO, are located in South and North America. In Europe, covering about 2 % of the world's CA area, the total area under CA has increased by 30 % from 2008/09 (1.6 M ha) to 2013/14 (2.0 M ha). By 2015/16, the area had further increased by 75 % to 3.6 M ha. Countries with significant CA adoption are Spain, Italy, Finland, France, Germany,

United Kingdom, Romania and Poland (Kassam *et al.*, 2019, 2015). Conservation agriculture's three key principles are

(1) *Minimum mechanical soil disturbance* which aims to introduce direct seeding, *i.e.* no tillage (NT) practices.
(2) *Permanent soil organic cover* which is achieved by crop residues left on the field and growing cover crops between harvest and seeding as well as during fallow periods.
(3) *Species diversification* which is achieved through crop rotation.

Although those three principles are key to a sustainable production intensification of agriculture, they must be accompanied by practices of integrated pest, weed and disease management, efficient water management and the use of high-yielding and adapted crop varieties (FAO and Collette, 2011). It was shown that it is of paramount importance to implement the other two principles along with NT. Otherwise, yield reductions can be expected affecting especially resource-poor countries (Pittelkow *et al.*, 2014).

The first key principle of CA states that the intensive mechanical disturbance of conventional annual tillage should be averted by practicing NT agriculture. Apart from no tillage at all, there are also reduced or mulch tillage and strip tillage, which are less intensive forms of tillage (*e.g.* Afshar *et al.*, 2019; Kassam *et al.*, 2019; Marandola *et al.*, 2019). In the remainder of the dissertation, the term conservation tillage will be used to address these variants of tillage other than conventional inversion tillage. Prior to the worldwide increasing adaptation of conservation tillage techniques, conventional tillage with a moldboard plow (CT) was the method of choice for loosening the soil, mixing organic residue post-harvest and preparing the seedbed. However, CT exposes the soil to the elements which makes it more vulnerable to wind and water erosion (Lal *et al.*, 2007). Conservation tillage can reduce such risks and, among others, improve soil water storage, increase soil organic matter and lower energy consumption (Holland, 2004; Williams *et al.*, 2018). No matter what the reason for adaptation of a certain tillage practice, it affects the underlying soil. The presence or absence of tillage or the intensity thereof has, among others, an impact on a soil's structure and with that its hydraulic properties (Horel *et al.*, 2015). How this relates to soil water, will be elaborated in the following sections.

1.2 Soil structure and soil hydraulic properties

Soil structure may be defined as the spatial arrangement of aggregates or solids and voids in a soil across different scales (Rabot *et al.*, 2018). Aggregation, *i.e.* the formation of soil aggregates, of the fine-grained primary soil particles into secondary units occurs through flocculation, *i.e.* coagulation, and cementation (Hillel, 2009) which is mediated by soil organic C (SOC), clay and carbonate contents as well as microorganisms and ionic bridging (Bronick and Lal, 2005). Aggregates can be differentiated according to their size into macroaggregates or peds (diameter $\varnothing > 250$ μm) and microaggregates ($\varnothing < 250$ - 53 μm) (Andruschkewitsch *et al.*, 2013; Edwards and Bremner, 1967). Microaggregates are generally more stable than macroaggregates which are more easily disrupted in a rapid wetting process (Golchin *et al.*, 1994; Tisdall and Oades, 1982). Breakdown of aggregates mainly occurs through slaking, *i.e.* compression of air contained in aggregates upon wetting, differential swelling and shrinking, mechanical impact of rainfall and physico-chemical dispersion of soil particles (Bissonnais, 1996).

The notion of looking at soil structure purely from the viewpoint of aggregates has drawn criticism. The connection between soil hydraulic properties (SHP) and soil structure may not be appropriate in the context of aggregates as mainly their mechanical stability is investigated, but not so much the structure with different configurations of voids and solids (Baveye, 2006; Letey, 1991; Rabot *et al.*, 2018). By looking at the soil structure from the pore perspective in terms of 'size, shape and arrangement of the solid particles and voids' (Letey, 1991), processes related to those properties may be explained much better (Baveye, 2006; Rabot *et al.*, 2018).

However, also in the characterization of the void space, *i.e.* pore space, between and within aggregates, no commonly agreed upon classification exists. Pores formed by primary soil particles can be called matrix or textural pores. Pores that originate from the interplay of factors such as biological activity, soil management in agriculture and climate can be called structural pores (Hillel, 2009; Rabot *et al.*, 2018). Kutilek (2004) categorized pores according to the laws of hydrostatics and hydrodynamics. Capillary pores were summarized with the term micropores, which from an aggregate perspective includes both intra-and inter-aggregate pores. According to his definition, macropores are non-capillary pores where the boundary to micropores is drawn at an equivalent pore radius (r) between 1 and 1.5 mm. Those pores develop through earthworm activity, decaying root systems, fissures and cracks from swelling-shrinking processes as well as soil tillage. In such pores, accelerated flow, *i.e.* preferential flow, occurs. In this thesis, the functional classification of Greenland (1981) is adhered to when

discussing results of changes in pore volume fractions. It assigns class boundaries according to the main pore functions with fissures (⌀ > 500 μm), transmission (⌀ 50 - 500 μm), storage (⌀ 0.5 - 50 μm), residual (⌀ 0.005 - 0.5 μm) and bonding pores (⌀ < 0.005 μm). Note that this definition of size classes is arbitrary, but it aims to capture a 'main function' regarding water transport and retention within each class. Additionally, pores formed through plant roots and earthworm burrows will be referred to as biopores which, along with desiccation cracks and inter-pedal voids, are sometimes also seen as structural porosity (Alaoui *et al.*, 2011). Biopores are of a cylindrical shape with low tortuosity, and a high vertical continuity (Koestel and Larsbo, 2014; Luo *et al.*, 2010). In agricultural systems, they may form wide networks across the profile important for gas and water transport and are sensitive to disturbances from soil tillage (Lucas *et al.*, 2019).

Soil structure inherently influences SHP governing water transport and storage through the configuration of soil pore space (Kutilek, 2004). Information on the pore size frequency distribution (PSD), *i.e.* 'the relative abundance of each pore size in a representative volume of soil' (Nimmo, 2004), is often obtained from the water retention characteristic (WRC) which describes the relationship between soil water content (θ) and soil water tension (h). The capillary theory relates the h at which a pore drains to a soil pore radius r which is given by

$$r = \frac{2\sigma_w \cos\gamma}{\rho_w g|h|} \qquad \text{(Eq. 1)}$$

where σ_w denotes the surface tension of water, γ is the contact angle of the air-water interface, ρ_w the density of water and g the gravity acceleration (Nimmo, 2004). Kosugi (1994) developed a water retention model based on the assumption of a lognormal PSD, which was later coupled to a modified version of Mualem's (1976) model to account for hydraulic conductivity (K) (Kosugi, 1996). A change in this PSD through factors such as climate, soil management and biological activity inherently affects the WRC and hydraulic conductivity characteristic (HCC) (Bodner et al., 2013a, 2014; Or and Ghezzehei, 2002; Pires et al., 2008).

At and near saturation, the bulk of the soil matrix or the majority of pores represented in a PSD may be bypassed by preferential flow through the structural porosity of a soil. Preferential or macropore flow may occur in biopores, as well as cracks and fissures of fine-textured soils. This has implications for flow and transport modeling, where a multicontinuum

approach may be preferred over the classic unimodal PSD to properly describe water movement in the soil (Gerke, 2006).

1.3 Effects of conservation tillage on soil hydraulic properties

After highlighting the relation between soil structure and SHP in Section 1.2, this section will particularly deal with the effects of both conventional and the increasingly adapted conservation tillage systems (see also Section 1.1) on the soil structure and consequently its hydraulic properties. Tillage is a mechanical disturbance of the arrangement of aggregates and the aggregates themselves. It leads to the disruption of a developed soil structure and changes the soil pore space and with that, the PSD (Or *et al.*, 2000). Apart from the direct physical impact, it also determines the distribution of soil organic matter originating from harvest residue across the soil profile (Jacobs *et al.*, 2015) which in turn influences aggregate stability (Andruschkewitsch et al., 2013, 2014b) and aggregation (Andruschkewitsch *et al.*, 2014a; De Gryze *et al.*, 2005). Further indirect effects are on root growth and biological activity (Horel *et al.*, 2015). For example, a global meta-analysis revealed that earthworm abundances increase by 137 and 127 % under NT and reduced tillage, respectively, compared to inversion tillage practices (Briones and Schmidt, 2017). Early root and shoot growth of winter wheat was shown to decrease with decreasing tillage intensity on sandy loam soils (Munkholm *et al.*, 2008).

A large body of literature about tillage system effects on soil structure (Blanco-Canqui and Ruis, 2018) and SHP (Horel *et al.*, 2015; Strudley *et al.*, 2008) as well as related soil functions, such as water purification and retention (Skaalsveen *et al.*, 2019) exists, which these review articles from the past decade show. Some of the main trends and recent findings will be presented here.

A general notion is that the lack of annual soil loosening in NT systems leads to a consolidation resulting in increased bulk densities (ρ_b) and compaction relative to CT systems. Blanco-Canqui and Ruis (2018) in their review found that results from the past 10 years were ambiguous with almost equally as many increases in ρ_b on NT compared to CT as no effects. Most of the observed changes were found in the top 10 cm of the soil. The time passed since the uptake of NT practices may be crucial in the evaluation of such effects. Reichert *et al.* (2016) monitored the evolution of different soil intensity and capacity properties over the course of 14 years since NT-implementation. Their proposed framework suggests an initial, intermediary, transitional and a more stabilized stage of soil structure development. While there may be an initial compaction with increased ρ_b shortly after its implementation,

pedogenetic processes form aggregates that lead to a new dynamic equilibrium of soil structure with decreases of ρ_b at the soil surface 14 years after NT-implementation. However, the authors also pointed out that those results are only verified for a highly-weathered clayey soil in southern Brazil but should also be applicable to more silty or sandy soils. Blanco-Canqui and Ruis (2018) made similar observations when comparing studies of short-and long-term implemented NT systems. Schwen *et al.* (2011b), on the other hand, found significantly increased ρ_b on NT at the soil surface of a long-term (12 - 14 years) tillage experiment with a silt loam soil in a semi-arid (pannonic) climate. In their review, Skaalsveen *et al.* (2019) focused on SHP and their related functions of NT-systems in North Western Europe. They found higher ρ_b for the majority of fields under NT compared to CT for various soil types and textural classes. While ρ_b under NT may increase with time in the absence of frequent loosening, *i.e.* tillage, due to natural compaction (Moret and Arrúe, 2007; Schwen *et al.*, 2011b; Soracco *et al.*, 2010), ρ_b under reduced (non-inversion) tillage practices often does not significantly differ from conventional (inversion) tillage practices (*e.g.* Blanco-Canqui *et al.*, 2017; Crittenden *et al.*, 2015; Schwen *et al.*, 2011b) or may even be lower (Peña-Sancho *et al.*, 2017) within the topsoil layer. Below the plowing horizon of a cultivator, a plow pan can form, which strongly increases ρ_b compared to the deeper reaching moldboard plow (Schlüter *et al.*, 2018).

The WRC, *i.e.* the relationship between θ and h, is key in describing retention and movement of water in the soil (Horel *et al.*, 2015). Generally, it is assumed that NT and non-inversion tillage improves soil water retention through the better maintenance of soil structure and residue retention at the soil surface (Blanco-Canqui and Ruis, 2018). In a study by Kargas and Londra (2015) on a loamy soil, water retention and porosity were higher about two months after roto-tillage compared to that on an NT plot. A comparison of CT- and NT-plots on a sandy clay revealed higher water retention close to saturation under CT. At more negative h, the trend was reversed with higher retention on NT (Martínez *et al.*, 2008) indicating the establishment of distinctly different PSDs between treatments with more macropores under CT and greater microporosity under NT. Reichert *et al.* (2016) found that under NT relatively small pores draining at $h < -60$ cm may form at the expense of larger pores improving water availability for plants and reducing rapid drainage of soil water. This change in PSD was attributed to initial soil compaction in the absence of annual soil loosening and the following re-arrangement of particles as a consequence of shrinking-swelling as well as biological processes. These ongoing changes in soil structure within the NT-system have been observed up to 14 years after its establishment. As opposed to the previous studies,

Blanco-Canqui *et al.* (2017) found no differences in WRC on a silty clay loam between long-term (35 years) NT, disk, chisel and CT systems. For North Western Europe (*i.e.* Ireland, the UK, Germany, the Netherlands, Belgium, Denmark, Norway, Sweden, Iceland, Northern France, Switzerland, Austria, Luxembourg), Skaalsveen *et al.* (2019) did not find conclusive evidence that point to a consistent improvement of water retention under NT compared to CT due to factors such as texture, climate and management-dependent factors. They concluded that NT-implementation here is challenging due to the wetter and colder climate compared to other parts of the world. This is in agreement with a meta-regression analysis by van den Putte *et al.* (2010) that observed yield decreases under NT in Western Europe. In more arid regions, *i.e.* Southern Europe, such losses in crop yield may not occur for clay and sandy soils under conservation tillage systems, because they seem to perform better than CT due to a decline in evaporation from the soil.

Hydraulic conductivity may or may not be increased under conservation tillage systems. In their review, Skaalsveen *et al.* (2019) found both increases (Kechavarzi *et al.*, 2009; Pelosi *et al.*, 2017; Ugarte Nano *et al.*, 2015) and decreases (Crittenden *et al.*, 2015; Schwen *et al.*, 2011b; Ulrich *et al.*, 2006) in K at and near saturation of soils under NT compared to those under CT in North Western Europe. Apart from great variability in K between soil types (*e.g.* Bodner *et al.*, 2007), the authors named temporal variability as a potential source of discrepancy between study results. They concluded that sampling on only one occasion cannot properly capture this seasonal variability in (near-) saturated K. According to the authors, studies are often based on sampling campaigns in spring. Castellini *et al.* (2019a), for example, determined saturated hydraulic conductivity (K_s) and HCC on short-(6 years) and long-term (14 years) NT on a clay soil in a Mediterranean environment in spring. Compared to CT, they found no effects of conservation tillage on K_s. Bulk density was significantly increased under NT which, however, did not affect the soil's permeability. The authors suggested that the presence of a better-connected network of comparably smaller pores under NT was responsible for that. However, as sampling was done only once, the authors emphasized that seasonal effects were not reflected in their results.

As this section has shown, observations of soil structural properties and SHP between studies are often ambiguous which is attributed to, among others, different classification systems (*e.g.* for soil types), sampling strategies, methodologies, time of implementation of a tillage system, climate and other site specific environmental factors, soil management and lack of documentation of the respective measures, as well as temporal variability of the properties

under investigation (Derpsch *et al.*, 2014; Horel *et al.*, 2015; Skaalsveen *et al.*, 2019; Strudley *et al.*, 2008).

1.4 Temporal variability of soil hydraulic properties

As already briefly addressed in Section 1.3, soil structure and thus SHP vary with time which complicates their quantification. In the past, many studies have only conducted one-off measurements disregarding the temporal component introduced by environmental and management factors (Skaalsveen *et al.*, 2019; Strudley *et al.*, 2008). Considering such variations in SHP in water transport and storage modeling was shown to significantly improve the outcomes of such simulations (Alletto *et al.*, 2015; Feki *et al.*, 2018; Schwen *et al.*, 2011a) which would ultimately improve soil management in agriculture and the ecosystems services soils provide (Vereecken *et al.*, 2016). This section will therefore outline the recent findings on time-variable soil physical and hydraulic properties.

Strudley *et al.* (2008) in their comprehensive review summarized results of various studies investigating temporal variability of SHP. Their findings suggest that there are no consistent effects of the tillage system on SHP. The effects of agricultural management on SHP is often overshadowed by temporal and spatial factors. Right after tillage, effects on SHP are most pronounced but already one wetting-drying cycle may diminish them. Generally, temporal variability was identified as a major obfuscating factor. Since the publication of this review, more than ten years have passed and the body of literature on the subject has further grown. The advances since then will be presented in this section.

Peña-Sancho et al. (2017) compared the impacts of CT (moldboard plowing), reduced tillage (RT; chisel plowing) and NT treatments on the WRC and inferred PSD as well as their changes with time. Their focus was on topsoil (0 - 10 cm) WRC of a loam-textured Hypercalcic Calcisol. Overall, they found higher θ at lower h under NT while the opposite was found at saturation. Primary tillage on CT and RT increased pore volume near saturation and led to an increase in the peak of the inferred PSD function as a result of interaggregate pore space forming. Post-tillage rainfall and wetting-drying cycles then reduced ρ_b and the WRC returned to pre-tillage conditions due to aggregate disintegration and deformation. Temporal variation on NT was assumed inert and therefore not investigated. Kargas *et al.* (2016) focused on the temporal evolution of the WRC under roto-tillage and NT. Here, roto-tillage caused a decrease in mesopores ($1000 > \varnothing > 10$ μm) and an increase in micropores ($\varnothing < 10$ μm). Water contents decreased from saturation down to h = -60cm. Compared to that, NT had more mesopores of smaller diameters than the roto-tilled soil. Kool *et al.* (2019) showed that

changes in WRC are closely related to variations of the ϱ_b. When ϱ_b decreases due to tillage, it affects the WRC. The PSD of freshly tilled soil has a bimodal shape with a structural and textural mode. However, such an artificially built-up structure is not stable and pore volumes decrease shortly after tillage. With post-tillage increases in ϱ_b, the WRC becomes steeper, *i.e.* water retention at h = -330 cm increases. Such changes were shown to be more pronounced with increasing depth (Kool *et al.*, 2019). Chandrasekhar *et al.* (2019) successfully modeled post-tillage PSD evolution using an existing model based on the Fokker-Planck equation (Or *et al.*, 2000) on published case studies throughout the world. They showed that it is possible to simulate an overall reduction in total porosity (Φ) and loss of interaggregate pores reasonably well. A change in soil management from CT to long-term NT was also predicted by the model. This also confirmed findings by Schwärzel *et al.* (2011) who were able to simulate an observed change in PSD from cropping to pasture with this model. Pelak and Porporato (2019) also based their study on the model of Or et al. (2000) but left out the diffusion term. They simulated PSD evolution considering tillage, consolidation and soil organic matter input. Predicted key soil properties such as K_s and Φ followed trends found commonly supported by the literature. These advances might make periodic sampling to quantify SHP for soil water modeling obsolete. Nevertheless, there is a shortage in available datasets for model calibration and validation (Chandrasekhar *et al.*, 2018). Different scenarios including the build-up of pore structure, heavy rainfall, irrigation and fertilization are not considered by such approaches so far (Chandrasekhar *et al.*, 2019; Pelak and Porporato, 2019).

As already discussed in Section 1.3, the effects of different tillage systems on K are rather ambiguous partly owing to temporal variability. Such temporal effects may for example be introduced by CT with a moldboard plow or RT with a cultivator creating a loose macroporous soil structure and distributing organic residue (Strudley *et al.*, 2008). The loosened soil matrix settles with time as a result of post-tillage rainfall and wetting-drying cycles which contributes to increased bulk densities during the growing season (Moret and Arrúe, 2007; Moret-Fernández et al., 2016; Peña-Sancho et al., 2017; Sandin et al., 2018). While ϱ_b may be an important measure to explain changes in (near-) saturated K, other soil structural properties need to be considered as well (Kool *et al.*, 2019). On the one hand, CT with a moldboard plow down to 20 – 30 cm may create a higher macroporosity with an increased connectivity compared to RT with a cultivator down to 12 – 15 cm (Schlüter *et al.*, 2018). However, CT also disrupts developed biopore networks reducing connectivity among pores which directly effects K at and near saturation (Jarvis, 2007). Many factors and processes such as biological activity, plant root growth (Bodner *et al.*, 2014; Kodešová *et al.*, 2006; Rasse

et al., 2000), organic matter input (Andruschkewitsch *et al.*, 2014a), as well as temperature and moisture fluctuations (Bodner *et al.*, 2013b), are continuously involved in soil structure formation. Yet, tillage may be the dominant factor in observed network changes over time (Lucas *et al.*, 2019). Tillage loosens the soil matrix, which eventually settles with time. Such changes can be observed over a wide range of the PSD (Chandrasekhar *et al.*, 2019). An untilled soil, on the other hand, can preserve a functional network of large biopores embedded in a comparably dense soil matrix (Pires *et al.*, 2019). This may result in a relative temporal stability of (near-) saturated *K* under NT systems as observed by Schwen *et al.* (2011b). Apart from variations associated to interference with the biopore system, changes have also been revealed in less saturated conditions. For example, observations of near-saturated *K* at an *h* of -3 cm, excluding the largest pores (equivalent $r > 0.5$ mm), on a silty loam under CT showed a ten times greater temporal than spatial variability between and within three growing seasons (Zumr *et al.*, 2019). However, no clear direction of change could be identified, which was attributed to variations between the precipitation regimes of the three years under investigation with one exceptionally dry year, agricultural management and the timing of sampling in spring. Similar observations were made by Keskinen *et al.* (2019), where temporal variability of near-saturated *K* at *h* of -1, -3, and -6 cm exceeded spatial variability. Changes in unsaturated *K* were attributed to post-tillage structural evolution and variability in antecedent soil moisture. Here, temporal variability was more pronounced on CT compared to NT soil. With decreasing *h* down to -6 (Keskinen *et al.*, 2019) or -10 cm (Bodner *et al.*, 2013b; Schwen *et al.*, 2011b), variability of *K* was shown to be lower than for *K* at or near saturation which reflected a reduced influence of the soil's structural pores. Annual precipitation and temperature may be important predictors of *K* in this range (Jorda *et al.*, 2015). The development of the entire HCC over time down to lower *h* has rarely been studied (*e.g.* Jirků *et al.*, 2013). Most studies investigating the temporal variability of SHP quantified the WRC and K_s (*e.g.* Kargas *et al.*, 2016; Kool *et al.*, 2019) or the range near saturation that can be measured in the field using tension infiltrometers (*e.g.* Alletto and Coquet, 2009; Bodner *et al.*, 2013b; Daraghmeh *et al.*, 2008; Schwen *et al.*, 2011b; Zumr *et al.*, 2019). However, a sensitivity study demonstrated that determining only K_s while ignoring the HCC from *h* -10 to -1000 cm in water flow modeling means ignoring the most important *h*-range under standard meteorological conditions, *i.e.* non-extreme weather events. Under such conditions, preferential flow only plays a minor role and the macropore fraction is excluded (De Pue *et al.*, 2019).

1.5 Objectives and hypotheses

Objectives and hypotheses for this dissertation were formulated based on the notion that soil physical properties and SHP of arable soils are temporally variable. Therefore, one-off or snapshot measurements do not properly capture the various properties such as water retention and transport. Factors that play a role in the variability of these properties are of both biotic and abiotic nature. Therefore, the aim of this dissertation was to better understand the impacts on the soil structure by the chosen tillage systems and other factors affecting soil hydraulic behavior. The experiments were done on a long-term tillage experiment in Eastern Germany with two main objectives outlined below.

Objective 1): Quantification of the temporal variability in soil pore size distribution

The first objective was to quantify SHP, *i.e.* the WRC and the HCC, over one winter wheat cropping season on one conventional tillage and two conservation tillage systems. Physical tillage intensity decreased from conventional tillage with a moldboard plow (CT), over reduced mulch tillage with a cultivator (RT) to no tillage with direct seeding of the crop (NT). From the obtained SHP, the aim was to indirectly obtain information on soil structural changes through evaluation of the inferred PSDs. The underlying hypotheses of this objective were:

Hypothesis A) The tillage system affects the modality of the PSD. Tilled soil, *i.e.* CT and RT, has a bimodal pore system with a distinct structural mode created by the mechanical loosening. Soil under NT tends to a unimodal pore system with one pronounced textural mode in the PSD due to compaction and the absence of annual loosening.

Hypothesis B) The PSD of soil under long-term NT is temporally more stable than that of the tilled soil. On the other hand, the more pronounced structural pore system of the CT and RT system is more instable with time. Therefore, the structural mode of the PSD will be reduced with increasing time after the last tillage operation.

Hypothesis C) Soil physical quality (SPQ) is in part dependent on the PSD and therefore differs between treatments and with time.

Objective 2): Characterization of the soil structure and the underlying water transport processes

The second objective was to characterize differences in soil structure between CT, RT and NT and understand how they affect water transport processes. To achieve this, both the temporal and spatial variability of the HCC over a wide soil moisture range was recorded using field and laboratory measurements. Finally, *K* at different saturation states were related to other soil properties such as ρ_b and SOC using correlation and multiple regression analyses. Supporting information came from a collaborative study (Schlüter et al., in press; see also Section 1.6) which provided X-ray μCT imaging of soil cores obtained from the CT and NT plot of the same field. The underlying hypotheses of this objective were:

Hypothesis D) Spatial variability, *i.e.* variability among samples taken at the same time and on the same treatment, of *K* at and near saturation is mainly governed by soil structure. With decreasing soil water tensions the influence of structure will diminish and the texture will gain relevance. This should be expressed in decreased variability towards drier soil moisture states.

Hypothesis E) Temporal variation in *K* is more pronounced on treatments under tillage, *i.e.* CT and RT, as soil under NT is more compacted in the absence of annual tillage.

Hypothesis F) On CT, a loose macroporous soil matrix created by annual tillage governs water transport at and near saturation. On NT, the soil matrix is denser compared to CT due to compaction. Large individual biopores conduct the bulk of the infiltrated water at and near saturation. RT takes a middle position with a comparably loose soil matrix but annually disturbed biopore networks.

1.6 Structure of the dissertation

The dissertation is partly based on results of one recently published and one submitted journal article as a first author and one accepted journal article with co-authorship:

1) **Kreiselmeier, J.**, Chandrasekhar, P., Weninger, T., Schwen, A., Julich, S., Feger, K.-H., Schwärzel, K., 2019. Quantification of soil pore dynamics during a winter wheat cropping cycle under different tillage regimes. Soil Tillage Res. 192, 222–232. https://doi.org/10.1016/j.still.2019.05.014
2) **Kreiselmeier, J.**, Chandrasekhar, P., Weninger, T., Schwen, A., Julich, S., Feger, K.-H., Schwärzel, K. Temporal variations of the hydraulic conductivity

characteristic under conventional and conservation tillage. Submitted to Geoderma. Status: under review.

3) Schlüter, S., Albrecht, L., Schwärzel, K., **Kreiselmeier, J.**, in press. Long-term effects of conventional tillage and no-tillage on saturated and near-saturated hydraulic conductivity – Can their prediction be improved by pore metrics obtained with X-ray CT?. Geoderma Special Issue 'Recent Advances in Pore-Scale Imaging of Soil Systems.

Articles 1) and 2) mostly summarize the results of Objectives 1) and 2), respectively. Previously unpublished work on soil physical quality completes Objective 1). The results of Article 3) are used to support the findings of Article 2). It partly presents the results of the B.Sc.-thesis of Lukas Albrecht under the supervision of Steffen Schlüter at the Helmholtz Centre for Environmental Research (UFZ) in Halle, Germany. The laboratory infiltration measurements, image analysis, flow simulation and statistical analysis of the data was done by Steffen Schlüter and Lukas Albrecht. Steffen Schlüter was the main and corresponding author of this manuscript. My contributions to Article 3) were

- involvement in the experimental design and selection of plots;
- conducting field infiltration measurements using the hood infiltrometer and consequently analyzing the data;
- acquiring yield data from the tillage experiment;
- manuscript writing (parts of the site description, parts concerning hood infiltration measurements) and general editing.

2 Materials and methods

2.1 Study area

2.1.1 Tillage experiment Lüttewitz ('Schlag Gasthof')

The site is located in the Central Saxon Loess Hill Country (*'Mittelsächsisches Lösshügelland'*), Eastern Germany (51°76 N, 13°1343 E, 275 m.a.s.l.; Figure 1), a landscape known for its extensive loess areas and fertile arable soils. In the past centuries, this region has suffered from severe soil erosion due to its topography with small-scale catchments and historically grown large agricultural field sizes (Wolf and Faust, 2013). The tillage experiment in Lüttewitz was established in 1993 with four treatments in order to investigate economic and ecological effects of different conservation tillage systems. It is one of a total of eight large-scale tillage experimental sites the Südzucker AG maintains in Germany (Südzucker AG, 2002). The soil type was classified as a Haplic Luvisol according to the World Reference Base for Soil Resources (WRB) system (IUSS Working Group WRB, 2015; Koch *et al.*, 2009). Soil texture on all measurement locations (Figure 1) was a homogeneous silt loam both at the surface from 0 to 0.05 m and from 0.25 to 0.30 m depth (Table 2).

Long-term (1981 - 2010) mean annual air temperature and precipitation of the nearby meteorological station in Nossen (~10 km linear distance) was at 8.7 °C and 753 mm (DWD, German Meteorological Service). Weather data was also available from a station directly on the field from 2011. However, precipitation data was largely fragmentary from January 2014 to October 2015. Therefore, no average values were calculated from this data set. Nevertheless, for most of the time of this study precipitation data was available which could be used for the interpretation of observed soil structural changes (Figure 2). Figure 2 gives an overview of the rainfall patterns during the observation period. Therein, an effective rainfall defined as > 10 mm d^{-1} is presented (Moret and Arrúe 2007). However, even at that magnitude precipitation can theoretically be distributed over 24 h with moderate intensities of only 0.4 mm h^{-1} which might not significantly contribute to mechanical breakdown of aggregates as this is dependent on the kinetic energy of rainfall (Bissonnais, 1996). Therefore, rainfall intensities in Figure 2 were based on half-hourly records from the on-site weather station and only intensities ≥ 5 mm h^{-1} are displayed. In the first couple of weeks after sowing, the station was not recording any rainfall, which was probably due to a malfunction. During

the remainder of the study, precipitation records are valid when compared to data from surrounding meteorological stations.

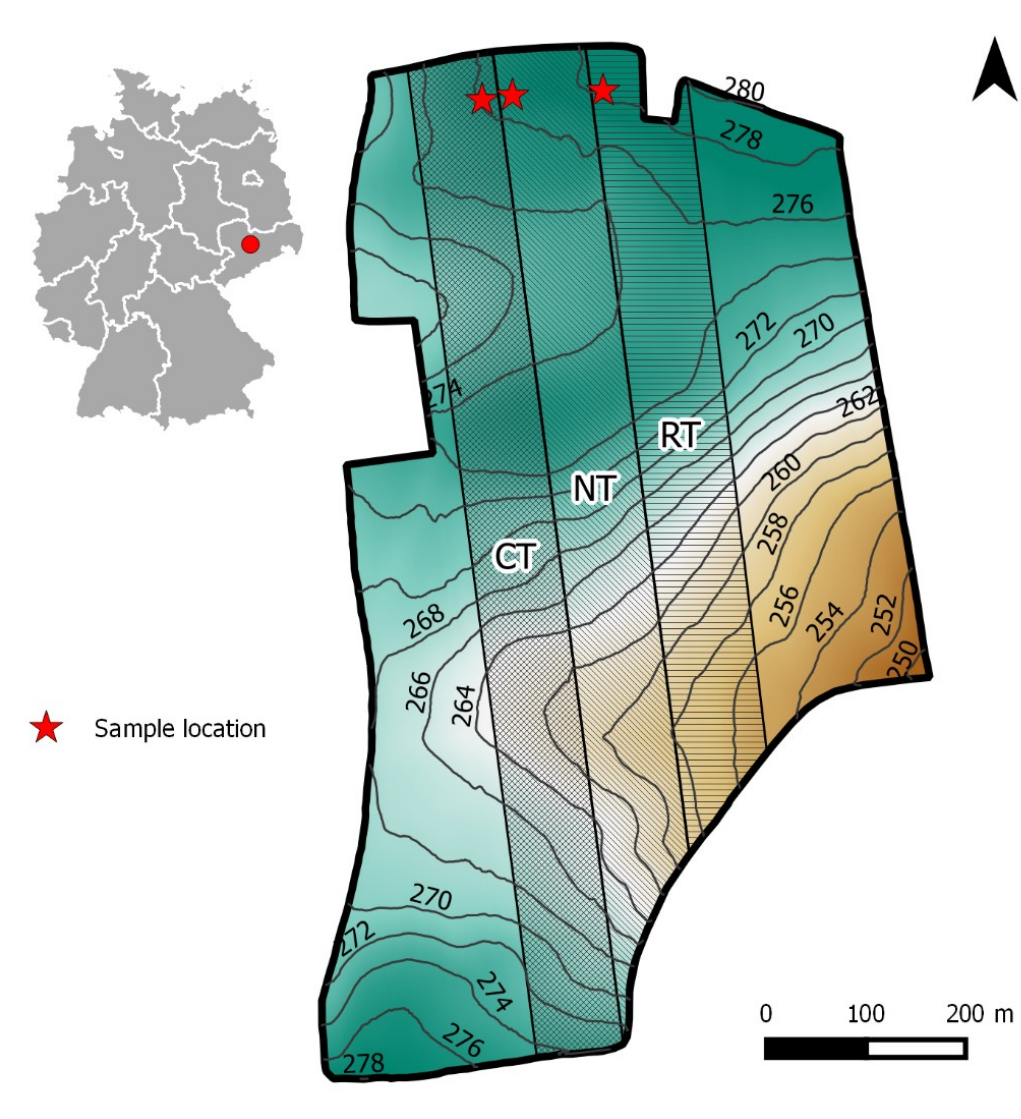

Figure 1 Experimental site Lüttewitz ('Schlag Gasthof') with location of sampling points on treatments conventional tillage (CT), reduced mulch tillage (RT) and no tillage (NT). Contour lines based on 2 m laser elevation data (Source: GeoSN, https://www.govdata.de/dl-de/by-2-0).

2.1.2 Treatments and agricultural management

There were no replicated plots of the treatments as the field was laid out in four large parallel strips with a size between 5.4 and 7.8 ha in north-south orientation. In this study, three treatments were investigated, namely CT, RT and NT (Figure 1). The main tillage and other agricultural operations are listed in Table 1 and displayed in Figure 2 along with the times of sampling. Organic residue from harvests and catch crops was retained on the field of all plots. During winter wheat harvest, straw was chopped, and, depending on the treatment, mixed

into the soil during stubble breaking (CT and RT) or left on the surface (NT). Conventional tillage entailed the use of a moldboard plow turning over the soil down to 25 to 30 cm during annual tillage and a cultivator for seedbed preparation and stubble breaking, *i.e.* the incorporation of stubbles and chopped organic residue into the soil following crop harvest. The less intensive RT only made use of a cultivator for both stubble breaking and seedbed preparation. With no annual tillage and no seedbed preparation prior to winter wheat seeding, NT was the least intensive tillage practice. Here, winter wheat was sown with a direct drill through the mulch left on the surface. Only before sugar beet, a shallow seedbed (8 cm in 2017; Table 1) was prepared in order to ensure a good enough emergence and establishment of seedlings through the organic residue layer covering the soil (Koch *et al.*, 2009).

Crop rotation at this site was two years of winter wheat (*Triticum aestivum* L.) followed by sugar beet (*Beta vulgaris* L.). Winter wheat was usually sown in autumn after the previous harvest. Before sugar beet sowing in spring, mustard was planted as a catch crop which was left on the field to freeze off. Its remains were later plowed into the soil during annual tillage (CT) and the seedbed preparation (RT, NT). In the year prior (2015) and during (2016) this study, winter wheat was grown (Figure 2). In April 2017, sugar beet was sown. Fertilization and pesticide usage represent common practice and did not differ between treatments.

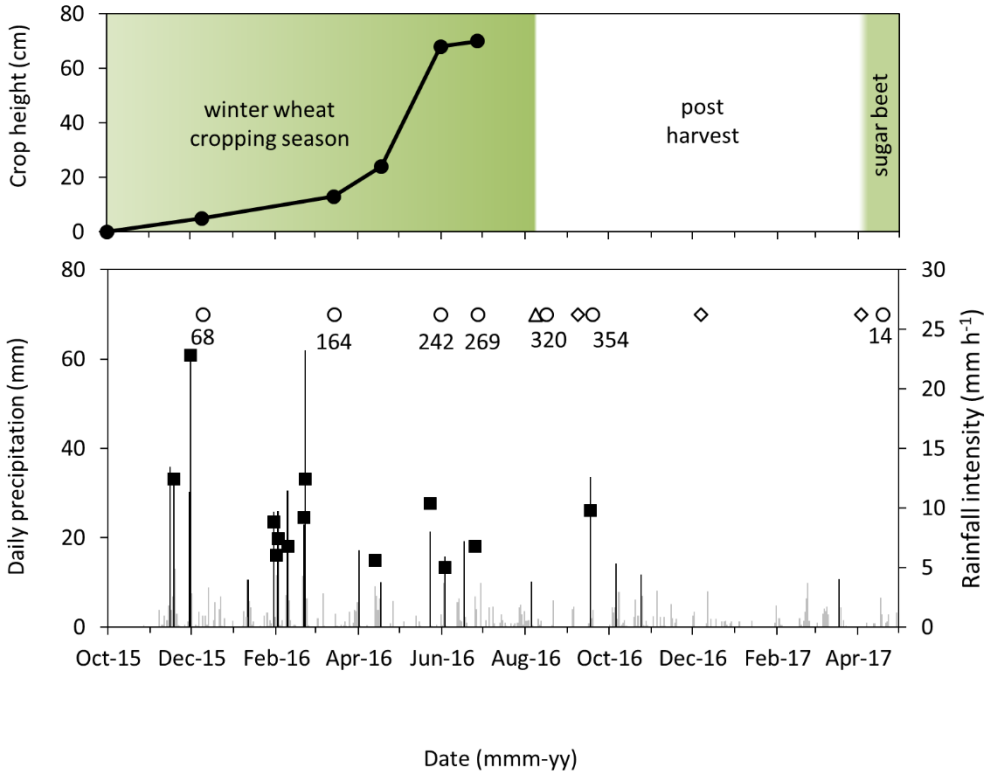

Figure 2 Daily precipitation (bottom diagram) for the measurement period since winter wheat sowing (1 October 2015). Effective rainfall (> 10 mm d^{-1}) as defined by Moret and Arrúe (2007) is highlighted in black. Largest rainfall intensities on any given day exceeding 5 mm h^{-1} are displayed as black squares. Times of sampling are marked by circles with days since last sowing of winter wheat or sugar beet, respectively. The triangle marks the time of harvest and the diamonds tillage on CT/RT (stubble breaking on 8 September 2016), CT (annual tillage on 7 December 2016) and seedbed preparation (CT & RT on 3 April 2017). The upper diagram depicts height of the winter wheat as determined during the measurement campaigns. The green background indicates the cropping season from sowing to harvest of winter wheat and sugar beet, respectively.

Table 1 Agricultural management in the study period mainly covering one cropping season of winter wheat. At the first two occasions, no hood infiltrometer measurements were done or results were not usable, respectively. Therefore, only undisturbed samples are presented for Dec-15 and Mar-16.

	Date	Agricultural Management	Details
2015	27 August	stubble breaking on CT and RT	cultivator (5 - 8 cm depth)
	10 September	tillage on CT	moldboard plow (25 cm depth)
	18 September	spraying	herbicide
	30 September	seedbed preparation	cultivator (15 cm depth on CT and RT)
	1 October	winter wheat sowing	*Triticum aestivum,* variety Kerubino; 320 seeds m^{-2}
	2 November	spraying	molluscicide
	9-10 December	**Soil core sampling: Dec-15**	
2016	**14-17 March**	**Soil core sampling: Mar-16**	
	8 April	spraying	herbicide, growth regulator
	28 April	fertilization	DAP: 0.42 t ha^{-1}
	7 May	spraying	fungicide, growth regulator
	18 May	fertilization	PK: 0.40 t ha^{-1}
	19 May	spraying	herbicide
	26 May	spraying	fungicide
	31 May	fertilization	DAP: 0.35 t ha^{-1}
	31 May - 2 June	**Hood infiltrometer-measurements and soil core sampling: May-16**	
	4 June	fertilization	CAN 27: 0.33 t ha^{-1}
	7 June	spraying	insecticide
	10 June	fertilization	DAP: 0.18 t ha^{-1}
	27-28 June	**Hood infiltrometer-measurements and soil core sampling: Jun-16**	
	8 August	harvest	fresh yield: 8.77, 9.06 and 9.13 t ha^{-1} on CT, RT and NT with 12.7, 12.4 and 12.6 % humidity
	16-22 August	**Hood infiltrometer-measurements and soil sampling: Aug-16**	
	8 September	stubble breaking on CT and RT	cultivator (5 - 8 cm depth)
	9 September	mustard sowing	catch crop
	19-22 September	**Hood infiltrometer-measurements and soil sampling: Sep-16**	
	6 December	soil rolling	roller
	7 December	tillage on CT	moldboard plow (30 cm depth)
2017	3 April	seedbed preparation	cultivator (15 cm depth on CT and RT, 8 cm on NT)
	5 April	sugar beet sowing	*Beta vulgaris*, variety BTS 770 1.17 U ha-1 ≙ 11.7 seeds m^{-2}
	19-20 April	**Hood infiltrometer-measurements and soil core sampling: Apr-17**	

PK	Phosphorus (P) and Potassium (K)
DAP	Diammonium phosphate (DAP); 18 % of Nitrogen (N) in the form of ammonium; 46 % of P in the form of ammonium phosphate
CAN 27	Calcium ammonium nitrate; 27 % N as nitrate and ammonium and 10 % Ca
CT	Conventional tillage with a moldboard plow
RT	Reduced mulch tillage with a cultivator
NT	No tillage with direct sowing

2.2 Sample design

All sampling and measurements in the field were done along a transect perpendicular to the crop rows with two-meter spacing between sample points. A total of five infiltration runs were done and as many undisturbed soil cores were taken per occasion and treatment plot. Transects were marked with plastic poles. Every occasion, the transect was moved two meters from the previous location to avoid disturbances from the previous sampling. The texture on all three plots was determined once in Mar-16 across such a transect (8 m with $n = 5$). Results between treatments were comparable (Table 2; see Section 2.4.3 for method description). To ensure further comparability between treatments, a relatively even area of the otherwise undulating site was chosen (Figure 1).

The main work flow is displayed in Figure 3. Details about each method are explained in Sections 2.3.1 to 2.4.2. First, infiltration measurements were conducted at the surface of the undisturbed soil. Unfortunately, HI measurements were not available for Dec-15. For Mar-16, most of the data had to be excluded due to malfunctions and erroneous measurements. From May-16 to Apr-17, HI-measurements could be used. More than 24 h after these measurements, undisturbed soil cores were retrieved and transported to the laboratory where they were stored in a fridge at about 4 °C. Before determining saturated K in the lab (K_{slab}), samples were gradually saturated in degassed tap water over the course of 24 h. Saturated samples were then transferred directly to the HYPROP® system for the determination of the drying WRC and HCC. Concluding the sequence, samples were oven-dried for 24 h at 105 °C to determine their dry weight and consequently the ρ_b.

Apart from the main work flow, a study on soil pore metrics from X-ray µCT scans and their relationship with K at and near saturation was done in corporation with the UFZ in Halle. The experimental design is briefly presented in Section 2.7. Results (Section 3.10) are discussed in connection with Objective 2) (Section 1.5) of this dissertation.

Table 2 Soil texture as obtained from the combined sieving and sedimentation method (n = 5). Standard deviation is displayed in brackets. Classification of the particle size fractions adheres to the World Reference Base for Soil Resources (WRB) of the FAO (IUSS Working Group WRB, 2015).

Treatment	Depth	Clay	Silt	Sand	WRB soil texture classification
		<2 µm	2-63 µm	63-2000 µm	
	(m)		% (w/w)		
CT	0.00-0.05	18.6 (0.8)	78.0 (1.4)	3.4 (0.2)	SiL, Silt Loam
	0.25-0.30	17.3 (0.8)	78.9 (1.0)	3.8 (0.2)	
RT	0.00-0.05	20.5 (1.2)	76.6 (0.8)	2.9 (0.4)	
	0.25-0.30	21.3 (2.2)	75.2 (1.8)	3.5 (0.7)	
NT	0.00-0.05	20.7 (0.9)	76.0 (1.6)	3.2 (0.1)	
	0.25-0.30	18.4 (1.4)	78.0 (1.2)	3.6 (0.2)	

CT: conventional tillage with a moldboard plow

RT: reduced mulch tillage with a cultivator

NT: no tillage with direct sowing

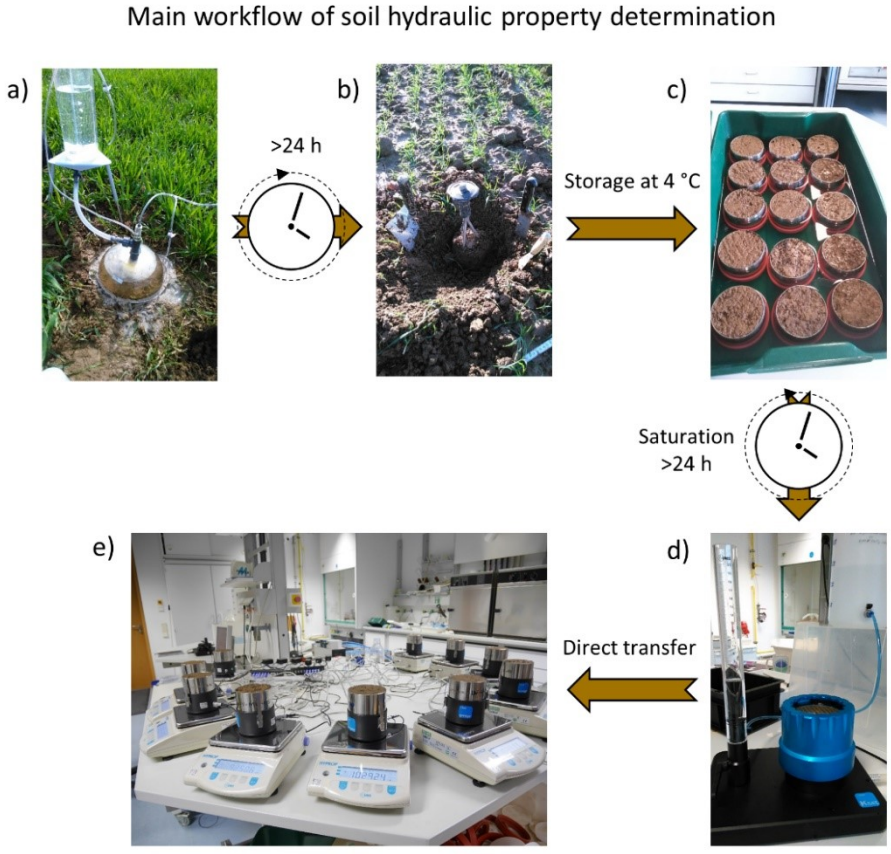

Figure 3 Main workflow of soil hydraulic property determination: a) *In-situ* (near-) saturated hydraulic conductivity with the hood infiltrometer; b) Undisturbed soil core sampling using 250 cm^3 stainless steel cylinders after > 24 h of the infiltration experiment; c) Gradual saturation of the retrieved soil cores in the laboratory with degassed tap water. The bottoms of the cylinders were fitted with previously saturated porous plates; d) Saturated hydraulic conductivity determination using the KSAT® device with the falling head method; e) Transient evaporation experiments with the HYPROP® system to determine the drying water retention and hydraulic conductivity characteristic at ambient atmospheric conditions.

2.3 Field measurements

2.3.1 Hood infiltrometer measurements

For the *in-situ* characterization of near-saturated K the hood infiltrometer (HI; UGT, Germany) was used. The HI is a type of tension infiltrometer (TI) which, like essentially all TIs, works with a Mariotte-type bubble tower to set a desired supply potential at the soil surface. Typically, TIs need a layer of sand or glass beads together with a nylon cloth to ensure a good hydraulic contact of the disk with the soil surface. For these TIs, the soil needs to be levelled in advance (Angulo-Jaramillo *et al.*, 2016). Instead of a disk, the HI operates with a water-filled hemispheric acrylic hood which is directly placed onto the soil surface. Therefore, the soil under investigation only needs little to no preparation before a measurement is started (Schwärzel and Punzel, 2007). Vegetation – in our case the crop or its stubbles after harvest – was carefully cut down to < 1 cm. Comparisons of the HI with a common TI (Schwärzel and Punzel, 2007) and minidisk infiltrometer (Matula *et al.*, 2015) have shown that the HI yields K_s and near-saturated K up to one and two orders of magnitude higher, respectively. This was mostly attributed to an improved hydraulic contact of the HI with the soil surface through the water-filled hood as compared to a minidisk infiltrometer (Matula *et al.*, 2015). Other factors may also be soil surface sealing, as well as smearing and clogging of pores caused by the surface preparation and the contact layer of the conventional TI (Schwärzel and Punzel, 2007). With 483 cm^2, the HI hood covers an infiltration area larger than many common commercially-available TIs such as the one by Eijkelkamp (314 cm^2; Eijkelkamp Soil & Water, 2019) and the minidisk infiltrometer (64 cm^2; METER Group Inc., 2019) or self-made solutions such as a malleable disk infiltrometer (314 cm^2; Moret-Fernández *et al.*, 2013) and an automated TI (170 cm^2; Špongrová *et al.*, 2009). Theoretically, using the HI instead of the alternative TIs should lead to an increased coverage of soil heterogeneity expressed in the distribution of macropores and cracks at the soil surface improving representativeness of the K_s and near-saturated K obtained from field infiltration measurements.

A schematic of the HI setup is displayed in Figure 4. The hemispheric hood is placed directly onto the soil surface framed by a retaining ring pushed about 1 cm into the soil. The space between hood and retaining ring is filled with a fine sand which is wetted in order to seal the hood from the ambient air. A reservoir in combination with the bubble tower ensures a constant supply of water to the hood, maintaining a constant water level and a negative h. By vertically moving the air intake pipe in the Mariotte-type bubble tower, h can be adjusted. The

U-tube manometer and the water level above the soil surface, as displayed in the stand pipe, provide information on the set *h*. For a more detailed description of the HI operation, please refer to the official manual (UGT, 2019) and the comprehensive and intelligible online tutorial by the Department of Water Resources of the Czech University of Life Sciences, Prague (Báťková *et al.*, 2013).

Negative *h* were set in descending order from close to saturation down to the bubbling pressure (BP) of the soil. The water level decline at each *h*-step was monitored until steady state, *i.e.* the state at which there are no more observable changes in water level decline per time step, was reached. Once *h* was low enough to draw air through the largest water-filled pore, the BP was recorded, and the measurement finalized. Depending on the BP, between two to four *h* were set and infiltration measured.

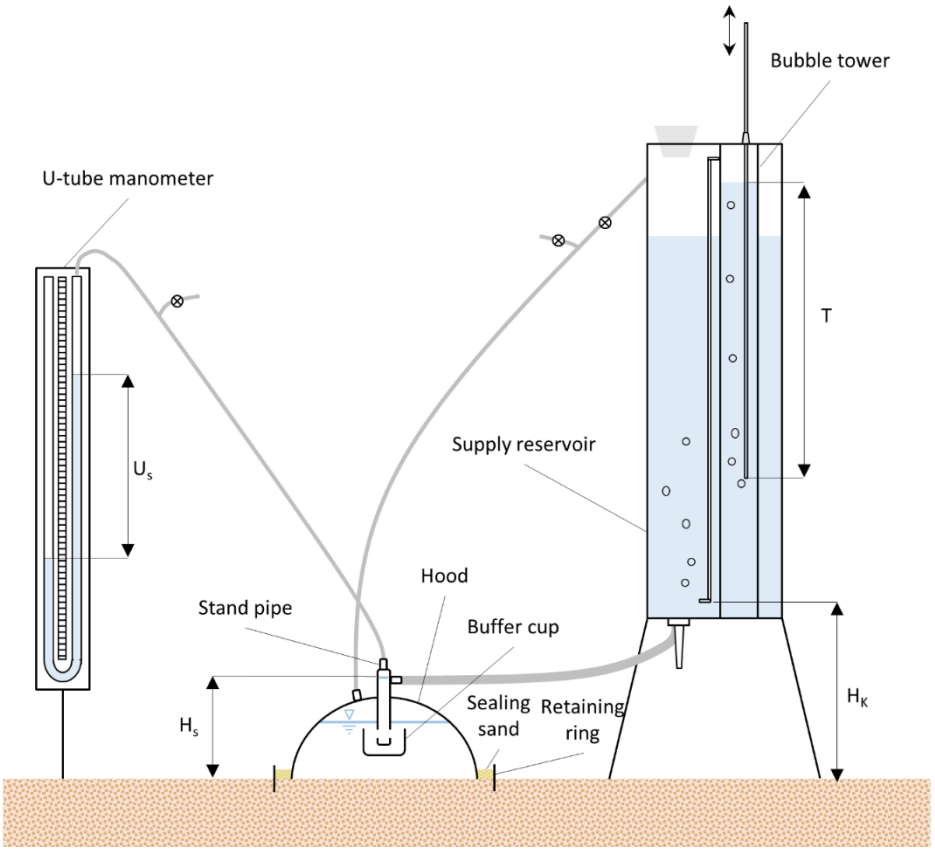

Figure 4 Schematic of the hood infiltrometer with its main components the hood, the supply reservoir and the U-tube manometer. The supply pressure head (*h*) at the soil surface can theoretically be set with an accuracy of 1 mm. It is determined as the difference between water level height in the stand pipe (H_S) and the negative pressure shown at the U-tube manometer (U_S). The set *h* is regulated by varying the submergence depth (T) of the air intake pipe in the bubble tower. The distance between reservoir and soil surface (H_K) serves as a reference for setting the initial T. Note that the schematic is not to scale. Redrawn and adapted from Schwärzel and Punzel (2007).

2.3.2 Analysis of hood infiltrometer measurements

In order to calculate K_s and K near saturation the steady-state infiltration data from field HI-measurements was analyzed by the linear interpolation procedures outlined in Reynolds and Elrick (1991) and Ankeny *et al.* (1991). As measurements were not always done at the same nominal h, the obtained K-h pairs were fitted with the two-line regression model proposed by Messing and Jarvis (1993) to obtain K_s and K at h = -2 cm (K_{-2cm}). The model is defined as

$$\ln K = \ln K^* + \alpha_1(h - h^*); h > h^* \quad \text{(Eq. 2)}$$

$$\ln K = \ln K^* + \alpha_2(h - h^*); h \leq h^* \quad \text{(Eq. 3)}$$

where α_1 and α_2 are the slopes of the respective regression line, h^* marks the h at the inflection point between the two regression lines and K^* is the respective K given by

$$\ln K^* = \ln K_s + \alpha_1 h^* \quad \text{(Eq. 4)}$$

Parameters ln K_s, ln K^*, h^*, α_1 and α_2 were estimated by means of non-linear least square analysis. The procedure is outlined in all detail by Jarvis and Messing (1995). As suggested therein, K was calculated at the midpoint of two consecutive h as well as between the smallest and largest h. With three to four set h steps for most infiltration runs the two-line regression model was expected to represent the K-h relationship within the estimated range well. Further h were not considered as most of the infiltration data was not obtained at h beyond -2 cm due to the BP ending measurements. As K may drop rapidly with decreasing h in structured soils due to drainage and consequent inactivation of macropores (Renger *et al.*, 1999; Schwärzel and Punzel, 2007), it was chosen to avoid extrapolation in this range.

2.3.3 Macropore stability indicator

At the end of each infiltration sequence the BP was determined which can be seen as an indicator for the presence or absence of macropores. Patra *et al.* (2019) proposed to calculate an equivalent threshold pore radius (r_{BP}) based on the well-known Young-Laplace capillary equation introduced in Section 1.2. Replacing $|h|$ with |BP| results in

$$r_{BP} = \frac{2\sigma_w \cos\gamma}{\rho_w g|BP|} \quad \text{(Eq. 5)}$$

where σ_w was set to 0.0713 N m^{-1}, γ was assumed to be 0, and ρ_w was set to 999 kg m^{-3}. The authors used r_{BP} as an indicator for the relative stability of the macropore system with time and between cropping systems based on the assumption of a correlation between prevalent mean macropore radius at the infiltration area and the BP. A higher mean macropore radius would mean a lower |BP| and following Eq. 5 a larger r_{BP} and *vice versa*. Patra *et al.* (2019) suggested to further test the suitability of this indicator on a higher number of observations to monitor its temporal evolution. Therefore, this measure was included here.

2.3.4 Undisturbed and disturbed soil sampling

For determining K_{slab} and the WRC in the laboratory, undisturbed soil cores (volume: 250 cm^3; height: 5 cm) were taken at least 24 h after the HI measurements. The cores were retrieved from directly underneath the previous hood position to make hydraulic properties from *in-situ* and laboratory measurements comparable. Where possible, the cylinders were pushed into the soil manually to avoid disturbances of the soil structure such as cracks and crevices potentially altering hydraulic properties. Especially K_{slab} determined with the falling or constant head method on such specimen was shown to be highly influenced by these artifacts extending through the entire length of a soil core (Reynolds *et al.*, 2000). Occasionally, simple pushing of cores was not possible due to high ρ_b. In these cases, a rubber hammer was used to drive cores into the soil. The cores were then carefully excavated using sharp knives and scissors severing roots and remaining organic material sticking out. For transport, the cylinders were closed with plastic caps and placed into foam boxes. Upon arrival in the laboratory, the samples were stored in a fridge at approximately 4 °C until further processing.

In addition to the undisturbed soil specimen, disturbed samples were collected in paper bags from the top 5 cm at every sampling spot. The soil was air-dried in the laboratory and sieved with a mesh size < 2 mm. This was used to determine soil texture and SOC and N concentrations. More details are given in Section 2.4.3.

2.4 Laboratory measurements

2.4.1 Saturated hydraulic conductivity

In the laboratory, soil cores were carefully trimmed with a knife at their edges and fitted with a previously saturated porous plate. The prepared samples were then placed in a trough and degassed tap water was filled to about two centimeters height (Figure 3c). Over the course of 24 h, the water level in the trough was gradually raised to ensure slow saturation of the specimen from bottom to top in order to minimize air entrapment in the soil pore system.

Upon saturation, the soil cores were moved to the KSAT® system (METER Group Inc., Germany) to determine K_{slab} (Figure 3d). As suggested by the manufacturer, the falling head method was employed. Originally, this method was only recommended for samples with a K_{slab} < 86 cm d^{-1}. Many of the samples here exhibited higher values and the constant head method would have been recommended (Klute and Dirksen, 1986). However, the KSAT® system is 'extremely precise' in measuring the water level decline with time through its internal pressure sensor. Therefore, the falling head method is the default setting for all kinds of permeabilities and was also used here (METER Group Inc., 2019a). The measured water level decline with time was then fitted with an exponential function by the KSAT® software. Only those samples with a coefficient of determination (R^2) > 0.999 were considered valid measurements. Saturated hydraulic conductivity was then calculated by the software making use of Darcy's law.

2.4.2 Water retention and hydraulic conductivity characteristic

Following the falling head procedure, the saturated soil cores were prepared for the determination of the drying WRC and HCC with the HYPROP® system (METER Group Inc., Germany). The HYPROP® system makes use of the simplified evaporation method (Peters and Durner, 2008), which is based on Wind's (1969) approach to linearly approximate vertical distributions of both θ and h in a sample. This method requires only two tensiometers inserted vertically at different depths of the soil sample (Figure 5). With help of an auger guide, holes for the tensiometers were carefully drilled into the core. Once assembled, the units were placed on scales connected to a computer and left to evaporate in ambient laboratory conditions at temperatures between 19 and 24 °C. A total of ten sensor units and balances were run at the same time (Figure 3e). The weight- and h-changes in time were recorded automatically every ten minutes except for the initial phase where measurements were taken at a higher frequency, which was the default setting in the HYPROP VIEW®

recording software (METER Group Inc, Germany) to account for the initial rapid redistribution of the water in the soil core. The samples were left to evaporate until the tensiometer reached their measurement limit where they drew air through the porous cup. When finished, samples were oven-dried at 105 °C for 24 h to determine their dry weight. With the known bulk soil volume (V_b) of 250 cm^3 and the dry soil mass (M_s), ϱ_b was calculated by $\varrho_b = M_s/V_b$.

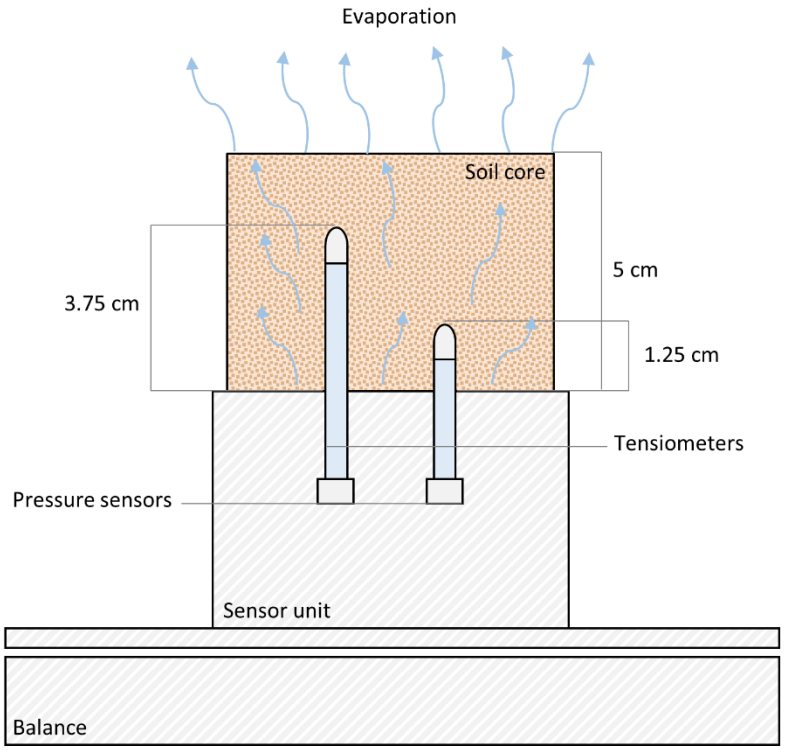

Figure 5 Schematic of the assembled HYPROP® sensor unit on the balance. Note that the schematic is not to scale. Redrawn and adapted from the HYPROP® operation manual (METER Group Inc., 2019b).

2.4.3 Other soil properties

Soil texture was determined with the combined sieving and sedimentation method only in Mar-16 as all measurement campaigns were done in proximity to each other. The property was not expected to vary notably with time. Prior to the sedimentation analysis, organic substance was removed by oxidation with hydrogen peroxide that was gradually added together with 2-Octanol to prevent the loss of sample through the formation of foam. The soil aggregates were dispersed by adding a sodium diphosphate solution.

Some of the air-dried material was further ground for CN analysis with the vario TOC cube (Elementar, Germany). As the soil was devoid of carbonates the measured total C content can be assumed to represent organic C. Soil organic C and N stocks were calculated

for the top five centimeters of the sampled soil using the results from the CN analysis and the ϱ_b following the procedure of Ellert and Bettany (1995).

2.5 Model fitting procedure

2.5.1 Bimodal models for the water retention and hydraulic conductivity characteristic

Agriculturally used soils can be expected to exhibit a bimodal soil structure with a textural and structural mode as a result of mechanical soil management and changes in SOC contents. When describing such soils, it has been shown that neglecting a multimodality in the model parametrization can introduce large errors (Jensen *et al.*, 2019). Even when disregarding only weak bimodality large epistemic errors may be introduced that lead to losses in accuracy of simulated soil water fluxes (Romano and Nasta, 2016). To accurately describe the PSD, the WRC and HCC were parametrized with the bimodal form of the Kosugi model (Kosugi, 1996) and the Mualem hydraulic conductivity model (Mualem, 1976) brought forward by Romano *et al.* (2011). The WRC is given by

$$S_e(h) = \frac{\theta - \theta_r}{\theta_s - \theta_r} = \sum_{i=1}^{k} w_i \left\{ \frac{1}{2} erfc \left[\frac{\ln\left(\frac{h}{h_{mi}}\right)}{\sqrt{2}\sigma_i} \right] \right\} \qquad \text{(Eq. 6)}$$

where S_e (-) is the effective saturation at h (cm), θ (cm^3 cm^{-3}) is the volumetric water content, θ_s and θ_r (cm^3 cm^{-3}) are the saturated and residual water content, respectively. Bimodality of the WRC is expressed by k = 2 defining a structural (i = 1) and a textural (i = 2) domain, w_i (-) is a factor assigning weights to both domains with $0 \leq w_i \leq 1$ and $\sum w_i = 1$, *erfc* is the complementary error function, h_{mi} (cm) is the median h at which the effective saturation of the respective subcurve $S_{ei}(h_{mi}) = 0.5$ and σ_i (-) is the standard deviation of the lognormal soil pore size distribution defining the width of the PSD. The HCC is given by

$$K(h) =$$

$$K_s \frac{S_e^{0.5}}{4\left[\sum_{i=1}^{k} \frac{w_i}{h_{mi}} exp\left(\frac{\sigma_i^2}{2}\right)\right]^2} \left\{\sum_{i=1}^{k} \frac{w_i}{h_{mi}} exp\left(\frac{\sigma_i^2}{2}\right) erfc\left[\frac{\sigma_i}{\sqrt{2}} erfc^{-1}(2\,S_{ei})\right]\right\}^2 \quad \text{(Eq. 7)}$$

The corresponding PSD is given by

$$g(r) = \; g(r) = \sum_{i=1}^{k} w_i \left(\frac{\Phi}{\sqrt{2\pi}\sigma_i r}\right) exp\left[-\frac{\ln\left(\frac{r}{r_{mi}}\right)^2}{2\sigma_i^2}\right] \quad \text{(Eq. 8)}$$

where Φ is here defined as θ_s - θ_r, r_{mi} is the median pore radius calculated from h_{mi} using the Young-Laplace equation that relates pore radii to h through r_{mi} = 0.149 cm^2 / h_{mi} (Seki, 2007). Normalizing this PSD from 0 to 1 (Romano *et al.*, 2011), Eq. 8 becomes

$$f(r) = \sum_{i=1}^{k} w_i \left(\frac{1}{\sqrt{2\pi}\sigma_i}\right) exp\left[-\frac{\ln\left(\frac{r}{r_{mi}}\right)^2}{2\sigma_i^2}\right] \quad \text{(Eq. 9)}$$

2.5.2 Parametrization to quantify changes in the pore size distributions and pore volume fractions

For the analysis of the soil pore dynamics during one cropping seasons of winter wheat from Dec-15 to Aug-16 (Table 1) as published in Kreiselmeier *et al.* (2019) the retention and conductivity data was lumped together per treatment and measurement occasion. This way, reference WRC and HCC data could be parametrized to ultimately yield a reference PSD using Eqs. 8 and 9. No HI-data was used as it was not available throughout the entire cropping season (see also explanation in Section 2.2).

To group the data from HYPROP® measurements (Section 2.4.2), it was fitted with a local polynomial regression to obtain both θ-h and K-h pairs from $|h|$ 0 to 3 $\log_{10}$[cm] at intervals of 0.1. From here on, $|h|$ ($\log_{10}$[cm]) will be referred to as pF (-). The regression fitting was done in R using the *loess* (local regression) function contained in the *stats* package (R Development Core Team, 2017). This function is fitted at individual data points such that

they are weighted towards the surrounding data points. The weighting, *i.e.* the degree of smoothing, is controlled by the 'span' parameter. Here, this parameter was subjectively chosen after trial and error at a value of 0.28 which was low enough to conserve local data variations while it was large enough to smoothen out random variations. The obtained values for each 0.1-pF-interval were averaged for each treatment and measurement occasion.

Consequently, group averaged θ-h and K-h pairs were simultaneously fitted with the bimodal Kosugi and Mualem model (Eqs. 6 and 7) by applying nonlinear least-square regression in the spreadsheet software Excel (Microsoft Corporation, USA). Hereby, the following objective function was minimized

$$SSD = w_\theta \sum_{i=1}^{k} w_{\theta i} \left[\theta_i - \hat{\theta}_i\right]^2 + w_K \sum_{i=1}^{k} w_{Ki} \left[\ln K_i - \ln(\hat{K}_i)\right]^2 \quad \text{(Eq. 10)}$$

where *SSD* is the total sum of squared differences of observed versus modelled results. The weight put on both the individual water retention and K data points is determined by the factors $w_{\theta i}$ and w_{Ki}, respectively. Measured K-h data was only available in a narrow range from about pF 2 to 3 owing to limitations of the simplified evaporation method. These limitations in the determination of K are associated with too small gradients between the two tensiometers in the wetter part of the HCC yielding unreliable results (De Pue *et al.*, 2019; Schwärzel *et al.*, 2006). Therefore, more weight ($\times 10^3$) was put on θ in the objective function which is also the standard setting in the fitting software HYPROP-FIT® (METER Group Inc, Germany). The observed data is represented by θ_i and ln (K_i) and the modelled data by $\hat{\theta}_i$ and ln ($\hat{K}_i$). The model parameters σ_i, h_{mi}, θ_s, θ_r and w_i were optimized. The K_s-parameter was fixed at the group geometric mean of K_{sdab} (Table 5). Additional data points at the dry end between pF 4 to 6 were added to the WRC from dewpoint potentiometer (WP4C; METER Group Inc, Germany) measurements. Within this pF-range soil texture was assumed to be the determining factor for water retention (Blume *et al.*, 2016) and therefore little to no temporal variations were expected here. Consequently, these measurements were only done for two occasions (Mar-16 and Aug-16) with sieved (< 2 mm) and mixed samples which were ultimately averaged to yield additional data points for each treatment at pF 4, 4.18 (*i.e.* permanent wilting point), 5 and 6. These added values constrained the possible range for θ_r such that it was not necessary to fix this parameter as is frequently done (*e.g.* Bodner *et al.*, 2013; Kosugi and Hopmans, 1998). The θ_s was constrained to just below Φ, as most of the data displayed a relatively smooth change close to saturation. All parametrized reference

curves and the underlying retention and *K* data are shown in Figure A1 and Figure A2 in the appendix.

In addition to the reference PSD, the pore volume fractions occupied by different pore size classes, as defined by Greenland (1981), were calculated for every treatment and occasion. The classes were fissures (⌀ > 500 µm), transmission (⌀ 50 - 500 µm), storage (⌀ 0.5 - 50 µm), residual (⌀ 0.005 - 0.5 µm) and bonding pores (⌀ < 0.005 µm). They were obtained by calculating the area under the curve of the bimodal reference PSD considering Φ, *i.e.* $\theta_s - \theta_r$, (Eq. 8) of each treatment and occasion using the *auc* function contained in the *MESS* package (Ekstrøm, 2018) in R (R Development Core Team, 2017).

2.5.3 Parametrization to infer unsaturated hydraulic conductivity for variability analysis

For the second parametrization, variability within treatments at every occasion was the focus of the investigation. Therefore, all WRC and HCC per treatment and occasion (n = 5) were parametrized individually. This was done from May-16 to Apr-17 (Table 1) where data from HI measurements, *i.e.* K_s and K_{2cm}, were available to be used for the HCC-fitting. Fitting was done using the same bimodal models outlined in Section 2.5 in the software HYPROP-FIT® (METER Group Inc, Germany) based on the SHYPFIT 2.0 software developed by Peters and Durner (2015) which applies a shuffled complex evolution algorithm (Duan *et al.*, 1992) for global parameter estimation.

The HCC was supplemented with one additional value between pF 3.7 and 3.8 for most samples. This was done by extending the measurement range making use of the air-entry pressure of the tensiometer ceramic cup which is typically around 80 kPa (Schindler *et al.*, 2010). An option for the automatic measurement range extension is integrated in the HYPROP-FIT® software which was used. Again, all parameters except K_s were optimized.

For the analysis of variability in the HCC, values at pF 2.0 ($k_{pF2.0}$), 2.5 ($k_{pF2.5}$) and 3.0 ($k_{pF3.0}$) were extracted from the parametrized model curves. Within this pF-range, most observed data was available in the HCC and a good fit of the data was expected here.

For correlation and regression analysis between porosities and conductivities (see also Objective 2) in Section 1.5), macro- (Φ_{mac}) and mesoporosities (Φ_{mes}) were derived from the retention data. Schwärzel et al. (2011) defined Φ_{mac} and Φ_{mes} as θ, i.e. porosity, at h > -4 cm and -4 > h > -12 cm, respectively. Following this definition, θ was extracted at the respective h by fitting the θ-h data pairs from transient evaporation experiments with a local polynomial regression in R as described in Section 2.5.2.

2.6 Capacitive soil physical quality indicators

Soil physical quality, as assessed by various indicators, can provide information on the state of a soil regarding crop production and soil degradation resulting in 'optimal' indicator ranges (A.R. Dexter, 2004; A.R Dexter, 2004; Reynolds *et al.*, 2009, 2002). Common (capacitive) indicators are relative field capacity (RFC), air capacity (AC) and available water capacity, macroporosity as well as ρ_b for which Reynolds *et al.* (2009) defined 'optimal' ranges based on a literature review (Table 3). Castellini *et al.* (2019) based their study on the same values. They found, using correlation and multivariate analysis, that it is possible to discriminate between minimum and NT treatments on a clay soil using the SPQ indicator RFC. Their analysis showed strong correlations between RFC and AC as well as AC and macroporosity. Based on their results and those of Cullotta *et al.* (2016), they arrived at an optimal AC-range of $0.10 \geq AC \geq 0.14$ cm^3 cm^{-3}. Due to its formulation, RFC implicitly also accounts for available water capacity. The authors concluded that for an SQP-assessment on fine-textured agricultural soils, it is sufficient to calculate RFC and AC as key indicators. This requires only two points of the WRC, *i.e.* θ_s at saturation (h = 0 cm) and at field capacity (h = -100 cm). Therefore, both RFC and AC were calculated from measured WRC data obtained from the smoothing fit of original HYPROP®-data, as outlined in Section 2.5.2, to allow for a statistical analysis looking at both temporal and treatment effects. This was done for all occasions from Dec-15 to Apr-17. The definition of both RFC and AC is given in Table 3. Another used indicator was ρ_b determined as outlined in Section 2.4.2.

Table 3 Definition and optimal range of soil physical quality indicators relative field capacity (RFC), air capacity (AC) and bulk density (ρ_b) as defined by a literature review of Reynolds *et al.* (2009). The optimal range of AC is based on more recent findings of Castellini *et al.* (2019).

Indicator	Definition	Optimal range
RFC (-)	$1 - (AC/\theta_s)$	$0.6 \leq RFC \leq 0.7$
AC (cm^3 cm^{-3})	$\theta_s - \theta_{FC}$	$0.10 \geq AC \geq 0.14$
ρ_b (g cm^{-3})		$0.9 \leq \rho_b \leq 1.2$

θ_s saturated water content; θ_m water content at h = -10cm; θ_{FC} water content at field capacity (h = -100 cm)

2.7 Relationship between imaged pore metrics and field near-saturated hydraulic conductivity

In spring 2018, a field campaign was done on CT and NT with the aim to relate (near-) saturated hydraulic K from HI measurements (K_s and K_{2cm}) to pore metrics such as critical and average pore diameter, macroporosity, pore connectivity and average pore diameter. These

pore metrics were obtained by X-ray μCT imaging on undisturbed soil cores (⌀: 10 cm, h: 10 cm; n = 13) at UFZ Halle which were taken at least 48 h after the infiltration procedure. The soil cores were taken at a depth of 10 - 20 cm so as to avoid disturbances from the previous sugar beet harvest in autumn 2017. At the time of sampling, winter wheat was grown. In addition to field measurements, a disk infiltrometer was used to measure infiltration directly on the soil cores and derived pore networks were used for a direct simulation (Stokes-Brinkmann solver) of water flow through the samples. For the lab measurements, the soil cores were saturated for 24 h from bottom to top. They were then transferred to a sand bed and h was adjusted according to the h set at the disk infiltrometer. For more details on the experimental design the reader is referred to Schlüter *et al.* (in press). Here, the focus will be put on the HI measurements as this technique was also used for the monitoring of the temporal variation in this dissertation.

2.8 Statistical analysis

All statistical analyses were performed in R 3.4.2. (R Development Core Team, 2017). Hydraulic conductivity data from KSAT® (K_{slab}), HI (K_s, K_{2cm}) and HYPROP® ($k_{pF2.0}$, $k_{pF2.5}$, $k_{pF3.0}$) measurements was visually assessed with normal Q-Q plots and consequently transformed with a logarithm to the base e (ln) prior to significance testing. This is a commonly observed statistical distribution for hydraulic conductivities (*e.g.* Bagarello *et al.*, 2014; Lee *et al.*, 1985; Reynolds *et al.*, 2000). Given the lognormal distribution, geometric means (GM) and geometric coefficients of variation (GCV) were calculated for all hydraulic conductivities according to Lee *et al.* (1985):

$$GM = \exp(AM) \quad \text{(Eq. 11)}$$

$$GCV = 100[exp(SD^2) - 1]^{0.5} \quad \text{(Eq. 12)}$$

where AM is the arithmetic mean and SD the standard deviation of the ln-transformed data.

One-way analyses of variance (ANOVA) were done on the quantities K_{slab}, K_s, K_{2cm}, $k_{pF2.0}$, $k_{pF2.5}$, $k_{pF3.0}$, RFC, AC, ρ_b, as well as SOC and N stocks to evaluate both the influence of the treatment (*TREAT*) and sampling occasion (*TIME*) on the respective property. Following significant one-way ANOVA test results, multiple comparisons were done using the least significant differences (LSD) test (Webster, 2007) included in the *emmeans* (estimated marginal

means) package in R (Lenth *et al.*, 2018). The significance level for all tests was defined to be $p < 0.05$. From here on, 'significant' results refer to a $p < 0.05$ if not stated otherwise.

Strengths and directions of relationships between ln-transformed K (K_{slab}, K_s, K_{-2cm}, $k_{pF2.0}$, $k_{pF2.5}$, $k_{pF3.0}$) and other recorded soil properties (SOC, |BP|, ϱ_b, Φ_{mac}, Φ_{mes}) were assessed by means of a Spearman rank correlation coefficient (ϱ). Only significant correlations are presented. Consequently, multiple linear regression with grouped treatment values was applied to look for factors explaining the observed variability in K.

3 Results

3.1 Rainfall patterns

In Dec-15, 68 days after last sowing and prior to the first sampling, a total of 171 mm effective rainfall (> 10 mm d^{-1}; Moret and Arrúe, 2007) was recorded (Figure 2). Several days had comparably high effective rainfall (35.8, 32.6, 30.2 and 59.8 mm d^{-1}). The event closest to the sampling date happened eight days before with a maximum intensity of 22.8 mm h^{-1}. After 164 days in Mar-16, 201 mm of effective rainfall had accumulated with the most intense event 20 days before sampling at a maximum intensity of 12.4 mm h^{-1}. During the growing season in May-16 and Jun-16, 242 and 269 days after sowing, respectively, 39 and 35 mm effective rainfall were recorded, respectively. Highest intensities were 10.4 and 4.2 mm h^{-1} seven and nine days before sampling, respectively. An example of a heavy rainfall event with a significant visible surface runoff on the field during the May-16 campaign is shown in Figure 6. That day, a total of 15.8 mm was recorded with a maximum intensity of only 5 mm h^{-1}. Directly after harvest, little effective rainfall was observed (10.2 mm) with a low maximum intensity of 0.8 mm h^{-1} eleven days before the field campaign. Only two days before the Sep-19 campaign, 33.6 mm d^{-1} effective rainfall came down with a maximum intensity of 9.8 mm h^{-1}.

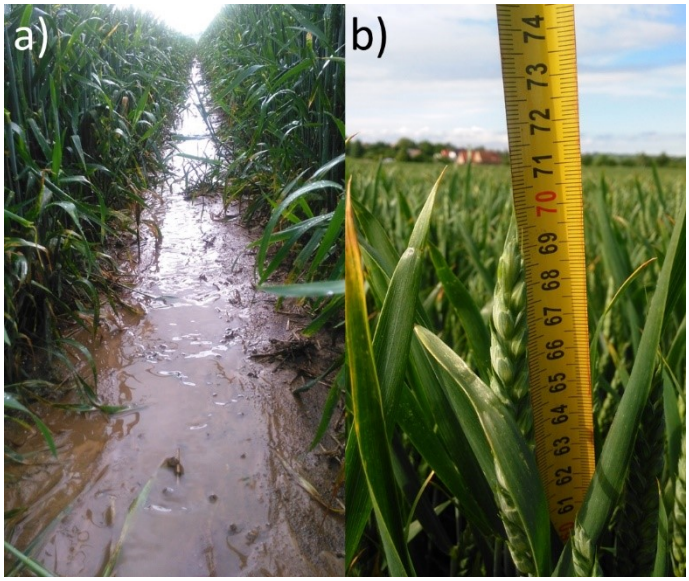

Figure 6 a) Water running down wheel tracks on 3 June 2016 after a heavy rainfall event. Measurements on all treatments were already completed shortly before. b) Winter wheat around the flowering phase end of May 2016.

3.2 Field (near-) saturated hydraulic conductivity

The two-line regression model described (near-) saturated *K* well with low root mean square errors (RMSE) and $R^2 > 0.9$ (Table 4). Overall, GMs of K_s and K_{2cm} were in the order RT > CT > NT which was only significant between RT and NT. The strength of temporal variation differed between treatments. On CT and RT, K_s increased consistently throughout the growing season from May-16 to after the harvest in Aug-16 by a factor of 2 and 6.6, respectively. Changes on NT throughout this time were negligible with averages varying by a maximum factor of 1.6. After stubble breaking with a cultivator in September, conductivities increased on CT while on RT they were reduced by more than 50 % on average coming from an already high GM of 2092 cm d^{-1}. Seedbed preparation on NT was the only occasion where K_s was strongly increased (factor of 2.5) compared to the previous sampling.

The GCV of K_s as an indicator for spatial variability of the individual occasions ranged from 23 to 184 % on CT, 35 to 177 % on RT and 19 to 127 % on NT (Figure 8). In May-16 and Apr-17, GCVs exceeded averages on CT by 42 and 80 %, respectively, which indicates a noteworthy change with time. For RT, this was only true for K_s in May-16 exceeding the overall GCV by 60 %. On NT, there were no mentionable differences between months. Geometric coefficients of variation of all treatments were well within a range commonly reported for (near-) saturated *K* of arable soils based on TI measurements (*e.g.* Deb and Shukla, 2012; Keskinen *et al.*, 2019; Reynolds *et al.*, 2000; Schwen *et al.*, 2011b).

Table 4 Geometric means of the hydraulic conductivity obtained from hood infiltration data fitted with the two-line regression model at saturation (K_s) and a pressure head of -2 cm (K_{2cm}) as well as from transient evaporation experiments at pressure heads of -100 ($k_{pF2.0}$), -316 ($k_{pF2.5}$) and -1000 cm ($k_{pF3.0}$). RMSE and R^2 were calculated between results obtained by piecewise linear interpolation and the two-line regression model.

Treat-ment	Date	K_s		K_{2cm}		RMSE	R^2	$k_{pF2.0}$		$k_{pF2.5}$		$k_{pF3.0}$	
		cm d^{-1}				ln[cm d^{-1}]		cm d^{-1}					
CT	May-16	459	Aa	204	Aa	0.0272	0.999	0.168	Aab	0.023	Aab	0.002	Aa
	Jun-16	689	Aa	431	Aabc	0.0097	0.999	0.119	Aac	0.017	Aabc	0.001	Aa
	Aug-16	910	Aab	589	Abc	0.0147	0.998	0.069	Ac	0.012	Ac	0.001	Aa
	Sep-16	1890	Ab	1106	Ab	0.0296	0.996	0.067	Ac	0.015	Aac	0.001	Aa
	Apr-17	436	Aa	217	Aac	0.0071	1.000	0.294	Ab	0.030	Ab	0.002	Aa
	overall	750	AB	416	AB			0.122	A	0.018	A	0.001	A
RT	May-16	315	Aa	116	Aa	0.0595	0.997	0.056	Ba	0.011	Ba	0.001	Aa
	Jun-16	1669	Bb	1089	Bb	0.0188	0.998	0.074	Aa	0.009	Aa	0.001	Aa
	Aug-16	2092	Bb	1023	Ab	0.0526	0.991	0.070	Aa	0.008	Ba	0.001	Ba
	Sep-16	1090	Ab	610	Abc	0.0242	0.998	0.058	Aa	0.012	Aa	0.001	Ba
	Apr-17	944	Ab	440	Ac	0.0302	0.997	0.077	Ba	0.010	Ba	0.001	Aa
	overall	1025	A	511	A			0.066	B	0.010	B	0.001	A
NT	May-16	511	Aa	291	Aa	0.0189	0.999	0.072	Ba	0.013	Ba	0.001	Aab
	Jun-16	536	Aa	263	Aa	0.0808	0.972	0.079	Aa	0.014	Aa	0.001	Aac
	Aug-16	333	Ca	224	Ba	0.0644	0.976	0.087	Aa	0.013	Aa	0.001	Aac
	Sep-16	355	Ba	242	Ba	0.0086	1.000	0.061	Aa	0.010	Aa	0.001	Abc
	Apr-17	890	Aa	558	Aa	0.0039	1.000	0.045	Ba	0.011	Ba	0.002	Ab
	overall	492	B	297	B			0.067	B	0.012	B	0.001	A

CT: conventional tillage; RT: reduced mulch tillage; NT: no tillage

RMSE: root mean square error; R^2: coefficient of determination

Same lowercase letters in a column indicate no significant differences within the same treatment ($p < 0.05$)

Same uppercase letters in a column indicate no significant differences between treatments on the same date ($p < 0.05$)

3.3 Threshold pore radius

Due to exceptional high spatial variability there was no significant difference in the overall r_{BP} between treatments with 0.40, 0.39 and 0.35 mm on CT, RT and NT, respectively (Figure 7). There were also no significant differences with time. In May-16, r_{BP} was notably higher on CT and so was the variance of observed values. Stubble breaking prior to Sep-16 did not affect observed r_{BP}. Seedbed preparation prior to the Apr-17 sampling seemed to have led to a reduction in r_{BP} on tilled plots, especially on CT, with low variability on all treatments. On NT, r_{BP} increased compared to Sep-16.

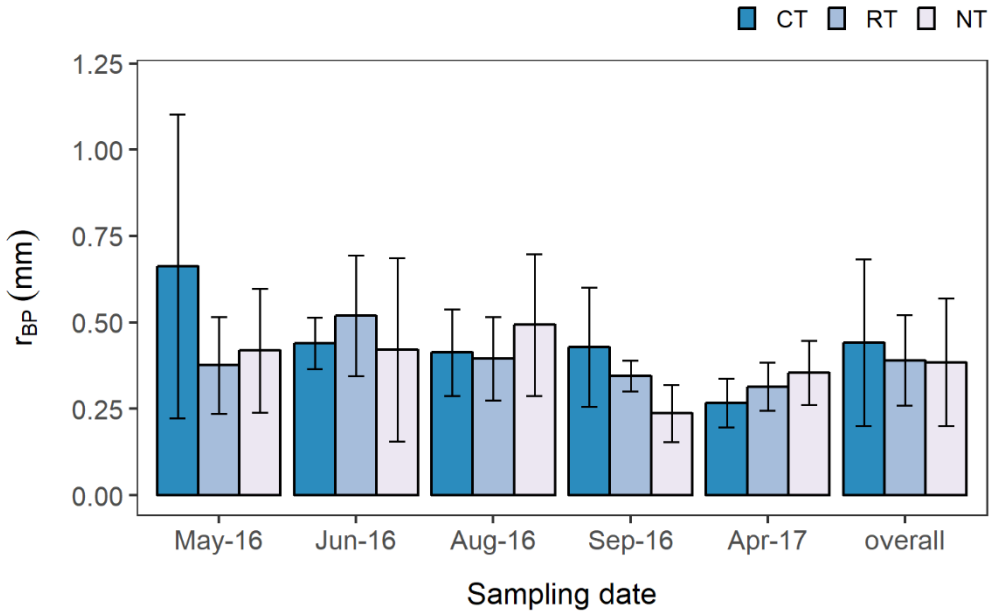

Figure 7 Mean threshold pore radius (r_{BP}) at the bubbling pressure (BP) as introduced by Patra *et al.* (2019). Treatments are conventional tillage (CT) with a moldboard plow, reduced mulch tillage (RT) with a cultivator and no tillage (NT) with direct sowing. Error bars denote one standard deviation from the mean (n = 5).

3.4 Laboratory saturated hydraulic conductivity

The falling head method proved to yield highly variable results between observation times. Overall, K_{slab} was in the order CT (GM 594 cm d^{-1}) > RT (GM 323 cm d^{-1}) > NT (GM 287 cm d^{-1}) (not significant) with high GCVs of 260, 425 and 373 %, respectively (Table 5). Only in Dec-15, the GMs of CT and RT were significantly larger than on NT. Statistically relevant temporal variations were only observed on tilled plots. On CT, a strong reduction was recorded between Sep-16 after stubble breaking and Apr-17 after seedbed preparation and sugar beet sowing. On RT, a significant reduction during winter from Dec-15 to Mar-16 was observed. On all treatments, K_{slab} rose from shortly before to after the harvest in Aug-16 by almost an order of magnitude. Variability was extremely high on some occasions with maximum GCVs of 1808, 601 and 1354% on CT, RT and NT, respectively. This can be attributed to a relatively low number of soil cores taken (n = 5) that was occasionally even reduced when samples had to be excluded because they did not match the criteria mentioned in Section 2.4.1 due to disturbance of the soil structure or large macropores.

Table 5 Geometric means (GM; (Eq. 11) and geometric coefficient of variation (GCV; (Eq. 12) of lab saturated hydraulic conductivity (K_{slab}) obtained from falling head experiments on undisturbed soil cores (250 cm^{-3}).

Date	Statistic	CT		RT		NT	
Dec-15	*GM (cm d⁻¹)*	1708	Aa	1557	Aa	302	Ba
	GCV (%)	58		61		420	
Mar-16	*GM (cm d⁻¹)*	505	Aa	109	Ab	549	Aa
	GCV (%)	35		790		27	
May-16	*GM (cm d⁻¹)*	535	Aa	330	Aab	256	Aa
	GCV (%)	155		75		1287	
Jun-16	*GM (cm d⁻¹)*	420	Aab	77	Ab	205	Aa
	GCV (%)	601		1808		1354	
Aug-16	*GM (cm d⁻¹)*	1236	Aa	2021	Aa	1248	Aa
	GCV (%)	88		259		58	
Sep-16	*GM (cm d⁻¹)*	1207	Aa	186	Ab	283	Aa
	GCV (%)	206		96		128	
Apr-17	*GM (cm d⁻¹)*	89	Ab	161	Ab	70	Aa
	GCV (%)	352		1110		418	
overall	*GM (cm d⁻¹)*	594	A	323	A	287	A
	GCV (%)	260		425		373	

CT	Conventional tillage with a moldboard plow
RT	Reduced mulch tillage with a cultivator
NT	No tillage with direct sowing

Same upper-and lowercase letters indicate no significant differences ($p < 0.05$) between and within treatments, respectively.

3.5 Unsaturated hydraulic conductivity

Overall, $k_{pF2.0}$ and $k_{pF2.5}$ obtained from the parametrization of the HCC data from transient evaporation experiments was in the order CT > RT ≈ NT where CT was significantly different from the other two (Table 4). Differences between treatments became less pronounced towards drier soil moisture states. The only significant change of $k_{pF2.0}$ of two consecutive occasions happened on CT from Sep-16 to Apr-17 with an increase. However, this was also the longest period between two observations which prevents a sensical interpretation.

Considering all occasions, variability expressed in the GCV was lower towards drier soil moisture states from $k_{pF2.0}$ to $k_{pF3.0}$ compared to field measurements on all treatments (Figure 8). Looking at individual observation periods, GCVs varied more on tilled plots, *e.g.* for $k_{pF2.0}$, where GCVs were particularly large on CT and RT following the stubble breaking in

Sep-16 compared to the previous post-harvest observation in Aug-16. Here, average GCVs of 89 and 70 % were exceeded by 85 and 55 % on CT and RT, respectively. On the untilled soil, differences in GCVs between occasions were negligible, *i.e.* they were close to the overall GCV.

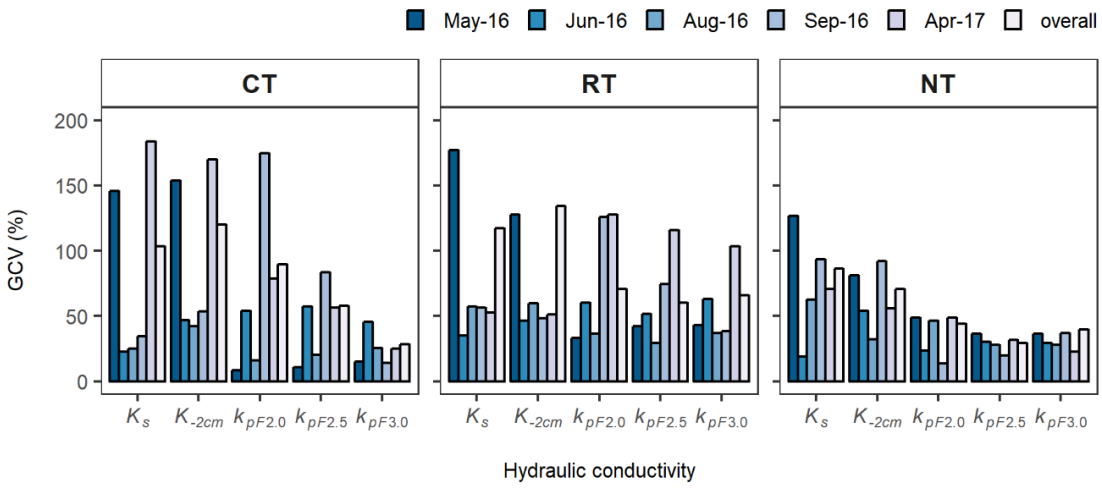

Figure 8 Geometric coefficients of variation (GCV; (Eq. 12) for hydraulic conductivity from field measurements at saturation (K_s) and a supply pressure head of -2 cm (K_{-2cm}) as well as from parametrized data from HYPROP® measurements at pressure heads of -100 cm ($k_{pF2.0}$), -316 ($k_{pF2.5}$) and -1000 cm ($k_{pF3.0}$).

3.6 Soil pore size distributions and pore volume fractions over one cropping season

The reference WRC and PSD are presented in their normalized form (Figure 9) due to their higher effectiveness in highlighting differences between textural and structural modes compared to the volumetric frequency. When considering Φ, *i.e.* θ_s - θ_r, the textural domain tended to overshadow the structural domain, making it impractical for a visual analysis of differences between treatments and variations with time as curves appeared unimodal (Figure A3).

Bimodal reference WRC and PSD curves differed distinctly between tilled (CT, RT) and untilled (NT) soil for most of the cropping period observed from Dec-15 to Aug-16 (Figure 9). While for CT and RT there were two clearly distinguishable modes for the majority of the season, NT soil tended towards a more unimodal distribution of pores with only a weakly expressed structural mode. The boundary between the two modes was somewhere around 30 to 40 µm. The representative mean pore radius of the structural mode (r_{m1}) indicating its location on the x-axis in Figure 9 was comparably high on all three treatments in

Dec-15 and Mar-16 (Table 6). During this time, the width of the mode, as expressed in the standard deviation of the lognormal PSD (σ_1), was largest for NT followed by RT in Dec-15 and CT in Mar-16. In May-16, the structural mode reverted to similar values as those of the mean pore radius of the textural mode (r_{m2}) effectively yielding a unimodal PSD like that of NT, albeit with an overall wider distribution. On tilled soil this was partly reversed towards the end of the season shortly before and after the harvest. Given that r_{m1} is related to Φ near saturation, it is not surprising that there was a positive trend with θ_s which was highest for all treatments in Dec-15, decreased towards May-16 and then increased again shortly before and after the harvest. Root mean square errors did not vary notably for both the WRC and HCC.

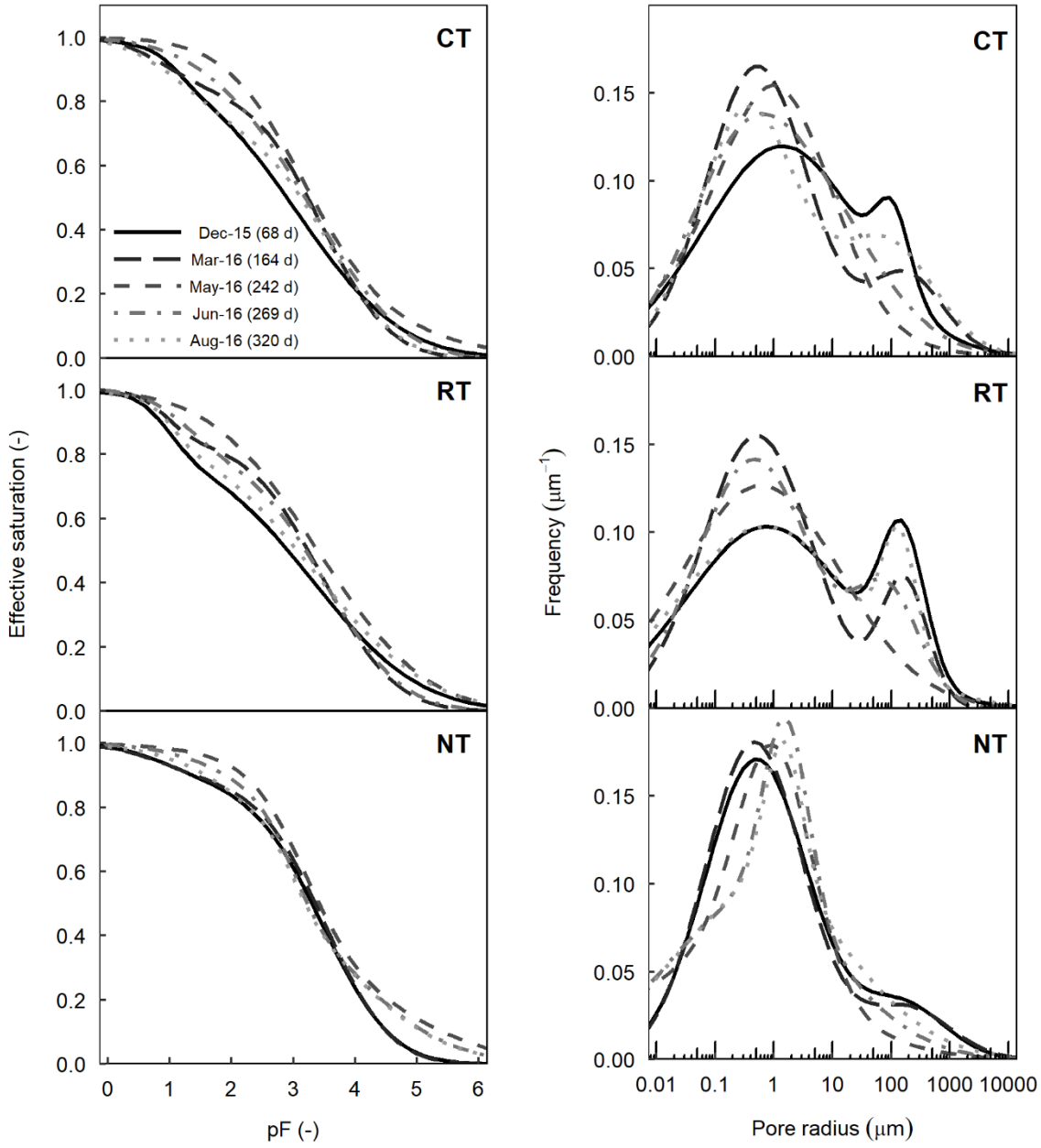

Figure 9 Temporal evolution of the normalized reference water retention (left) and pore size distribution curves calculated with Eqs. 6 and 9, respectively, for the treatments conventional tillage (CT), reduced mulch tillage (RT) and no tillage (NT). Lines represent different dates with days passed since last sowing on 1 October 2015 in brackets.

Table 6 Reference curve parameters residual (θ_r) and saturated (θ_s) water content, pressure heads at effective saturation $S_{ei}(h_{mi}) = 0.5$ for both the structural (h_{m1}) and textural (h_{m2}) domains, their respective standard deviations of the lognormal pore radius distribution σ_1 and σ_2, and the weighting factor for the structural domain (w_1). The weighting factor of the textural domain (w_2) can be obtained by 1-w_1. Saturated hydraulic conductivity (K_s) is presented as geometric mean of laboratory falling head measurements. Goodness of fit between observed and modeled values is expressed by the root mean square error (RMSE) for both the water retention and hydraulic conductivity characteristic. Time since last sowing refers to days passed since 1 October 2015.

	Date	Time since last sowing	θ_r	θ_s	h_{m1}	h_{m2}	r_{m1}	r_{m2}	σ_1	σ_2	w_1	K_s	RMSE θ	RMSE $K(h)$
		d	$cm^3\ cm^{-3}$		cm		µm		-	-	-	$cm\ d^{-1}$	$cm^3\ cm^{-3}$	ln [$cm\ d^{-1}$]
CT	Dec-15	68	0.0241	0.4582	14	1068	107.8	1.4	0.68	3.08	0.07	1708	0.0025	0.0028
	Mar-16	164	0.0326	0.4487	8	2866	180.5	0.5	1.47	2.00	0.17	505	0.0033	0.0180
	May-16	242	0.0118	0.4078	1304	8732	1.1	0.2	2.13	3.80	0.65	535	0.0018	0.0377
	Jun-16	269	0.0273	0.4094	384	6826	3.9	0.2	2.68	2.16	0.56	420	0.0034	0.0776
	Aug-16	320	0.0317	0.4444	19	4098	79.5	0.4	1.89	1.95	0.31	1236	0.0042	0.0194
RT	Dec-15	68	0.0174	0.4842	9	1938	156.9	0.8	0.87	3.18	0.18	1557	0.0033	0.0293
	Mar-16	164	0.0345	0.4449	9	2905	166.2	0.5	0.91	2.15	0.16	109	0.0025	0.0054
	May-16	242	0.0076	0.4253	2434	2654	0.6	0.6	3.12	3.29	0.83	330	0.0061	0.0302
	Jun-16	269	0.0329	0.4289	17	3225	87.2	0.5	1.27	2.26	0.20	77	0.0025	0.0075
	Aug-16	320	0.0108	0.4569	11	2085	137.9	0.7	0.67	3.38	0.12	2021	0.0035	0.0117
NT	Dec-15	68	0.0368	0.4605	10	2948	150.4	0.5	1.69	2.02	0.13	302	0.0039	0.0088
	Mar-16	164	0.0390	0.4490	8	3218	180.4	0.5	1.72	1.93	0.13	549	0.0034	0.0089
	May-16	242	0.0057	0.4235	1469	10000	1.0	0.1	1.46	3.76	0.48	256	0.0018	0.0150
	Jun-16	269	0.0146	0.4403	927	3333	1.6	0.4	0.88	3.33	0.25	205	0.0016	0.0082
	Aug-16	320	0.0146	0.4495	1015	2236	1.5	0.7	0.76	3.44	0.16	1248	0.0014	0.0139

CT Conventional tillage with a moldboard plow

RT Reduced mulch tillage with a cultivator

NT No tillage with direct sowing

Figure 10 shows the volume fractions of individual pore size classes derived from the area under the PSD considering Φ (Eq. 8). The volume fractions reflect the temporal evolution of the PSD shown in Figure 9, especially that of the structural mode, with decreases in transmission pores (⌀ 50 - 500 µm) from Dec-15 to May-16 and a consequent (partial) restoration towards the end of the growing period. While this trend could also be identified for NT, the pore volume fraction of transmission pores was much lower than on tilled soil. The same was true for fissures (⌀ < 0.005 µm). On the other hand, the pore volume fraction taken up by storage pores (⌀ 0.5 - 50 µm) was higher on untilled soil, pointing towards an improved water retention in the absence of annual tillage and consequent soil structural disturbances. Fissures and transmission porosities showed a moderate positive linear trend with pooled group GMs of K_{slab} (n = 15; R^2 = 0.30 at $p < 0.05$ and R^2 = 0.53 at $p < 0.01$, respectively) which highlights the importance of those size classes for infiltration processes. The correlation is not entirely surprising as the pore volume fractions were derived from models parametrized with the group GMs of K_{slab}. Nevertheless, when differentiating between treatments, the trend between transmission pores and K_{slab} was especially pronounced on CT (n = 5; R^2 = 0.87 at $p < 0.05$) while for RT and NT no significant relationship could be identified. Porosities of other size classes did not yield any notable trends with K_{slab}.

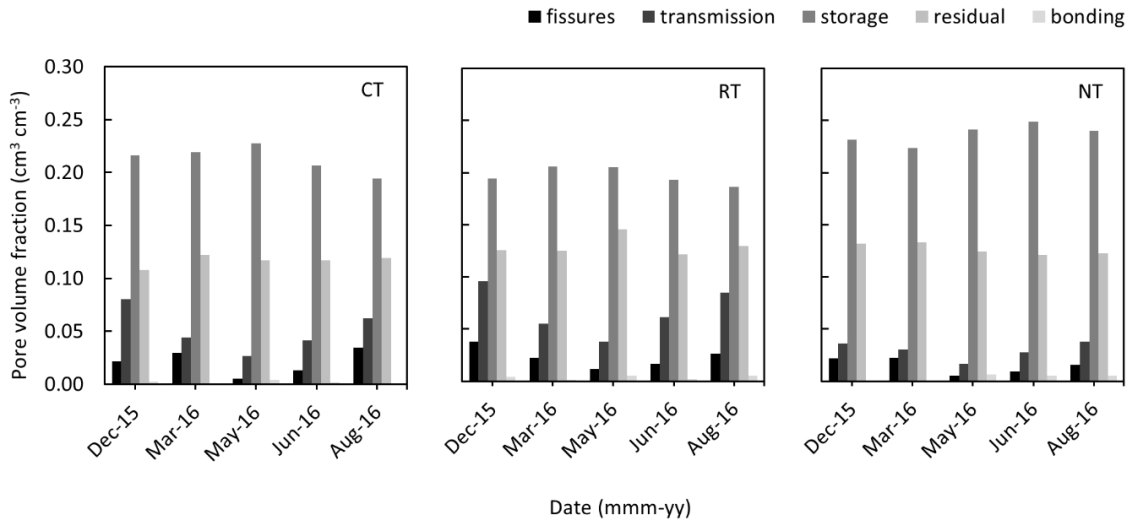

Figure 10 Pore volume fractions derived from the area under the curve of bimodal pore size distributions (Eq. 8). The classes were fissures (⌀ > 500 µm), transmission (⌀ 50 - 500 µm), storage (⌀ 0.5 - 50 µm), residual (⌀ 0.005 - 0.5 µm) and bonding pores (⌀ < 0.005 µm).

3.7 Capacitive soil physical quality indicators

The average RFC was outside of the optimum range for almost all occasions on all three treatments (Figure 11). Overall, the order was NT (0.889) > CT (0.798) > RT (0.788) where RFC under NT was significantly higher compared to the other two with a consistently narrower range for most of the times. Values larger 0.7 indicate an aeration deficit. Only under RT in the beginning of the cropping seasons some measurements were within a range considered positive for crop growth. During winter and until Jun-16, RFCs increased on all treatments (significant for CT and NT) whereas shortly before and after harvest an improvement could be observed which was most pronounced on RT.

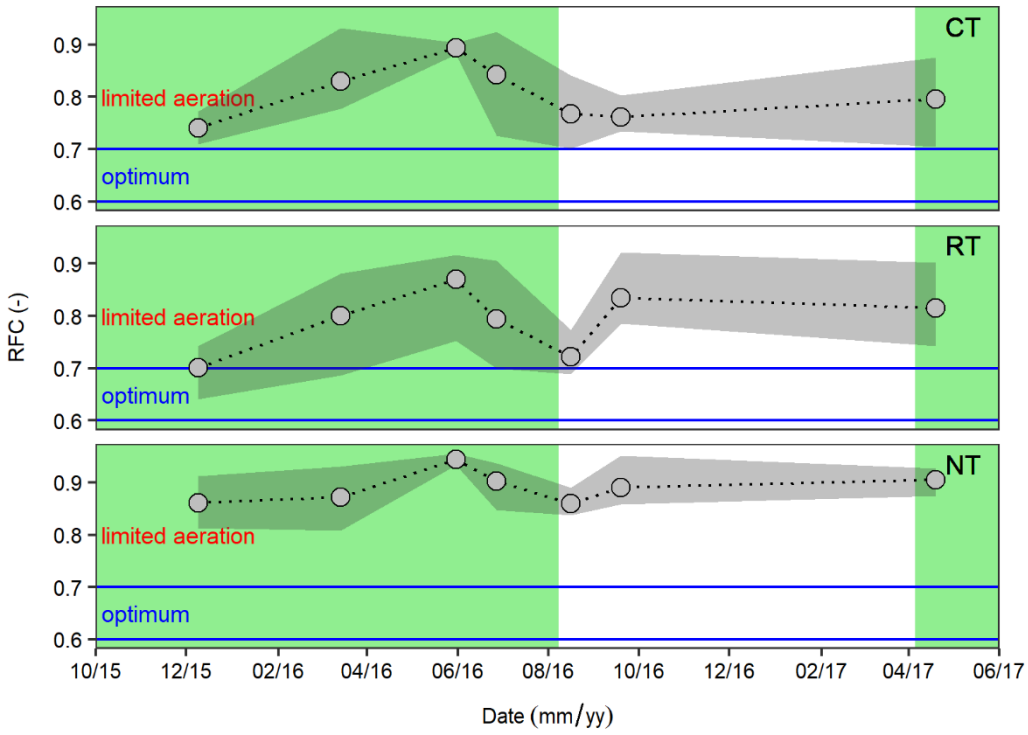

Figure 11 Temporal evolution of relative field capacity (RFC) under conventional tillage (CT), reduced mulch tillage (RT) and no tillage (NT). Dots represent group arithmetic means and ribbon marks range (min-max) of measured values. Green background marks cropping period defined as the time from sowing to harvest. Blue lines mark optimum range while the area above is considered a soil with limited aeration. Definition according to Reynolds *et al.* (2009).

Similar as RFCs, ACs of all treatments were within a suboptimal range for most of the times (Figure 12). The overall order was RT (0.096 cm^3 cm^{-3}) > CT (0.088 cm^3 cm^{-3}) > NT (0.049 cm^3 cm^{-3}) again significant between NT and CT/RT. Only tilled soils reached intermediate levels with highest values in Dec-15 where RT even reached an optimum of 0.143 cm^3 cm^{-3}. Towards Jun-16 a decrease in AC was observed on all treatments. For CT and RT, AC then rose back to intermediate levels shortly after harvest. Following stubble

breaking, AC on RT decreased significantly. This was, however, not the case under CT where stubble breaking had no evident impact.

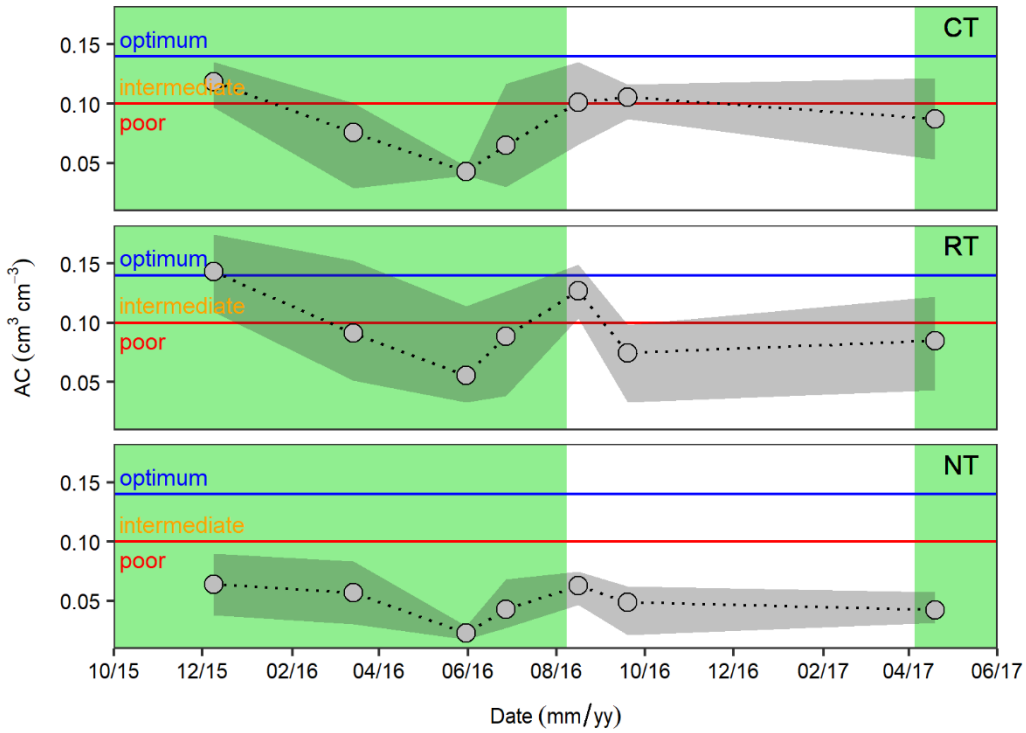

Figure 12 Temporal evolution of air capacity (AC) under conventional tillage (CT), reduced mulch tillage (RT) and no tillage (NT). Dots represent group arithmetic means and ribbon marks range (min-max) of measured values. Green background marks cropping period defined as the time from sowing to harvest. The area above the blue line marks the optimum range followed by an intermediate (orange) and poor (red) aeration range. Definitions according to Reynolds *et al.* (2009) and Castellini *et al.* (2019).

3.8 Correlation and linear regression of hydraulic conductivity with other soil properties

Spearman's ϱ indicated distinct effects of the soil tillage treatment on the relationships between hydraulic conductivities and the other selected soil properties (Figure 13). Both plots under annual tillage showed moderate negative correlations of K_s and K_{2cm} with ϱ_b. Given the strong negative correlation between ϱ_b and Φ_{mac} and Φ_{mes} it is not surprising that HI-derived conductivities were positively correlated with those properties as well. An increase in SOC occurred alongside conductivities measured with the HI on CT. The BP did not yield any significant relationships. On NT, none of the investigated properties was relevant for the interpretation of field-derived conductivities.

For unsaturated K obtained from transient evaporation measurements, the picture was less clear. On the conventionally-tilled field both Φ_{mac} and Φ_{mes} showed a moderated negative relationship with $k_{pF2.0}$, $k_{pF2.5}$ and $k_{pF3.0}$. Under mulch tillage this was only the case for $k_{pF3.0}$

while under the untilled soil no such relationship was observed. A moderate negative correlation was only found between ρ_b and $k_{pF2.0}$ on RT and NT.

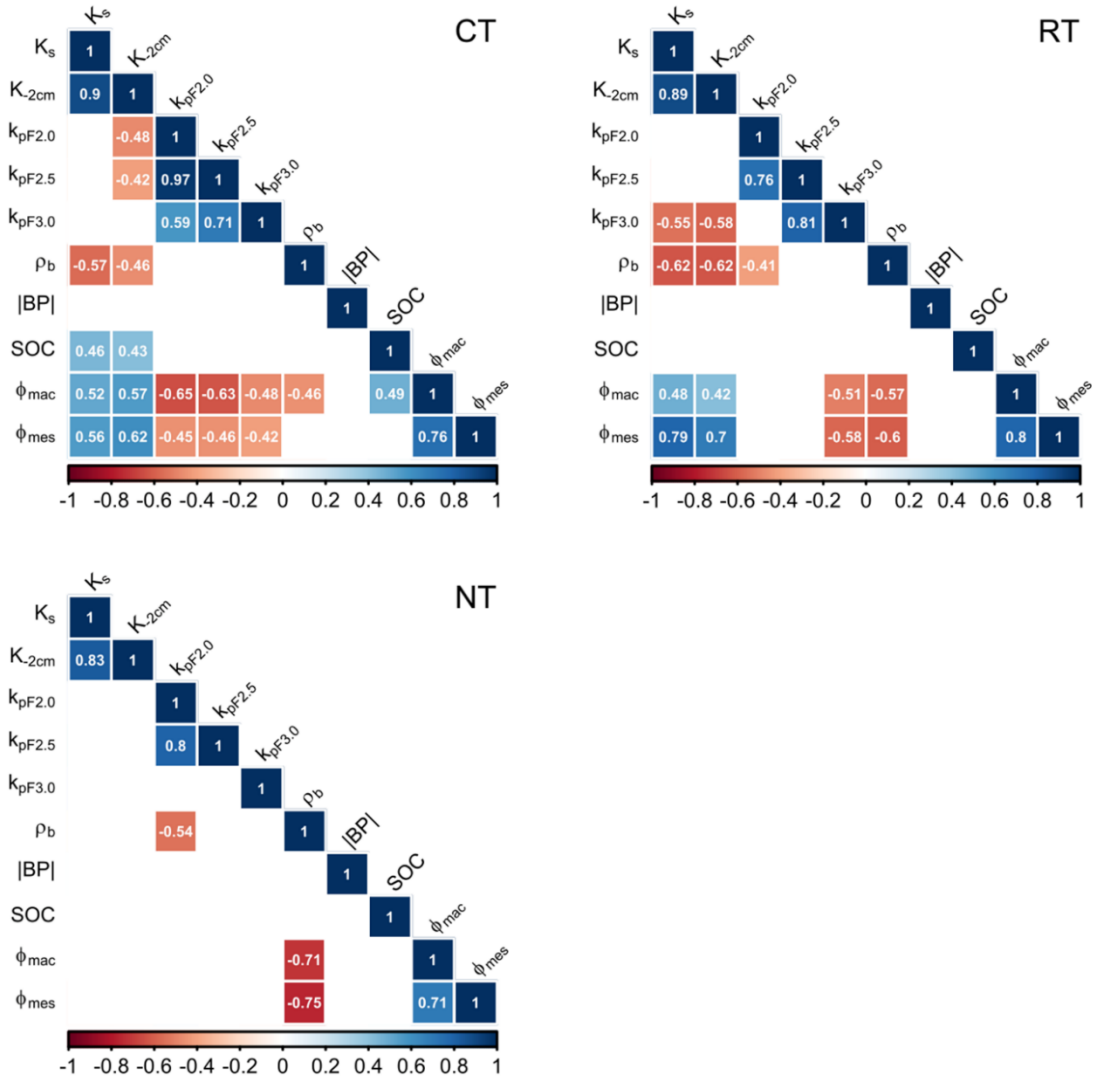

Figure 13 Correlation matrix displaying Spearman's rank correlation coefficient ϱ at $p < 0.05$ between ln-transformed hydraulic conductivities from hood infiltrometer measurements at saturation (K_s) and a supply pressure head (h) of -2 cm (K_{2cm}) as well as from HYPROP measurements at h = -100 ($k_{pF2.0}$), -316 ($k_{pF2.5}$) and -1000 cm ($k_{pF3.0}$) and bulk density (ρ_b), the absolute bubbling pressure (|BP|), soil organic C concentrations (SOC), macro- (Φ_{mac}) and mesoporosity (Φ_{mes}). Treatments are conventional tillage (CT), reduced mulch tillage (RT) and no tillage (NT).

The multiple linear regression of the properties already investigated in the Spearman rank correlation analysis was not constructive for (near-) saturated K on NT. As could be expected from the results presented in Figure 13, the tilled plots were more suitable for this undertaking. Given the multicollinearity between ρ_b and Φ_{mac} and Φ_{mes}, it was decided to drop ρ_b and instead add both porosities ($\Phi_{mac+mes}$) for further analysis as they anyway had a strong positive correlation with a ϱ of 0.76 and 0.80 ($p < 0.05$) under CT and RT, respectively (Figure 13). For the |BP|, no positive correlation was identified with K_s and K_{2cm}. Nevertheless, it

proved to be a good predictor on CT explaining 61 % of the variance (adjusted R^2) in K_s together with $\Phi_{mac+mes}$ with $p < 0.001$ for both predictors (Table 7). Following these results, higher K_s-values can be expected with decreasing |BP| and increasing $\Phi_{mac+mes}$. On the RT plot, $\Phi_{mac+mes}$ alone only explained 49 % of the variance ($p < 0.001$) where after removal of a strongly influential outlier (Cook's distance > 0.5) |BP| became insignificant as a predictor. For K_{2cm}, the response of the predictors also used for the regression with K_s was similar for both CT and RT. Overall, they explained less of the observed variance. Therefore, they are not shown here to avoid redundancies.

There was a negative or positive relationship between $k_{pF2.0}$ and ϱ_b or Φ_{mac}, respectively. However, those properties only explained 41, 21 and 29 % of the observed variation on CT, RT and NT, respectively (Table 8). The relation with both predictors was inverse. An increase in ϱ_b would mean a reduction in $k_{pF2.0}$. An increase in Φ_{mac} on the other hand came along with a reduction in $k_{pF2.0}$. None of the other predictors were meaningful for both $k_{pF2.5}$ and $k_{pF3.0}$.

Table 7 Coefficients and standard error (in brackets) of the (multiple) linear regression on ln-transformed saturated hydraulic conductivity versus the absolute bubbling pressure (|BP|) and the sum of macroporosity and mesoporosity ($\Phi_{mac+mes}$) for conventional tillage (CT) and $\Phi_{mac+mes}$ for reduced mulch tillage (RT) with n = 25 and 24, respectively.

	CT	**RT**
|BP|	-0.23*** (0.05)	
$\Phi_{mac+mes}$	25.03*** (6.07)	27.85*** (5.81)
adj. R^2	0.61	0.49
p	< 0.001	< 0.001

Table 8 Coefficients and standard error (in brackets) of the linear regression on ln-transformed hydraulic conductivity at h = -100 cm ($k_{pF2.0}$) versus macroporosity (Φ_{mac}) for conventional tillage (CT) with n = 25 and bulk density (ρ_b) on reduced mulch tillage (RT) and no tillage (NT) with n = 24 and n = 25, respectively.

	CT	RT	NT
ρ_b		-3.18* (1.20)	-3.52** (1.10)
Φ_{mac}	-92.34*** (22.05)		
adj. R^2	0.41	0.21	0.29
p	< 0.001	0.015	0.004

3.9 Other soil properties

3.9.1 Bulk density

Overall, ρ_b was in the order NT (1.33 g cm^{-3}) > CT ≈ RT (1.28 g cm^{-3}) (significant). Significant changes with time were only observed under CT and RT with increases during winter from Dec-2015 to Mar-16 and a consequent steady decrease throughout the winter wheat growing season until shortly before the harvest at the end of Jun-16 (Figure 14). Stubble breaking in Sep-16 following the harvest did significantly decrease ρ_b on CT while there was a slight increase under RT. Overall, ρ_b on NT remained temporally more stable. It was significantly larger than what was found on tilled plots in Dec-15. The NT-treatment also exhibited greater values during the growing season in the end of May-16 and Jun-16 and following stubble breaking on the tilled plots. Seedbed preparation in Apr-17 and sugar beet sowing had no significant effect on neither of the treatments compared to the previous sampling.

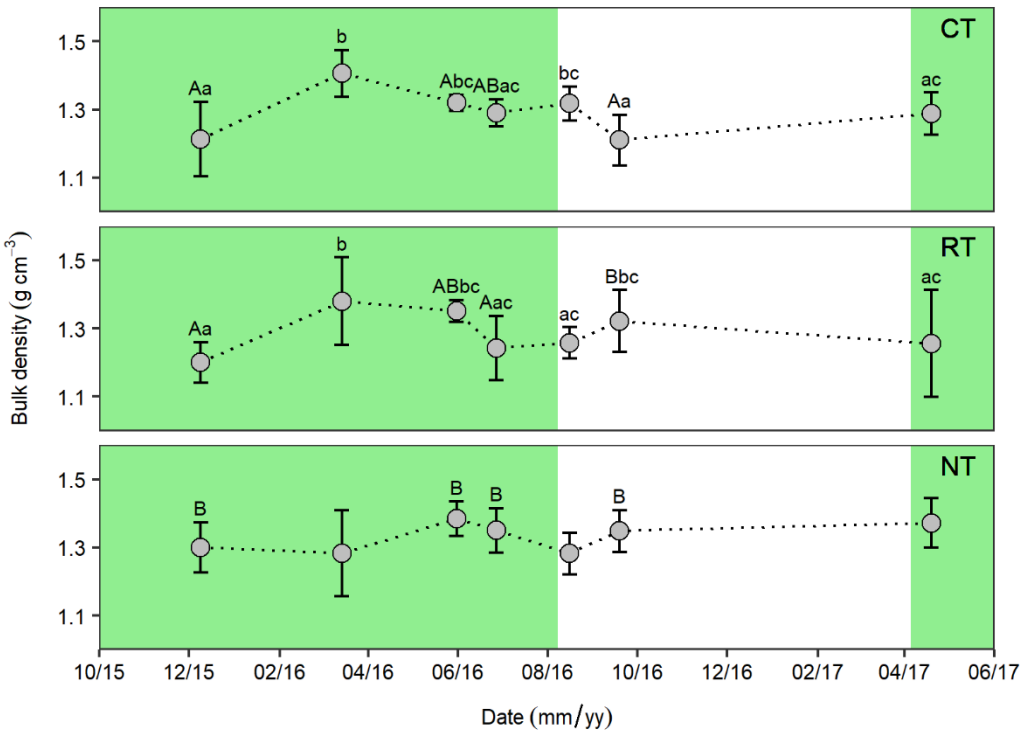

Figure 14 Temporal evolution of the bulk density under conventional tillage (CT), reduced mulch tillage (RT) and no tillage (NT). Error bars indicate the standard deviation from the mean. Green background marks cropping period defined as the time from sowing to harvest. Same upper-and lowercase letters indicate no significant differences ($p < 0.05$) between and within treatments, respectively.

3.9.2 Soil organic carbon and nitrogen

Soil organic C and N concentrations were higher on NT topsoil compared to CT and RT for all occasions (Table 9). Consequently, SOC and N stocks in the top five centimeters were always larger on NT compared to CT and RT (Figure 15). The same was true for the variability of measured data expressed in the standard deviation. Overall, the order was NT (1.2 kg m^{-2}) > RT (0.9 kg m^{-2}) > CT (0.8 kg m^{-2}) (significant) for SOC stocks and NT (0.12 kg m^{-2}) > RT (0.10 kg m^{-2}) > CT (0.08 kg m^{-2}) (significant) for N stocks.

Significant temporal variations of SOC stocks were only observed on RT where there was an increase during winter from Dec-15 to Mar-16 and after the harvest (Aug-16) to after the stubble breaking (Sep-16). The same pattern occurred for the N stocks on RT.

Table 9 Soil organic C (SOC) and N concentrations within the top five cm of the soil under conventional tillage (CT), reduced mulch tillage (RT) and no tillage (NT) plots. Standard deviation in brackets.

Treat-ment	Date	SOC		N	
		%			
CT	Dec-15	1.17	(0.08)	0.121	(0.005)
	Mar-16	1.16	(0.05)	0.123	(0.005)
	May-16	1.13	(0.06)	0.122	(0.003)
	Jun-16	1.17	(0.03)	0.132	(0.004)
	Aug-16	1.15	(0.03)	0.123	(0.002)
	Sep-16	1.33	(0.18)	0.129	(0.010)
	Apr-17	1.14	(0.02)	0.121	(0.002)
RT	Dec-15	1.25	(0.08)	0.136	(0.010)
	Mar-16	1.34	(0.14)	0.142	(0.014)
	May-16	1.32	(0.05)	0.148	(0.004)
	Jun-16	1.31	(0.10)	0.147	(0.010)
	Aug-16	1.34	(0.10)	0.147	(0.010)
	Sep-16	1.48	(0.05)	0.155	(0.005)
	Apr-17	1.53	(0.14)	0.164	(0.011)
NT	Dec-15	1.75	(0.12)	0.176	(0.011)
	Mar-16	1.88	(0.15)	0.192	(0.012)
	May-16	1.79	(0.17)	0.185	(0.016)
	Jun-16	1.85	(0.14)	0.186	(0.014)
	Aug-16	1.77	(0.17)	0.183	(0.014)
	Sep-16	1.81	(0.11)	0.181	(0.008)
	Apr-17	1.73	(0.05)	0.180	(0.006)

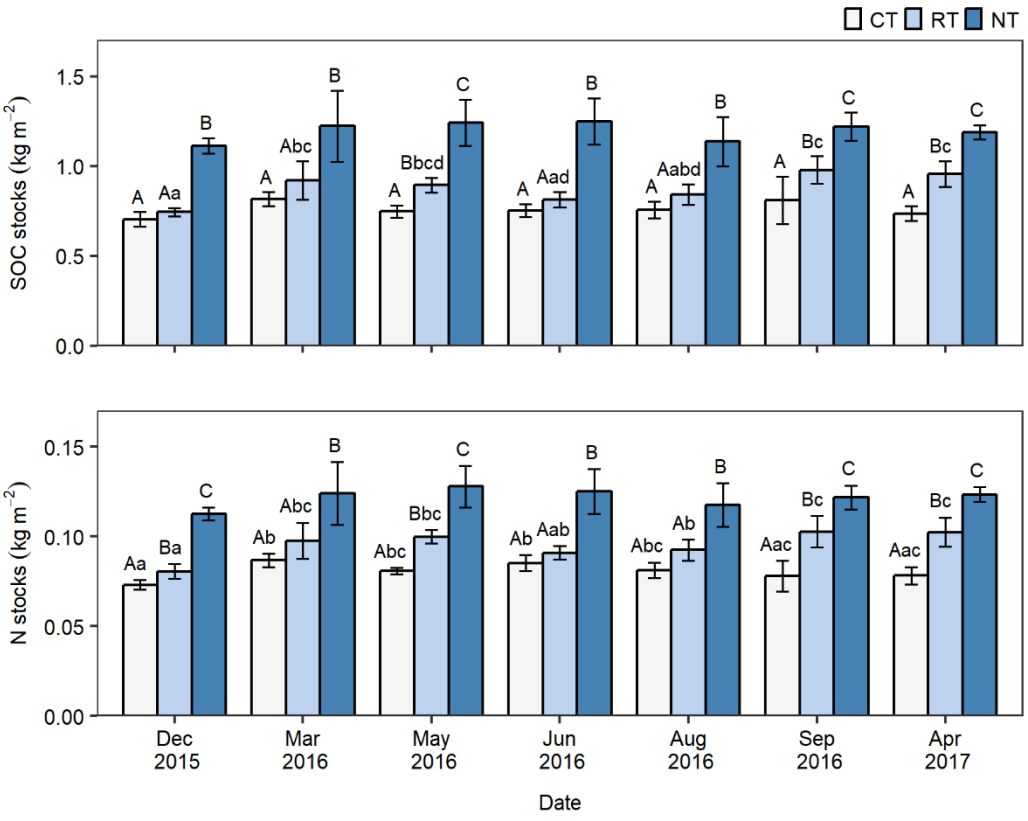

Figure 15 Soil organic C (SOC) and N stocks for the top 5 cm of the soil. Error bars indicate the standard deviation from the mean. Same upper-and lowercase letters indicate no significant differences ($p < 0.05$) between and within treatments, respectively.

3.10 Imaged soil structure and hydraulic conductivity

3.10.1 Comparison of hydraulic conductivity obtained through three methods in Spring 2018

Field (near-) saturated *K* measured at the soil surface with the HI was higher under NT (K_s GM 1175 cm d^{-1}) compared to CT (K_s GM 776 cm d^{-1}) ($p < 0.1$). These estimates were substantially higher than the estimates of the laboratory disk infiltrometer directly measured on the soil cores. Here, the trend was reversed between CT (K_s GM 288 cm d^{-1}) and NT (K_s GM 138 cm d^{-1}) ($p < 0.1$). Direct simulations based on imaged pore space undoubtedly yielded the highest values with no significant differences between CT (K_s GM 12,882 cm d^{-1}) and NT (K_s GM 23,442 cm d^{-1}).

3.10.2 Soil pore metrics

Analysis of the imaged pore space showed that macroporosity, *i.e.* visible porosity ⌀ > 60 µm, was much lower in NT than CT soil cores ($p < 0.001$), which agrees with higher ρ_b in the NT cores. Along with a lower macroporosity, critical macroporosity, *i.e.* minimum macroporosity

in the direction of flow, was reduced ($p < 0.001$) leading also to a lower connectivity ($p < 0.001$). Despite these results, the average pore diameter, derived from a pore diameter histogram, was greater under NT. Here, large biopores contributed the most to macroporosity, while on CT pores with a diameter < 0.5 mm embedded in the loose soil matrix contributed most to the frequency.

3.10.3 Correlation between hydraulic conductivity and pore metrics

Correlation analysis using the Spearman rank correlation analysis and following partial least square regression was used to show the relationship and contribution of the pore metrics or combinations thereof to the (near-) saturated hydraulic *K* obtained from the three methods, *i.e.* HI, disk infiltrometer and direct simulation. Correlation analysis showed that for all three methods, pore metrics correlated better with K_{2cm} than with K_s. Using all pore metrics, the partial least square analysis could explain more of the variability in K_s from the HI for CT (72.9 %) than NT (43.4 %) soil. Reasons may be that CT soil cores with their loose soil matrix are more representative than the NT soil core with fewer large biopores. However, also the pore metrics may be less suitable for flow prediction within this specific NT soil structure. Individual linear regression revealed the importance of each pore metric for K_s derived from HI measurements. For CT, the sequence in decreasing importance was average pore diameter (62.6 %), average pore distance (34.7 %) and pore connectivity (8.7 %). This indicates water transmission through the loose soil matrix. For NT, the sequence was pore connectivity (34.9 %), macroporosity (10 %) and average pore distance (6.6 %). As opposed to CT, the soil matrix here was denser. Therefore, connectivity of few large biopores gains importance in the water transmission process. This is confirmed by the connectivities, which under CT in the soil matrix was high anyway. For NT, pore connectivity was in a critical range between 0.4 and 0.8.

4 Discussion

4.1 Soil pore size distributions over one cropping cycle

This chapter presents the results concerning Objective 1) (Section 1.5) and its associated hypotheses. It discusses possible causes for the observed differences in soil structure expressed in the bimodal PSD of the three tillage treatments and their respective evolution with time over one cropping season from Dec-15 to Aug-16. Further, it looks at derived pore size classes and SPQ indicators to investigate the impact of soil tillage on soil health.

4.1.1 Soil pore size distribution is bimodal on tilled soil and varies with time

Despite 164 days passed since the last sowing, the effects of annual tillage on the WRC and with this the PSD persisted. In Dec-15, a distinct bimodal PSD with a textural and a structural mode could be identified on CT and RT distinguishing it from NT with a mostly unimodal PSD (Figure 9). Abundant fissures and transmission pores highlight those differences from the untilled soil (Figure 10) despite large amounts of effective rainfall received (Figure 2). Similarly, Moret-Fernández *et al.* (2016) found such a bimodal pore system under CT (moldboard plowing down to 30 – 40 cm) and RT (chisel plowing 25 – 30 cm), whereas the investigated NT soil was well described by a unimodal WRC model. Prior to the first sampling here, bimodality may have been more pronounced. However, intense precipitation events (maximum intensity eight days prior: 22.8 mm h^{-1}) on the bare field lead to aggregate disintegration as a consequence of slaking and mechanical breakdown (Xiao *et al.*, 2018) which likely caused a substantial amount of interaggregate porosity to degrade. Further, pore loss directly following tillage, defined as complete closure of interaggregate pores due to gravity and rainfall, may have added to a decline in structural pores (Alletto and Coquet, 2009; Or *et al.*, 2000) and increases in ρ_b (Moret-Fernández *et al.*, 2016; Peña-Sancho *et al.*, 2017). In Dec-15, the structural domain was more pronounced under RT compared to CT (Figure 9) which is probably related to the different mechanical impacts of both techniques. While inversion tillage with a moldboard plow creates large clods of soil with little physical aggregate disruption (Andruschkewitsch *et al.*, 2014b), tillage with a cultivator creates a more heterogeneous structure as expressed in the distinct modes of PSD (Figure 9). Further, more abundant water-stable macroaggregates (> 250 µm) with higher SOC contents have been found on RT (and NT) compared to CT on the same field (Andruschkewitsch *et al.*, 2014b)

thus making RT (and NT) soil structure more resilient towards precipitation impacts. Andruschkewitsch *et al.* (2014b) attributed these findings to higher organic matter incorporation into the first 15 cm under RT as opposed to moldboard plowing on CT that transported organic material down to 30 cm depth. Observations of SOC stocks made in this study and those of Jacobs *et al.* (2015) confirmed the organic matter distribution as influenced by the tillage system (Figure 15) which may also favor root development in the topsoil of RT and NT as a result of greater soil structural stability (Martínez *et al.*, 2008).

Despite the intense rainfalls (Figure 2) and assumed loss in porosity since the last tillage, K_S was comparably high on tilled plots (Table 5). Abundant fissures and transmission pores under CT and RT (Figure 10) together with comparably low ρ_b (Figure 14) and high Φ favored rapid infiltration on these plots. Additionally, on RT more plant residues were mixed into the top soil after the previous harvest providing additional flow paths. Therefore, a factor explaining the large variability in K_{slab} throughout the season are the relatively short soil cores (height = 5 cm) used for measurements where individual large biopores such as earthworm burrows and root channels reaching from top to bottom dominated flow processes in few of the cores (Mallants *et al.*, 1997; Reynolds *et al.*, 2000).

By Mar-16 (164 days after last sowing), the significant increase in ρ_b (Figure 14) points to the continuing post-tillage compaction of the soil due to effective rainfall (201 mm; Figure 2) as observed by other authors (Moret and Arrúe, 2007; Peña-Sancho *et al.*, 2017; Schwen *et al.*, 2011b). Saturated hydraulic conductivity was further reduced (Table 5) following the loss in transmission pores on CT and RT that were almost halved in volume. As for the PSD, intraaggregate pores were created at the expense of interaggregate pores (Figure 9). Freeze-thaw cycles may have disintegrated larger aggregates (1000 - 5000 µm) favoring the formation of smaller aggregates (250 - 1000 µm) (Li and Fan, 2014) thereby homogenizing the soil structure towards a more unimodal PSD. Again, lower macroaggregate stability on CT might explain the shift of the structural domain towards smaller pores while on RT only a decrease in volumetric frequency was observed. On NT there was barely any change in the PSD by that time indicating persistence of the prevalent soil structure against freeze-thaw cycles. Chopped straw residues and remaining stubbles from the last winter wheat harvest possibly moderated extremes in moisture and temperature in addition to the positive effects of organic matter incorporation on aggregate stability and the absence of mechanical disturbance (Blanco-Canqui and Ruis, 2018). Nevertheless, r_{m1} increased slightly during winter on all treatments (Table 6). Bodner *et al.* (2013) found an increase in Kosugi parameter r_m and a decrease of σ connected to increasing wetting-drying cycle intensities. With frequent precipitation events

prior to the Mar-16 sampling this may explain the larger r_{m1} values despite aggregate disintegration through freeze-thaw cycles. Converse to Bodner *et al.* (2013), the corresponding σ_1 in this study increased which might be due to the bimodal parameterization we used where the additional width in the structural curve could be to some extent balanced by a decline in the textural heterogeneity σ_2 (Table 6).

By the end of May-16 (242 days after last sowing), the structural mode on all plots had practically disappeared with hardly any difference between r_{m1} and r_{m2} (Table 6) apparent in a nearly unimodal homogeneous PSD (Figure 9). The transmission pore volume fraction was also at a minimum on all treatments (Figure 10). As pointed out in the previous paragraph, r_{m1} has been found to be positively correlated to the intensity of wetting-drying cycles. However, during a phase of water deficit, r_m was found to decrease together with slight increases in σ due to aggregate coalescence in favor of smaller pore size classes (Bodner *et al.*, 2013a) as also seen in a slight increase of storage pore volume on all plots. On all treatments such a decrease in r_{m1} together with an increase of σ_1 (only on CT and RT) was observed (Table 6). Since the last sampling 78 days prior, comparably little effective rainfall (39 mm) had accumulated (Figure 2). In addition to the lack of effective rainfall, crop growth tends to increase evapotranspiration throughout the season, especially in the flowering phase of winter wheat (Kang *et al.*, 2003). This potentially aggravated water availability and lead to the observed reduction in interaggregate pores. While the structural domain disappeared, the overall pore volume increased as indicated by a reduction in ρ_b under CT and RT (Figure 14) resulting in a unimodal but wider PSD (Figure 9).

By the end of Jun-16 (269 days after last sowing), some of the structural PSD domain was restored on RT (Figure 9). Here, continued decay of abundant organic matter mixed into the upper soil layer may have contributed to the regeneration of the structural domain. In addition to decaying organic matter, weather conditions could have played a role again. Within about 27 days since the last sampling 35 mm effective rainfall had accumulated together with increased evapotranspiration which could have intensified wetting-drying cycles again compared to the previous period leading to an increase in r_{m1} or macroporosity (Bodner *et al.*, 2013b, 2013a). This would also explain the continuing decrease in ρ_b on CT and RT (Figure 14) while on NT wetting-drying cycles were moderated through straw residue covering the surface. Despite a distinctly higher transmission pore volume (Figure 10), K_{slab}-values did not increase, which points to a poor connectivity of the newly developed macropores.

In the 51 days to the next sampling after harvest, only 10.2 mm h^{-1} effective rainfall was observed with weak intensities (maximum intensity: 0.8 mm h^{-1}; Figure 2). Larger K_{slab}-

values (Table 5) despite higher ρ_b in Aug-16 (Figure 14) suggest that fissures or biopores, *i.e.* earthworm burrows, decaying stalks and especially root channels (Blanco-Canqui and Ruis, 2018; Strudley *et al.*, 2008) together with newly formed transmission pores (Figure 10) governed the percolation process. Swinnen et al. (1995) showed that up to 43 and 36 % of winter wheat roots grown at tillering and ear emergence stages, respectively, already had decayed by the end of the growing season shortly before harvest. This underlines their potential to provide root channels for infiltration but also their contribution to a more heterogeneous and stable soil structure at this crop growth stage as observed in the PSDs (Figure 9) and increases in pore size classes with ⌀ > 50 µm on all treatments (Figure 10).

4.1.2 Summary Objective 1) Hypotheses A and B

Overall, temporal variability in PSD was more pronounced on tilled plots. This was also true for ρ_b, which showed significant changes over time confirming the hypothesis of a comparably inert soil structure on NT. Nevertheless, PSD under NT showed changes in its structural domain. Seasonal averages in ρ_b and K_{slab} were not significantly different between treatments, which raises the question when and how often SHP and soil physical properties need to be quantified for modeling applications. In case of modeling, *e.g.* irrigation schedules (Feki *et al.*, 2018), a seasonal quantification may be warranted while for studies covering a larger time span beyond a cropping season, *i.e.* more than one year, a less detailed description with one or two observations per year may be sufficient. The results of this study can be summarized to four distinct phases of a winter wheat cropping cycle on a silt loam soil that should be observed especially on tilled plots such as CT and RT:

1. Some weeks after (annual) tillage (here 68 days) with the newly created loose macropore-rich structure as the initial phase of the cycle when instantaneous pore loss (Or *et al.*, 2000) has already closed the larger instable void spaces. Volume taken up by transmission pores is still high (RT > CT) at that time highlighting the difference to the untilled system (NT) (Figure 10).
2. After winter (164 days) when environmental conditions (mostly temperature and moisture) have led to a continued settling of the structural domain as built up by tillage. The tillage effect is still visible in abundant fissures and transmission pores but a tendency to a shift towards the textural domain with a decline in overall Φ can be observed. Pore volumes under NT hardly experienced any changes by that time (Figure 10).

3. Mid to end of the growing season before harvest (242 days) when bimodality has disappeared (Figure 9) because of rainfall impact and intensified soil drying through increased evapotranspiration. Volume taken up by fissures and transmission pores is at a seasonal minimum (Figure 10).
4. Shortly before and after harvest (269 and 320 days, respectively) when effects of root growth and organic matter decay come to show with a restoration of the soil structural domain, as seen in increases in fissures and transmission pores (Figure 10) as well as a general loosening process with lower ρ_b (Figure 14) and increasing K_{slab} (Table 5).

With respect to Objective 1), as stated in Section 1.5, the two Hypotheses A and B can be confirmed. Differences in PSD between tilled and untilled soil were evident in a distinct structural mode on CT and RT (Hypothesis A). While this mode could be observed in the beginning and towards the end of the growing season, it diminished mid to end of it. On NT, such variability was less pronounced, mostly due to the lack of a structural mode with overall less fissures and transmission pores and a more compacted state (Hypothesis B).

It needs to be stressed that these results are site-specific and restricted to the top soil layer. For other tillage/cropping systems, soil types and depths soil structure may respond differently towards the influence of environmental conditions. In this case, RT, for example, was more resilient against environmental conditions degrading soil structure compared to CT due to higher SOC stocks incorporated into the top soil layer. On the other hand, the CT system may be more resilient towards aggregate disintegration and compaction in greater depths due to a more balanced organic matter distribution. In systems where organic residue is removed, overall soil structure may be more vulnerable to external forcing of temperature and rainfall as well as an inherent instability of soil aggregates.

4.2 The effects of a changing pore system on soil physical quality

This chapter deals with tillage effects on SPQ and the temporal variation thereof. Capacitive SPQ indicators, such as RFC and AC used here, are directly derived from the WRC (Castellini *et al.*, 2019b) and therefore are inherently linked to soil pore space changes which were discussed in Section 4.1. Such temporal variability proved to be most relevant for tilled soil. Thus, it is reasonable to assume that an evolving PSD also leads to evolving SPQ indicators on these treatments.

4.2.1 Suboptimal soil physical quality indicators change with time

Weninger *et al.* (2019) already investigated SPQ in Lüttewitz based on the same data used here. However, the focus of this study was laid on the overall differences between tillage treatments. They found overall favorable available water capacity conditions for crop growth on all treatments with $\theta > 0.2$ cm^3 cm^{-3}. However, aeration was poor across all investigated treatments. This was especially pronounced on NT. The temporal component of this study's investigation revealed the same pattern (Figure 12). No tillage soil had suboptimal AC-values on every observed date while for tilled soil the optimum to intermediate AC-values were reached in Dec-15, Aug-16 and Sep-16 (only CT). At the same time, the abundance of transmission pores was increased (Figure 10). These results imply that tillage improves SPQ but its beneficial effects are lost during winter and the beginning of the growing season. Nevertheless, SPQ may be restored to some extent by root growth, organic matter decomposition and biological activity as discussed in Section 4.1.1. The plot under NT on the other hand, with its overall higher ρ_b (Section 3.9.1) and lower transmission pores, was too compacted to revert to more favorable conditions. Weninger *et al.* (2019) attributed this vulnerability to compaction and lack of aeration in the absence of annual tillage to pore clogging due to low colloid content and weak structure in silt-dominated soils, as discussed in Horn *et al.* (1995). Similar to AC, ρ_b was not within an optimum range for arable soils ($0.9 \leq \rho_b \leq 1.2$ g cm^{-3}; Table 3) for all times on NT and most occasions on CT and RT (Figure 14).

Castellini *et al.* (2019) identified RFC as a key or summary SPQ indicator because it could be used to discriminate between agronomic treatments and combined aspects of both AC and available water capacity. In this study, RFC indicated limited aeration conditions for most dates and all treatments (Figure 11) as already shown for AC. In Dec-15, RFC on RT was closest to optimum conditions (Table 3). However, further in the cropping season, conditions deteriorated, and optimum values were not restored anymore. On NT, the range of measured RFC was narrower than on CT and RT which indicates a more homogeneous pore system.

In contrast to this study, Soracco *et al.* (2018) found similar temporal patterns of capacitive indicators such as AC and RFC on both CT and NT treatments on a Luvic Phaeozem (IUSS Working Group WRB, 2015) with a loam texture and 2.85 % SOC. On both treatments, SPQ indicators followed the same trends, particularly evident after harvest where traffic likely led to a reduction in macroporosity and AC. They also observed significant changes in ρ_b under NT, which was overall more favorable than that on CT. However, the observations were made during a corn cropping season and the treatment on NT included

tillage (z = 5 cm) to prepare the seedbed. The CT site was plowed with a disc plow and a tooth harrow (Villarreal *et al.*, 2017) which might further explain the differences to our study where SOC was lower (Table 9) and CT entailed the more intense turnover moldboard plowing. Here, stubble breaking before the Sep-16 sampling and seedbed preparation before the Apr-17 sampling (Table 1) apparently did not improve AC and RFC.

To summarize, SPQ, as expressed in AC and RFC, on the investigated silt loam soil exhibited an overall lack of aeration. Temporal variations of the chosen SPQ indicators were related to changes in transmission pore volume. Positive effects of NT and RT, *e.g.* soil erosion control, need to be weighed against an increased risk of compaction due to low organic matter contents (Weninger *et al.*, 2019). A meta-regression analysis of the effects of conservation agriculture on crop yields in Europe (van den Putte *et al.*, 2010) showed that overall yields are decreased on RT and NT-systems compared to CT with tillage depth as an important factor. Winter crop yields in Western Europe were shown to be reduced by 7 % under NT, which may also be associated with ongoing compaction. The sugar beet yield decline under NT is substantial and may even be economically unviable. For example, Koch *et al.* (2009) found a significant sugar beet yield decrease on NT and to a lesser extent on RT of the Südzucker experimental plots, including that in Lüttewitz. This was related to higher penetration resistance and increased ϱ_b which lead to a reduced AC. In the case of loess soils, they concluded that it is necessary to mechanically loosen the soil for an optimal sugar beet yield. A small but consistent yield decrease in winter wheat was previously observed for the NT treatment in Lüttewitz (Jacobs *et al.*, 2015; Schlüter *et al.*, in press). In some years, grain yields may even be higher than for conventionally tilled soil. For example, the 2016 winter wheat harvest in Lüttewitz yielded the most grain under NT (9.13 t ha^{-1} with 12.6 % moisture) closely followed by RT (9.06 t ha^{-1} with 12.4 % moisture) and finally CT (8.77 t ha^{-1} with 12.7 % moisture) (Table 1). Despite the general trend for yield reductions under NT in Lüttewitz, winter wheat may still be produced economically due to lower production costs under conservation tillage compared to CT (Dieckmann, 2008). Therefore, to evaluate the overall feasibility of a specific CA system, one should not only focus on yields but rather all aspects of agricultural management practices such as costs, labor and effectiveness to counter adverse environmental effects, *e.g.* soil erosion. For example, it was shown that profitability of conservation tillage versus conventional tillage is strongly related to prices of glyphosate and diesel. The former is used more frequently on minimum tillage systems and these systems profit from falling prices of the herbicide. Increasing prices of the latter may further create

favorable conditions for reduced soil tilth which requires less energy, *i.e.* diesel, input than CT (Nail *et al.*, 2007).

4.2.2 Summary Objective 1) Hypothesis C

To summarize, the changes in the soil pore system, as discussed in Section 4.1.1, are reflected in the temporal variations of RFC and AC. Optimum to intermediate conditions as defined by Reynolds *et al.* (2009) and Castellini *et al.* (2019) were only reached on tilled soil close to the last tillage (Dec-15) and towards the end of the growing season. No till soil with higher compaction levels had comparably less changes in RFC and AC and always remained at suboptimum levels. Therefore, Hypothesis C of Objective 1) can be confirmed. Despite suboptimum SPQ, winter crop production may still be economically viable (Dieckmann, 2008) while the increased compaction under NT hampers growth of sugar beet (Koch *et al.*, 2009).

4.3 Tillage effects on variability of hydraulic conductivity

This chapter presents both the spatial and temporal variability of (near-) saturated and unsaturated *K* obtained from HI-and HYPROP®-experiments from May-16 to Apr-17. Results are discussed with respect to Hypothesis D and E pertaining to Objective 2) as outlined in Section 1.5.

4.3.1 (Near-) saturated hydraulic conductivity

The tillage treatment had a distinct influence on the overall topsoil *K* obtained from hood infiltration runs with clear temporal patterns (Table 4). Chopped straw and stubbles from the previous harvest mixed into the top 15 and 30 cm on RT and CT, respectively, had a distinct effect on *K* at and near saturation. The decomposing organic material likely led to the formation of macropores (Strudley *et al.*, 2008) which in turn resulted in an increase in *K* during the first three occasions from May-16 to Aug-16. The increase in mean pore radius due to wetting-drying cycles (Bodner *et al.*, 2013b, 2013a) may have further promoted a re-formation of soil structure as already discussed in Section 4.1.1. In this section, it was shown that the pore volume fraction of transmission pores (⌀ 50 – 500 µm) and fissures (⌀ > 500 µm) increased on those plots during that time. Transmission pores were also shown to be correlated to changes in K_{slab}. This indicated that these pore size classes are important factors for infiltration processes at saturation, especially on CT. The increases in *K* were

stronger on RT, which may be explained by the relatively higher availability of organic material in the top 15 cm compared to CT. On CT, a similar amount of material was distributed over a larger vertical profile of 30 cm caused by the moldboard plowing as also observed in consistently lower SOC stocks in the top 5 cm compared to RT (Figure 15). Variability in May-16 was high on CT and RT but then decreased with time (Figure 8). This may point to a continuing homogenization of the soil where rather the loose soil matrix influences *K* than individual large pores that may be subject to a more heterogeneous distribution and therefore exhibit a more variable infiltration behavior.

Stubble breaking post-harvest on RT (Table 1) interrupted the rise in *K* by cutting through the pore network that had developed up to that point. Due to that, pore continuity, an important metric for *K* near saturation (Soracco *et al.*, 2019), was reduced. On the other hand, in the conventionally tilled soil with comparingly less 'building material' for the soil aggregates, the stubble breaking lead to a further increase in *K* by loosening the soil matrix as seen in decreased ϱ_b (Figure 14). On NT, *K* near saturation was comparably lower (Table 4) which is probably associated to the overall increased ϱ_b (Figure 14). Along with a distinct lack of fissures and transmission pores compared to tilled soil (Weninger *et al.*, 2019; Figure 10), this limited infiltration through the soil matrix. In their study on loam and silt loam soils, Soracco *et al.* (2019) also reported reduced (near-) saturated *K* on NT compared to CT. While the continuity of big macropores or biopores ($\varnothing > 1$ mm) expressed in a continuity index (Lozano *et al.*, 2013) was higher on untilled soil, porosities of those biopores were lower. In part, this could also be seen in reduced fissures on NT (Figure 10), although the bigger biopores were probably not captured entirely by the evaporation experiments. The higher continuity was attributed to a well-developed soil structure, biological activity and abundant root channels on NT.

Temporal variation on NT was comparably low as also observed by Schwen *et al.* (2011b) and Keskinen *et al.* (2019). Unlike the tilled plots, organic material from the previous harvest remained on the soil surface acting as a moderator for soil moisture and temperature reducing the effects of wetting-drying cycles and the destructive impact of the kinetic energy received from heavy rainfall (see also Discussion-Section 4.1.1). Overall, ϱ_b was higher which prevented a preferred infiltration through the soil matrix. Only following seedbed preparation for sugar beets in Apr-17, comparable levels to those of CT and RT were observed. Nevertheless, ϱ_b remained high indicating little influence of this mechanical manipulation on the spatial arrangement of the soil aggregates on NT. The effect of seedbed preparation was

also limited as it only affected the top 8 cm (Table 1) while the comparably denser layer below (Jacobs *et al.*, 2015) introduced a resistance towards infiltrating water.

Many studies looked into the effects of conventional and conservation agriculture on soil hydraulic properties with rather ambiguous results especially when it comes to *K* (Blanco-Canqui and Ruis, 2018). Weninger *et al.* (2019) analyzed the overall differences in (near-) saturated *K* on this field as well as on two sites in Austria (both Chernozem with silt loam texture). Like Blanco-Canqui and Ruis (2018), they did not find systematic differences between tillage treatments. However, NT exhibited a tendency for reduced *K*. As discussed in the introduction, temporal variation might explain part of the disagreement between studies, especially if only 'snapshot' measurements were done (Strudley *et al.*, 2008). A good example is K_s in May-16, where overall values were rather similar with 459, 315 and 511 cm d^{-1} for CT, RT and NT, respectively. This was also true for associated CVs with 146, 177 and 127 %, respectively. Less than one month later with pesticide spraying as the only management action in between (Table 1), K_s was significantly increased on RT compared to NT. On CT, K_s was now greater than on NT. Schwen *et al.* (2011a) significantly improved soil water modeling by using time-variable hydraulic parameters despite much lower variations in topsoil (near-) saturated *K* than those observed here. This shows that one-off estimations of this hydraulic property are not sufficient to determine differences in soil hydraulic properties of conventional and conservation agriculture, and variability in (near-) saturated *K* needs to be included in the modeling process.

4.3.2 Unsaturated hydraulic conductivity

Under drier conditions, *i.e.* more negative *h*, overall variability of *K* decreased due to decreasing influence of larger pores emphasizing the increasing relevance of soil texture over soil structure (Bodner *et al.*, 2013b; Schwen *et al.*, 2011b) Nevertheless, a significant temporal variation of $k_{pF2.0}$ could be seen on CT which may also be an artifact of the parameterization with the bimodal Mualem model as with increases in K_s and especially K_{2cm} (see also positive correlation in Figure 13), $k_{pF2.0}$ decreased and vice versa. However, the same pattern was not present on RT and NT. Given the generally low values of $k_{pF2.0}$, $k_{pF2.5}$ and $k_{pF3.0}$, the temporal variability may not be meaningful for modeling studies and it may be reasonable to assume an invariant *K* in this *h*-range.

Laboratory data in the unsaturated moisture range in combination with the field measurements representing the soil structural part is essential for an adequate description of the HCC (Weninger *et al.*, 2018). These results showed that there is a difference between field

and lab data from three to almost five orders of magnitude. For the simulation of unsaturated flow processes this data combination is essential in the parametrization of the respective hydraulic models (Schwärzel and Bohl, 2003). Consideration of only K_s in the parametrization of the HCC as many modeling studies do may lead to overestimations of K at h between -10 and -100 cm (De Pue *et al.*, 2019).

4.3.3 Summary: Objective 2) Hypothesis D and E

Spatial variability across the HCC, as expressed in the GCVs, was shown to be reduced with increasing h. This was mostly true for NT and on some occasions for CT and RT. Therefore, Hypothesis D can partly be confirmed. Temporal variability of the HCC was comparably high on plots under tillage (CT and RT), especially at and near saturation, where GCVs differed greatly between occasions. Structural changes throughout the season seemed to occur long after primary tillage and initial void closure. Abundant fissures and transmission pores under CT and NT were linked to changes in (near-) saturated K. With its denser soil matrix, *i.e.* higher ϱ_b, K near saturation was temporally more stable on untilled soil and Hypothesis E can be confirmed.

4.4 Factors influencing water transmission and its temporal variation

This chapter deals with Objective 2) and the respective Hypothesis F as set out in Section 1.5. Correlation analysis and multiple regression analyses of K with other soil properties, *i.e.* BP, ϱ_b, $\Phi_{mac+mes}$ and SOC were done to infer information about differences in soil structure on the three tillage treatments. Supporting information came from a study (Schlüter et al., in press) using undisturbed soil cores for an X-ray μCT image analysis which yielded pore metrics for CT and NT plots (Section 2.7).

4.4.1 Soil properties partly explain variability in hydraulic conductivity on CT

Predictions of WRC and HCC parameters from other (more readily available) soil properties such as soil texture, ϱ_b, soil organic matter and moisture are often made using pedotransfer functions (Vereecken *et al.*, 2010). Here, it was possible to explain up to 61 % of the variance observed in K_s of CT soil pooling all data collected on different occasions (Table 7). With decreasing tillage intensity, *i.e.* from CT over RT to NT, the usefulness of predictors like $\Phi_{mac+mes}$ (and the closely related ϱ_b) and BP decreased. On NT, there was no statistically

significant correlation with any of those properties which indicates distinctly different water transport mechanisms between treatments. Flow through the soil matrix may therefore be more relevant on tilled plots. Another indicator for that is the SOC content, which stabilizes the fundamental building blocks of an agricultural soil, *i.e.* aggregates. It was found that the higher the SOC, the higher the yield of water-stable macroaggregates ($r > 250$ µm) on our tillage experiment and three similarly treated sites in Germany (Andruschkewitsch *et al.*, 2013). Here, SOC was only positively correlated with K_s and K_{2cm} on CT (Figure 13), where the SOC concentrations and stocks in the top 5 cm were lowest compared to the other two treatments (Figure 15). This may be attributed to the fact, that the infiltration front of the HI integrates over a larger depth profile than just the measured top 5 cm. On CT, residue from the harvest is more equally distributed with depth down to 30 cm while on RT and NT it is accumulated in the very topsoil layer (Andruschkewitsch *et al.*, 2013). The correlation between conductivity and SOC that in turn is related to the macroaggregate yield is then obscured by the layering on RT and NT. On NT, the overall higher ρ_b in the top 5 cm (Figure 14) and deeper down the profile (Jacobs *et al.*, 2015) restricted infiltration through the intraaggregate pore space reducing its importance as a predictor for K_s and K_{2cm}.

The BP may be used as a rather quickly determined soil structural property compared to sometimes lengthy tension infiltration measurements (Klípa *et al.*, 2015; Špongrová *et al.*, 2009). It is related to the largest present soil pore under the hood infiltration area or rather the critical pore radius or 'bottleneck' of the pore system connected to the soil surface (Patra *et al.*, 2019). However, r_{BP} calculated from BP barely showed notable differences between treatments and with time (Figure 7). This may be attributed to the very high spatial variability of macropores on arable soils due to biological activity, *i.e.* earthworm activity, root growth and decomposition of organic material. Therefore, temporal trends are difficult to identify with infiltration measurements (Rienzner and Gandolfi, 2014). The HI used here captures flow through macropores well compared to other TIs (Matula *et al.*, 2015; Schwärzel and Punzel, 2007) that were shown to be more indicative of K in the soil matrix (Fodor *et al.*, 2011; Rienzner and Gandolfi, 2014). Hence, spatial variability of macropores should translate to spatial variability in estimated K_s and K_{2cm}-values here. Following the interpretation of Patra *et al.* (2019), a lack of temporal variation would mean a relative stability of the macropore system under all treatments. However, this is questionable as great changes in K_s and K_{2cm} were observed on tilled plots. The correlation and regression analysis showed that some of the conductivity changes can be explained by a changing $\Phi_{mac+mes}$ (Figure 13; Table 7) which should then also be expressed in changes of r_{BP} or BP. One of the reasons for the lack of a

response may be the assumption that r_{BP} is indicative of the entire macropore system underneath the infiltration hood. Depending on the treatment, one large biopore, *i.e.* a pore created by earthworms and other soil macrofauna, embedded in an otherwise dense soil matrix, may lead to a relatively high BP and consequently a large r_{BP}. One would expect such a setup rather for the untilled soil where the soil matrix is comparably dense and ρ_b is increasing with depth as previously observed on this field (Jacobs *et al.*, 2015). Here, BP, ρ_b and $\Phi_{mac+mes}$ were not meaningful in correlation and regression analyses suggesting a distinctly different soil structure and hence different SHP. A more regular macropore distribution can be expected on CT, where BP was also a significant predictor in explaining variability in K_s (Table 7). Mulch tillage lies in between those two treatments. Here (near-) saturated *K* showed a similar correlation with ρ_b as on CT (Figure 13).

Existing pedotransfer functions use easily obtainable soil properties such as ρ_b, SOC and soil texture to predict *K* at and near saturation (Tóth *et al.*, 2015; Vereecken *et al.*, 2010). This study suggests that agricultural management practices such as the tillage system greatly influence soil structure which makes it difficult to choose suitable predictors of (near-) saturated *K* with justifiable effort. While on tilled plots ρ_b and the closely-related $\Phi_{mac+mes}$ could to some extent be used as predictors, it proved to be meaningless for the long-term NT soil. The same was true for the other soil structural indicator BP that proved potentially useful only on CT.

4.4.2 Imaged pore metrics explain differences in field hydraulic conductivity

Hydraulic conductivity measured with the HI in spring 2018 showed a completely different trend than what was observed during the 2016 and early 2017 campaigns. Saturated hydraulic conductivity and K_{2cm} were much greater under NT than CT which was only observed once in Apr-17 (Table 4) where the shallow seedbed preparation (Table 1) may have contributed to an increase. The previous sugar beet harvest in autumn 2017 may have contributed to these unusually high *K*-values in spring 2018 under NT.

The quantified pore metrics confirmed the findings already discussed in Section 4.4.1 where easily quantifiable soil properties such as ρ_b and Φ_{mac} and Φ_{mes} were useful for predicting (near-) saturated *K* on CT and to some extent on RT soil. As the image analysis showed, this is due to the prevalent soil structure. Conventionally tilled soil exhibited a comparably looser soil matrix than long-term untilled soil. Under NT, the soil matrix is denser. Therefore, it does not substantially contribute to water transmission. Instead, few large biopores conduct most

of the water. Soil pore metrics from imaging analysis could visualize this typical NT structure (Borges *et al.*, 2019; Pires *et al.*, 2019). It was possible to relate those soil pore metrics to some extent to (near-) saturated *K*, even though these measurements were taken at the topsoil, while soil cores were taken from 10 - 20 cm depth. Conservative estimates of the infiltration front depths yielded wetting front advances from 19 to 33 cm on CT and NT, respectively, during the conducted experiments. Therefore, topsoil measurements should have encompassed the sampled soil core volume. To quantify the governing soil structural metrics on NT in the field was shown to be more difficult due to the nature of spatially heterogeneous biopores (Rienzner and Gandolfi, 2014) with potentially turbulent flow (Beven and Germann, 2013). On CT, on the other hand, Φ or macroporosity as defined in the imaging study ($\varnothing > 60$ µm) is a relatively good metric to predict (near-) saturated *K*. For more in-depth discussions on differences of predictions for all three methods, the interested reader is referred to Schlüter *et al.*, (in press).

4.4.3 Summary Objective 2) Hypothesis F

Correlation and regression analysis indicated distinct differences in the infiltration processes among treatments. While ϱ_b, Φ_{mac} and Φ_{mes} were found to be most determining for K_s and K_{2cm} on CT and RT, they were not on NT. A reverse influence of Φ_{mac} and Φ_{mes} on $k_{pF2.0}$, $k_{pF2.5}$ and $k_{pF3.0}$ was observed especially for CT but also to some extent for RT. This suggests that increases in both Φ_{mac} and Φ_{mes} are coupled to decreases in smaller pore sizes on tilled soils. Under NT, the soil matrix is comparably denser and none of the investigated properties was relevant in correlation and regression analyses.

The layering of SOC on RT and NT likely obfuscated a correlation with K_s and K_{2cm} as observed under CT. Here, SOC was more evenly distributed and water transmission likely occurred mostly through the soil matrix, as confirmed by pore metric quantification with X-ray µCT imaging. On untilled soil, larger biopores embedded in the otherwise dense soil matrix conduct water. Considering these results, Hypothesis F can be confirmed.

5 Summary and outlook

Soil structure and the associated WRC and HCC of arable soils change in the short-term, *e.g.* over a cropping season, and in the long-term as result of a change in soil management, *e.g.* from CT to NT. Such temporal variability is a major obfuscating factor in the quantification of SHP. An accurate modeling of soil water dynamics needs to consider these variations in order to make well-founded management decisions, *e.g.* when drafting an irrigation schedule or when estimating how a land-use or soil management change will affect a soil's water availability. The development of models that predict the evolution in PSD from which SHP can be inferred might help reduce quantification efforts in the field and laboratory. Data availability has increased in the past decade which also helps in the development of pedotransfer functions to estimate SHP from more easily-available soil properties. Yet, few studies have quantified soil structural and SHP changes over time. Which soil structural or pore metrics govern water transmission under conventional and conservation tillage practices needs to be understood better.

In light of these issues, two objectives were formulated for this dissertation:

- Objective 1) was to quantify SHP and PSD changes over one winter wheat cropping season.
- Objective 2) was to characterize the soil structure and the associated SHP.

The frequent observation of SHP within a winter wheat cropping season (Objective 1) showed distinct temporal variations in the derived PSD of tilled plots CT and RT. Here, changes in soil pore space occurred mostly in pore classes with ⌀ > 50 µm which are associated with water transport. Saturated hydraulic conductivity varied together with abundances of transmission pores highlighting the susceptibility of water flow at saturation towards changes in PSD. Soil structure under NT was temporally more stable with its comparably lower transmission (⌀ 50-500 µm) but more storage pores (⌀ 0.5 - 50 µm). Under tilled soil, a built-up of the structural pores could be observed later in the season.

These results highlight the need to explicitly consider the evolution of the structural domain of tilled soils in modeling frameworks. This may especially be relevant when simulating soil water fluxes over a short time period, *e.g.* a cropping season. Going one step further than a mere stepwise implementation of SHP into hydrological models, as outlined in the introduction section would be to predict the evolution of soil pore space using an existing model (Chandrasekhar *et al.*, 2018). In the long run, predicting such soil pore space changes

would ideally replace the majority of costly and time-consuming field and laboratory measurements. However, existing PSD-modeling approaches see soil structural changes mostly as a short-term post-tillage loss in Φ and a consequent shift to smaller pores (*e.g.* Chandrasekhar et al., 2019, 2018; Or et al., 2000; Pelak and Porporato, 2019). Here, results pointed towards a build-up of new structural pores as a result of soil organic matter decomposition, biological activity as well as root growth and decay later in the growing season which should be considered when trying to predict the evolution of PSD (Pelak and Porporato, 2019). Challenges for such endeavors are site- and management-specific conditions that hamper comparison and generalization of quantified soil structural changes.

Soil physical quality represented by RFC, AC and ρ_b was shown to be at suboptimum levels for most of the times on all three treatments. All three indicators varied with changes in the PSD and therefore they were most variable on tilled soil. Despite comparably worse SPQs on NT, winter wheat yields were previously shown to be reduced only marginally here (Jacobs *et al.*, 2015) and it may even be economically more viable than the CT system. Evaluation of such a conservation tillage system should therefore consider all aspects such as positive and adverse environmental effects, *e.g.* erosion control, water storage and compaction, and production costs, *e.g.* labor and fuel costs. Ultimately, conservation tillage is only one aspect of CA and for a successful implementation the other principles need to be considered as well (Pittelkow *et al.*, 2014). A recommendation for or against one of the investigated systems in this specific case, however, would be out of scope of this dissertation as the focus was mainly on process understanding of the tillage effects on soil structure.

The characterization of soil structure and the underlying water transport processes (Objective 2) revealed distinct differences between tilled and untilled soil. Structural changes throughout the season seemed to occur long after primary tillage and initial void closure. With its denser soil matrix, *i.e.* higher ρ_b, K near saturation was temporally more stable on untilled soil. While ρ_b and $\Phi_{mac+mes}$ were found to be most determining on CT and RT, they were not on NT. Image analysis confirmed the hypothesized different soil structure and hence water transmission processes between CT and NT soil resulting in completely different pore or soil physical property metrics for the prediction of K near saturation.

These results highlight that the intensity of tillage affects water transmission properties by either loosening or compacting the soil matrix. The choice of tillage system may either destroy or preserve large vertically-oriented soil pores, *i.e.* mostly biopores created by earthworms, but also macroporosity built up by organic matter decomposition, distributed across different vertical profiles. This has consequences for the validity of pedotransfer

functions that may not be universally applied. It needs to be kept in mind that the mechanical disturbances that is tillage or the absence thereof, likely results in different structural properties and consequently different SHP. Therefore, the pool of soil physical and chemical properties used as predictors in pedotransfer functions may vary for different tillage treatments. Apart from tillage, a selection of suitable predictors should also include other aspects of agricultural management that influence (near-) saturated *K*, such as residue management and crop rotation (Patra et al., 2019).

Although the results from this study were from unreplicated plots, they consistently showed distinct differences between tilled and untilled soil in soil structure as revealed by the periodic field and laboratory experiments. Despite shedding light on processes of soil structure and hence SHP development under conservation and conventional tillage of a silt loam soil, this study raises more questions. To what extent would observed changes in SHP affect simulated water dynamics? How can SHP be reliably predicted for various practices when already at one site this is a difficult endeavor and conservation tillage systems around the world differ in a multitude of aspects (Derpsch et al., 2014). Future work will need to enhance our process understanding and integrate this knowledge in tools to predict the soil structural evolution for various scenarios of agricultural management. In light of a changing climate and an increasing demand for food, such knowledge is crucial in sustaining both soil and water resources (Vereecken et al., 2016).

References

Afshar, R.K., Nilahyane, A., Chen, C., He, H., Bart Stevens, W., Iversen, W.M., 2019. Impact of conservation tillage and nitrogen on sugarbeet yield and quality. Soil Tillage Res. 191, 216–223. https://doi.org/10.1016/j.still.2019.03.017

Alaoui, A., Lipiec, J., Gerke, H.H., 2011. A review of the changes in the soil pore system due to soil deformation: A hydrodynamic perspective. Soil Tillage Res. 115/116, 1–15. https://doi.org/10.1016/j.still.2011.06.002

Alletto, L., Coquet, Y., 2009. Temporal and spatial variability of soil bulk density and near-saturated hydraulic conductivity under two contrasted tillage management systems. Geoderma 152, 85–94. https://doi.org/10.1016/j.geoderma.2009.05.023

Alletto, L., Pot, V., Giuliano, S., Costes, M., Perdrieux, F., Justes, E., 2015. Temporal variation in soil physical properties improves the water dynamics modeling in a conventionally-tilled soil. Geoderma 243/244, 18–28. https://doi.org/10.1016/j.geoderma.2014.12.006

Andruschkewitsch, R., Geisseler, D., Dultz, S., Joergensen, R.-G., Ludwig, B., 2014a. Rate of soil-aggregate formation under different organic matter amendments - A short-term incubation experiment. J. Plant Nutr. Soil Sci. 177, 297–306. https://doi.org/10.1002/jpln.201200628

Andruschkewitsch, R., Geisseler, D., Koch, H.-J., Ludwig, B., 2013. Effects of tillage on contents of organic carbon, nitrogen, water-stable aggregates and light fraction for four different long-term trials. Geoderma 192, 368–377. https://doi.org/10.1016/j.geoderma.2012.07.005

Andruschkewitsch, R., Koch, H.-J., Ludwig, B., 2014b. Effect of long-term tillage treatments on the temporal dynamics of water-stable aggregates and on macro-aggregate turnover at three German sites. Geoderma 217–218, 57–64. https://doi.org/10.1016/j.geoderma.2013.10.022

Angulo-Jaramillo, R., Bagarello, V., Iovino, M., Lassabatere, L., 2016. Unsaturated soil hydraulic properties, in: Angulo-Jaramillo, R., Bagarello, V., Iovino, M., Lassabatere, L. (Eds.), Infiltration measurements for soil hydraulic characterization. Springer International Publishing, Cham, pp. 181–287. https://doi.org/10.1007/978-3-319-31788-5_3

Ankeny, M.D., Ahmed, M., Kaspar, T.C., Horton, R., 1991. Simple field method for determining unsaturated hydraulic conductivity. Soil Sci. Soc. Am. J. 55, 467-470. https://doi.org/10.2136/sssaj1991.03615995005500020028x

Bagarello, V., Baiamonte, G., Castellini, M., Di Prima, S., Iovino, M., 2014. A comparison between the single ring pressure infiltrometer and simplified falling head techniques: comparing pressure infiltrometer and SFH techniques. Hydrol. Process. 28, 4843–4853. https://doi.org/10.1002/hyp.9980

Báťková, K., Matula, S., Miháliková, M., 2013. Hood Infiltrometer [WWW Document]. URL http://hydropedologie.agrobiologie.cz/en-hood.html (accessed 7.22.19).

Baveye, P., 2006. Comment on "Soil structure and management: A review" by C.J. Bronick and R. Lal. Geoderma 134, 231–232. https://doi.org/10.1016/j.geoderma.2005.10.003

Beven, K., Germann, P., 2013. Macropores and water flow in soils revisited: Review. Water Resour. Res. 49, 3071–3092. https://doi.org/10.1002/wrcr.20156

Bissonnais, Y., 1996. Aggregate stability and assessment of soil crustability and erodibility: I. Theory and methodology. Eur. J. Soil Sci. 47, 425–437. https://doi.org/10.1111/j.1365-2389.1996.tb01843.x

Blanco-Canqui, H., Ruis, S.J., 2018. No-tillage and soil physical environment. Geoderma 326, 164–200. https://doi.org/10.1016/j.geoderma.2018.03.011

Blanco-Canqui, H., Wienhold, B.J., Jin, V.L., Schmer, M.R., Kibet, L.C., 2017. Long-term tillage impact on soil hydraulic properties. Soil Tillage Res. 170, 38–42. https://doi.org/10.1016/j.still.2017.03.001

Blume, H.-P., Brümmer, G.W., Fleige, H., Horn, R., Kandeler, E., Kögel-Knabner, I., Kretzschmar, R., Stahr, K., Wilke, B.-M., 2016. Physical properties and processes, in: Scheffer/Schachtschabel Soil Science. Springer Berlin Heidelberg, Berlin, Heidelberg, pp. 175–283. https://doi.org/10.1007/978-3-642-30942-7_6

Bodner, G., Leitner, D., Kaul, H.-P., 2014. Coarse and fine root plants affect pore size distributions differently. Plant Soil 380, 133–151. https://doi.org/10.1007/s11104-014-2079-8

Bodner, G., Loiskandl, W., Kaul, H.-P., 2007. Cover crop evapotranspiration under semi-arid conditions using FAO dual crop coefficient method with water stress compensation. Agric. Water Manag. 93, 85–98. https://doi.org/10.1016/j.agwat.2007.06.010

Bodner, G., Scholl, P., Kaul, H.-P., 2013a. Field quantification of wetting–drying cycles to predict temporal changes of soil pore size distribution. Soil Tillage Res. 133, 1–9. https://doi.org/10.1016/j.still.2013.05.006

Bodner, G., Scholl, P., Loiskandl, W., Kaul, H.-P., 2013b. Environmental and management influences on temporal variability of near saturated soil hydraulic properties. Geoderma 204/205, 120–129. https://doi.org/10.1016/j.geoderma.2013.04.015

Borges, J.A.R., Pires, L.F., Cássaro, F.A.M., Auler, A.C., Rosa, J.A., Heck, R.J., Roque, W.L., 2019. X-ray computed tomography for assessing the effect of tillage systems on topsoil morphological attributes. Soil Tillage Res. 189, 25–35. https://doi.org/10.1016/j.still.2018.12.019

Briones, M.J.I., Schmidt, O., 2017. Conventional tillage decreases the abundance and biomass of earthworms and alters their community structure in a global meta-analysis. Glob. Change Biol. 23, 4396–4419. https://doi.org/10.1111/gcb.13744

Bronick, C.J., Lal, R., 2005. Soil structure and management: A review. Geoderma 124, 3–22. https://doi.org/10.1016/j.geoderma.2004.03.005

Castellini, M., Fornaro, F., Garofalo, P., Giglio, L., Rinaldi, M., Ventrella, D., Vitti, C., Vonella, A., 2019a. Effects of no-tillage and conventional tillage on physical and hydraulic properties of fine textured soils under winter wheat. Water 11, 484. https://doi.org/10.3390/w11030484

Castellini, M., Stellacci, A.M., Barca, E., Iovino, M., 2019b. Application of multivariate analysis techniques for selecting soil physical quality indicators: A case study in long-term field experiments in Apulia (Southern Italy). Soil Sci. Soc. Am. J. 83, 707. https://doi.org/10.2136/sssaj2018.06.0223

Chandrasekhar, P., Kreiselmeier, J., Schwen, A., Weninger, T., Julich, S., Feger, K.-H., Schwärzel, K., 2019. Modeling the evolution of soil structural pore space in agricultural soils following tillage. Geoderma 353, 401–414. https://doi.org/10.1016/j.geoderma.2019.07.017

Chandrasekhar, P., Kreiselmeier, J., Schwen, A., Weninger, T., Julich, S., Feger, K.-H., Schwärzel, K., 2018. Why we should include soil structural dynamics of agricultural soils in hydrological models. Water 10, 1862. https://doi.org/10.3390/w10121862

Crittenden, S.J., Poot, N., Heinen, M., van Balen, D.J.M., Pulleman, M.M., 2015. Soil physical quality in contrasting tillage systems in organic and conventional farming. Soil Tillage Res. 154, 136–144. https://doi.org/10.1016/j.still.2015.06.018

Cullotta, S., Bagarello, V., Baiamonte, G., Gugliuzza, G., Iovino, M., La Mela Veca, D.S., Maetzke, F., Palmeri, V., Sferlazza, S., 2016. Comparing different methods to determine soil physical quality in a mediterranean forest and pasture land. Soil Sci. Soc. Am. J. 80, 1038. https://doi.org/10.2136/sssaj2015.12.0447

Daraghmeh, O.A., Jensen, J.R., Petersen, C.T., 2008. Near-saturated hydraulic properties in the surface layer of a sandy loam soil under conventional and reduced tillage. Soil Sci. Soc. Am. J. 72, 1728. https://doi.org/10.2136/sssaj2007.0292

De Gryze, S., Six, J., Brits, C., Merckx, R., 2005. A quantification of short-term macroaggregate dynamics: influences of wheat residue input and texture. Soil Biol. Biochem. 37, 55–66. https://doi.org/10.1016/j.soilbio.2004.07.024

De Pue, J., Rezaei, M., Van Meirvenne, M., Cornelis, W.M., 2019. The relevance of measuring saturated hydraulic conductivity: Sensitivity analysis and functional evaluation. J. Hydrol. 576, 628–638. https://doi.org/10.1016/j.jhydrol.2019.06.079

Deb, S.K., Shukla, M., 2012. Variability of hydraulic conductivity due to multiple factors. Am. J. Environ. Sci. 8, 489–502. https://doi.org/10.3844/ajessp.2012.489.502

Derpsch, R., Franzluebbers, A.J., Duiker, S.W., Reicosky, D.C., Koeller, K., Friedrich, T., Sturny, W.G., Sá, J.C.M., Weiss, K., 2014. Why do we need to standardize no-tillage research? Soil Tillage Res. 137, 16–22. https://doi.org/10.1016/j.still.2013.10.002

Dexter, A.R., 2004. Soil physical quality: Part I. Theory, effects of soil texture, density, and organic matter, and effects on root growth. Geoderma 120, 201–214. https://doi.org/10.1016/j.geoderma.2003.09.004

Dexter, A.R, 2004. Soil physical quality: Part II. Friability, tillage, tilth and hard-setting. Geoderma 120, 215–225. https://doi.org/10.1016/j.geoderma.2003.09.005

Dieckmann, J., 2008. Zur Bedeutung der Bodenstruktur für den Ertrag von Zuckerrüben - eine pflanzenbauliche und ökonomische Analyse in einer Zuckerrüben-Getreide-Fruchtfolge mit dauerhaft differenzierter Bodenbearbeitung (In German, with English abstract). Dissertation, Göttingen.

Duan, Q., Sorooshian, S., Gupta, V., 1992. Effective and efficient global optimization for conceptual rainfall-runoff models. Water Resour. Res. 28, 1015–1031. https://doi.org/10.1029/91WR02985

Edwards, A.P., Bremner, J.M., 1967. Microaggregates in soils. J. Soil Sci. 18, 64–73. https://doi.org/10.1111/j.1365-2389.1967.tb01488.x

Eijkelkamp Soil & Water, 2019. Tension infiltrometer set [WWW Document]. URL https://en.eijkelkamp.com/products/field-measurement-equipment/tension-infiltrometer.html (accessed 20.11.2019).

Ekstrøm, C.T., 2018. MESS: Miscellaneous Esoteric Statistical Scripts. R package version 0.5.2.

Ellert, B.H., Bettany, J.R., 1995. Calculation of organic matter and nutrients stored in soils under contrasting management regimes. Can. J. Soil Sci. 75, 529–538. https://doi.org/10.4141/cjss95-075

FAO, 2019. What is Conservation Agriculture? FAO CA website [WWW Document]. URL http://www.fao.org/conservation-agriculture/overview/what-is-conservation-agriculture/en/ (accessed 20.11.2019).

FAO, Collette, L. (Eds.), 2011. Save and grow: a policymaker's guide to the sustainable intensification of smallholder crop production. FAO, Rome.

FAO, International Fund for Agricultural Development, UNICEF, World Food Programme, World Health Organization, 2019. The state of food security and nutrition in the world: safeguarding against economic slowdowns and downturns.

Feki, M., Ravazzani, G., Ceppi, A., Mancini, M., 2018. Influence of soil hydraulic variability on soil moisture simulations and irrigation scheduling in a maize field. Agric. Water Manag. 202, 183–194. https://doi.org/10.1016/j.agwat.2018.02.024

Fodor, N., Sándor, R., Orfanus, T., Lichner, L., Rajkai, K., 2011. Evaluation method dependency of measured saturated hydraulic conductivity. Geoderma 165, 60–68. https://doi.org/10.1016/j.geoderma.2011.07.004

Gerke, H.H., 2006. Preferential flow descriptions for structured soils. J. Plant Nutr. Soil Sci. 169, 382–400. https://doi.org/10.1002/jpln.200521955

Godfray, H.C.J., Beddington, J.R., Crute, I.R., Haddad, L., Lawrence, D., Muir, J.F., Pretty, J., Robinson, S., Thomas, S.M., Toulmin, C., 2010. Food security: the challenge of feeding 9 billion people. Science 327, 812–818. https://doi.org/10.1126/science.1185383

Godfray, H.C.J., Garnett, T., 2014. Food security and sustainable intensification. Philos. Trans. R. Soc. B Biol. Sci. 369, 20120273. https://doi.org/10.1098/rstb.2012.0273

Golchin, A., Oades, J., Skjemstad, J., Clarke, P., 1994. Soil structure and carbon cycling. Soil Res. 32, 1043. https://doi.org/10.1071/SR9941043

Greenland, D.J., 1981. Soil management and soil degradation. J. Soil Sci. 32, 301–322. https://doi.org/10.1111/j.1365-2389.1981.tb01708.x

Hillel, D., 2009. Soil structure and aggregation, in: Environmental Soil Physics. AP, Acad. Press, Amsterdam, pp. 101–125.

Holland, J.M., 2004. The environmental consequences of adopting conservation tillage in Europe: reviewing the evidence. Agric. Ecosyst. Environ. 103, 1–25. https://doi.org/10.1016/j.agee.2003.12.018

Horel, Á., Tóth, E., Gelybó, G., Kása, I., Bakacsi, Z., Farkas, C., 2015. Effects of Land Use and Management on Soil Hydraulic Properties. Open Geosci. 7, 742-754. https://doi.org/10.1515/geo-2015-0053

Horn, R., Domżżał, H., Słowińska-Jurkiewicz, A., van Ouwerkerk, C., 1995. Soil compaction processes and their effects on the structure of arable soils and the environment. Soil Tillage Res. 35, 23–36. https://doi.org/10.1016/0167-1987(95)00479-C

IUSS Working Group WRB, 2015. World reference base for soil resources 2014, update 2015 International soil classification system for naming soils and creating legends for soil maps (No. 106), World Soil Resources Reports. FAO, Rome.

Jacobs, A., Jungert, S., Koch, H.-J., 2015. Soil organic carbon as affected by direct drilling and mulching in sugar beet – wheat rotations. Arch. Agron. Soil Sci. 61, 1079–1087. https://doi.org/10.1080/03650340.2014.981669

Jarvis, N.J., 2007. A review of non-equilibrium water flow and solute transport in soil macropores: principles, controlling factors and consequences for water quality. Eur. J. Soil Sci. 58, 523–546. https://doi.org/10.1111/j.1365-2389.2007.00915.x

Jarvis, N.J., Messing, I., 1995. Near-saturated hydraulic conductivity in soils of contrasting texture measured by tension infiltrometers. Soil Sci. Soc. Am. J. 59, 27. https://doi.org/10.2136/sssaj1995.03615995005900010004x

Jensen, J.L., Schjønning, P., Watts, C.W., Christensen, B.T., Munkholm, L.J., 2019. Soil water retention: uni-modal models of pore-size distribution neglect impacts of soil Management. Soil Sci. Soc. Am. J. 83, 18. https://doi.org/10.2136/sssaj2018.06.0238

Jirků, V., Kodešová, R., Nikodem, A., Mühlhanselová, M., Žigová, A., 2013. Temporal variability of structure and hydraulic properties of topsoil of three soil types. Geoderma 204–205, 43–58. https://doi.org/10.1016/j.geoderma.2013.03.024

Jorda, H., Bechtold, M., Jarvis, N., Koestel, J., 2015. Using boosted regression trees to explore key factors controlling saturated and near-saturated hydraulic conductivity. Eur. J. Soil Sci. 66, 744–756. https://doi.org/10.1111/ejss.12249

Kang, S., Gu, B., Du, T., Zhang, J., 2003. Crop coefficient and ratio of transpiration to evapotranspiration of winter wheat and maize in a semi-humid region. Agric. Water Manag. 59, 239–254. https://doi.org/10.1016/S0378-3774(02)00150-6

Kargas, G., Kerkides, P., Sotirakoglou, K., Poulovassilis, A., 2016. Temporal variability of surface soil hydraulic properties under various tillage systems. Soil Tillage Res. 158, 22–31. https://doi.org/10.1016/j.still.2015.11.011

Kargas, G., Londra, P.A., 2015. Effect of tillage practices on the hydraulic properties of a loamy soil. Desalination Water Treat. 54, 2138–2146. https://doi.org/10.1080/19443994.2014.934110

Kassam, A., Friedrich, T., Derpsch, R., 2019. Global spread of conservation agriculture. Int. J. Environ. Stud. 76, 29–51. https://doi.org/10.1080/00207233.2018.1494927

Kassam, A., Friedrich, T., Derpsch, R., Kienzle, J., 2015. Overview of the worldwide spread of conservation agriculture. Field Actions Sci. Rep. 8, 1–11.

Kechavarzi, C., Špongrová, K., Dresser, M., Matula, S., Godwin, R.J., 2009. Laboratory and field testing of an automated tension infiltrometer. Biosyst. Eng. 104, 266–277. https://doi.org/10.1016/j.biosystemseng.2009.06.014

Keskinen, R., Räty, M., Kaseva, J., Hyväluoma, J., 2019. Variations in near-saturated hydraulic conductivity of arable mineral topsoils in south-western and central-eastern Finland. Agric. Food Sci. 28. 70-83. https://doi.org/10.23986/afsci.79329

Klípa, V., Sněhota, M., Dohnal, M., 2015. New automatic minidisk infiltrometer: design and testing. J. Hydrol. Hydromech. 63, 110–116. https://doi.org/10.1515/johh-2015-0023

Klute, A., Dirksen, C., 1986. Hydraulic conductivity and diffusivity: laboratory methods, in: Klute, A. (Ed.), Methods of soil analysis. Part 1. Physical and mineralogical methods. ASA and SSSA, Madison, WI., pp. 687–734.

Koch, H.-J., Dieckmann, J., Büchse, A., Märländer, B., 2009. Yield decrease in sugar beet caused by reduced tillage and direct drilling. Eur. J. Agron. 30, 101–109. https://doi.org/10.1016/j.eja.2008.08.001

Kodešová, R., Kodeš, V., Žigová, A., Šimůnek, J., 2006. Impact of plant roots and soil organisms on soil micromorphology and hydraulic properties. Biologia (Bratisl.) 61, 339-343. https://doi.org/10.2478/s11756-006-0185-7

Koestel, J., Larsbo, M., 2014. Imaging and quantification of preferential solute transport in soil macropores. Water Resour. Res. 50, 4357–4378. https://doi.org/10.1002/2014WR015351

Kool, D., Tong, B., Tian, Z., Heitman, J.L., Sauer, T.J., Horton, R., 2019. Soil water retention and hydraulic conductivity dynamics following tillage. Soil Tillage Res. 193, 95–100. https://doi.org/10.1016/j.still.2019.05.020

Kosugi, K., 1996. Lognormal distribution model for unsaturated soil hydraulic properties. Water Resour. Res. 32, 2697–2703. https://doi.org/10.1029/96WR01776

Kosugi, K., 1994. Three-parameter lognormal distribution model for soil water retention. Water Resour. Res. 30, 891–901. https://doi.org/10.1029/93WR02931

Kosugi, K., Hopmans, J.W., 1998. Scaling water retention curves for soils with lognormal pore-size distribution. Soil Sci. Soc. Am. J. 62, 1496-1505. https://doi.org/10.2136/sssaj1998.03615995006200060004x

Kreiselmeier, J., Chandrasekhar, P., Weninger, T., Schwen, A., Julich, S., Feger, K.-H., Schwärzel, K., 2019. Quantification of soil pore dynamics during a winter wheat cropping cycle under different tillage regimes. Soil Tillage Res. 192, 222–232. https://doi.org/10.1016/j.still.2019.05.014

Kutilek, M., 2004. Soil hydraulic properties as related to soil structure. Soil Tillage Res. 79, 175–184. https://doi.org/DOI 10.1016/j.still.2004.07.006

Lal, R., Reicosky, D.C., Hanson, J.D., 2007. Evolution of the plow over 10,000 years and the rationale for no-till farming. Soil Tillage Res. 93, 1–12. https://doi.org/10.1016/j.still.2006.11.004

Lee, D.M., Elrick, D.E., Reynolds, W.D., Clothier, B.E., 1985. A comparison of three field methods for measuring saturated hydraulic conductivity. Can. J. Soil Sci. 65, 563–573. https://doi.org/10.4141/cjss85-060

Lenth, R., Singmann, H., Love, J., Buerkner, P., Herve, M., 2018. emmeans: estimated marginal means, aka least-squares means. R package version 1.2.3.

Letey, J., 1991. The study of soil structure - Science or art. Soil Res. 29, 699. https://doi.org/10.1071/SR9910699

Li, G.-Y., Fan, H.-M., 2014. Effect of freeze-thaw on water stability of aggregates in a black soil of Northeast China. Pedosphere 24, 285–290. https://doi.org/10.1016/S1002-0160(14)60015-1

Lozano, L.A., Soracco, C.G., Cornelis, W.M., Gabriels, D., Sarli, G.O., Villarreal, R., 2013. Anisotropy of pore size classes' connectivity related to soil structure under no tillage: Soil Sci. 178, 612–617. https://doi.org/10.1097/SS.0000000000000027

Lucas, M., Schlüter, S., Vogel, H.-J., Vetterlein, D., 2019. Soil structure formation along an agricultural chronosequence. Geoderma 350, 61–72. https://doi.org/10.1016/j.geoderma.2019.04.041

Luo, L., Lin, H., Li, S., 2010. Quantification of 3-D soil macropore networks in different soil types and land uses using computed tomography. J. Hydrol. 393, 53–64. https://doi.org/10.1016/j.jhydrol.2010.03.031

Mallants, D., Mohanty, B.P., Vervoort, A., Feyen, J., 1997. Spatial analysis of saturated hydraulic conductivity in a soil with macropores. Soil Technol. 10, 115–131. https://doi.org/10.1016/S0933-3630(96)00093-1

Marandola, D., Belliggiano, A., Romagnoli, L., Ievoli, C., 2019. The spread of no-till in conservation agriculture systems in Italy: Indications for rural development policy-making. Agric. Food Econ. 7, 7. https://doi.org/10.1186/s40100-019-0126-8

Martínez, E., Fuentes, J.-P., Silva, P., Valle, S., Acevedo, E., 2008. Soil physical properties and wheat root growth as affected by no-tillage and conventional tillage systems in a Mediterranean environment of Chile. Soil Tillage Res. 99, 232–244. https://doi.org/10.1016/j.still.2008.02.001

Matula, S., Miháliková, M., Lufinková, J., Báťková, K., 2015. The role of the initial soil water content in the determination of unsaturated soil hydraulic conductivity using a tension infiltrometer. Plant Soil Environ. 61, 515–521. https://doi.org/10.17221/527/2015-PSE

Messing, I., Jarvis, N.J., 1993. Temporal variation in the hydraulic conductivity of a tilled clay soil as measured by tension infiltrometers. J. Soil Sci. 44, 11–24. https://doi.org/10.1111/j.1365-2389.1993.tb00430.x

METER Group Inc., 2019a. Mini disk infiltrometer. http://library.metergroup.com/Manuals/10564_Mini%20Disk%20Infiltrometer_Web.pdf (accessed 4.9.2019).

METER Group Inc., 2019b. KSAT operation manual. https://metergroup-83d0.kxcdn.com/app/uploads/2018/12/KSAT_Manual.042019.pdf (accessed 23.4.2019).

METER Group Inc., 2019c. HYPROP operation manual. http://library.metergroup.com/Manuals/18263_HYPROP_Manual_Web.pdf (accessed 23.4.2019).

Moret, D., Arrúe, J.L., 2007. Dynamics of soil hydraulic properties during fallow as affected by tillage. Soil Tillage Res. 96, 103–113. https://doi.org/10.1016/j.still.2007.04.003

Moret-Fernández, D., Blanco, N., Martínez-Chueca, V., Bielsa, A., 2013. Malleable disc base for direct infiltration measurements using the tension infiltrometry technique. Hydrol. Process. 27, 275–283. https://doi.org/10.1002/hyp.9206

Moret-Fernández, D., Peña-Sancho, C., López, M.V., 2016. Influence of the wetting process on estimation of the water-retention curve of tilled soils. Soil Res. 54, 840. https://doi.org/10.1071/SR15274

Mualem, Y., 1976. A new model for predicting the hydraulic conductivity of unsaturated porous media. Water Resour. Res. 12, 513–522.

Munkholm, L.J., Hansen, E.M., Olesen, J.E., 2008. The effect of tillage intensity on soil structure and winter wheat root/shoot growth. Soil Use Manag. 24, 392–400. https://doi.org/10.1111/j.1475-2743.2008.00179.x

Nail, E., Young, D., Schillinger, W., 2007. Diesel and glyphosate price changes benefit the economics of conservation tillage versus traditional tillage. Soil Tillage Res. 94, 321–327. https://doi.org/10.1016/j.still.2006.08.007

Nimmo, J.R., 2004. Porosity and pore size distribution, in: Encyclopedia of soils in the environment. Elsevier, London, pp. 295–303.

Or, D., Ghezzehei, T.A., 2002. Modeling post-tillage soil structural dynamics: A review. Soil Tillage Res. 64, 41–59. https://doi.org/10.1016/S0167-1987(01)00256-2

Or, D., Leij, F.J., Snyder, V., Ghezzehei, T.A., 2000. Stochastic model for posttillage soil pore space evolution. Water Resour. Res. 36, 1641–1652. https://doi.org/10.1029/2000WR900092

Patra, S., Julich, S., Feger, K.-H., Jat, M.L., Jat, H., Sharma, P.C., Schwärzel, K., 2019. Soil hydraulic response to conservation agriculture under irrigated intensive cereal-based cropping systems in a semiarid climate. Soil Tillage Res. 192, 151–163. https://doi.org/10.1016/j.still.2019.05.003

Pelak, N., Porporato, A., 2019. Dynamic evolution of the soil pore size distribution and its connection to soil management and biogeochemical processes. Adv. Water Resour. 131, 103384. https://doi.org/10.1016/j.advwatres.2019.103384

Pelosi, C., Grandeau, G., Capowiez, Y., 2017. Temporal dynamics of earthworm-related macroporosity in tilled and non-tilled cropping systems. Geoderma 289, 169–177.

Peña-Sancho, C., Lopez, M.V., Gracia, R., Moret-Fernandez, D., 2017. Effects of tillage on the soil water retention curve during a fallow period of a semiarid dryland. Soil Res. 55, 114. https://doi.org/10.1071/SR15305

Peters, A., Durner, W., 2015. SHYPFIT 2.0 user's manual (Research Report). Institut für Ökologie, Technische Universität Berlin, Germany.

Peters, A., Durner, W., 2008. Simplified evaporation method for determining soil hydraulic properties. J. Hydrol. 356, 147–162. https://doi.org/10.1016/j.jhydrol.2008.04.016

Pires, L., Cassaro, F., Reichardt, K., Bacchi, O., 2008. Soil porous system changes quantified by analyzing soil water retention curve modifications. Soil Tillage Res. 100, 72–77. https://doi.org/10.1016/j.still.2008.04.007

Pires, L.F., Roque, W.L., Rosa, J.A., Mooney, S.J., 2019. 3D analysis of the soil porous architecture under long term contrasting management systems by X-ray computed tomography. Soil Tillage Res. 191, 197–206. https://doi.org/10.1016/j.still.2019.02.018

Pittelkow, C.M., Liang, X., Linquist, B.A., van Groenigen, K.J., Lee, J., Lundy, M.E., van Gestel, N., Six, J., Venterea, R.T., van Kessel, C., 2014. Productivity limits and potentials of the principles of conservation agriculture. Nature 517, 365–368. https://doi.org/10.1038/nature13809

R Development Core Team, 2017. R: A language and environment for statistical computing. R Foundation for Statistical Computing.

Rabot, E., Wiesmeier, M., Schlüter, S., Vogel, H.-J., 2018. Soil structure as an indicator of soil functions: A review. Geoderma 314, 122–137. https://doi.org/10.1016/j.geoderma.2017.11.009

Rasse, D.P., Smucker, A.J.M., Santos, D., 2000. Alfalfa root and shoot mulching effects on soil hydraulic properties and aggregation. Soil Sci. Soc. Am. J. 64, 725-731. https://doi.org/10.2136/sssaj2000.642725x

Reichert, J.M., da Rosa, V.T., Vogelmann, E.S., da Rosa, D.P., Horn, R., Reinert, D.J., Sattler, A., Denardin, J.E., 2016. Conceptual framework for capacity and intensity physical soil properties affected by short and long-term (14 years) continuous no-tillage and controlled traffic. Soil Tillage Res. 158, 123–136. https://doi.org/10.1016/j.still.2015.11.010

Renger, M., Stoffregen, H., Klocke, J., Facklam, M., Wessolek, G., Roth, C.H., Plagge, R., 1999. Ein autoregressives Verfahren zur Bestimmung der gesättigten und ungesättigten hydraulischen Leitfähigkeit. (In German, with English abstract). J. Plant Nutr. Soil Sci. 162, 123–130.

Reynolds, W.D., Bowman, B.T., Brunke, R.R., Drury, C.F., Tan, C.S., 2000. Comparison of tension infiltrometer, pressure infiltrometer, and soil core estimates of saturated hydraulic conductivity. Soil Sci. Soc. Am. J. 64, 478-484. https://doi.org/10.2136/sssaj2000.642478x

Reynolds, W.D., Bowman, B.T., Drury, C.F., Tan, C.S., Lu, X., 2002. Indicators of good soil physical quality: density and storage parameters. Geoderma 110, 131–146. https://doi.org/10.1016/S0016-7061(02)00228-8

Reynolds, W.D., Drury, C.F., Tan, C.S., Fox, C.A., Yang, X.M., 2009. Use of indicators and pore volume-function characteristics to quantify soil physical quality. Geoderma 152, 252–263. https://doi.org/10.1016/j.geoderma.2009.06.009

Reynolds, W.D., Elrick, D.E., 1991. Determination of hydraulic conductivity using a tension infiltrometer. Soil Sci. Soc. Am. J. 55, 633-639. https://doi.org/10.2136/sssaj1991.03615995005500030001x

Rienzner, M., Gandolfi, C., 2014. Investigation of spatial and temporal variability of saturated soil hydraulic conductivity at the field-scale. Soil Tillage Res. 135, 28–40. https://doi.org/10.1016/j.still.2013.08.012

Romano, N., Nasta, P., 2016. How effective is bimodal soil hydraulic characterization? Functional evaluations for predictions of soil water balance: Functional evaluations for bimodal soil. Eur. J. Soil Sci. 67, 523–535. https://doi.org/10.1111/ejss.12354

Romano, N., Nasta, P., Severino, G., Hopmans, J.W., 2011. Using bimodal lognormal functions to describe soil hydraulic properties. Soil Sci. Soc. Am. J. 75, 468-480. https://doi.org/10.2136/sssaj2010.0084

Sandin, M., Jarvis, N., Larsbo, M., 2018. Consolidation and surface sealing of nine harrowed Swedish soils. Soil Tillage Res. 181, 82–92. https://doi.org/10.1016/j.still.2018.03.017

Schindler, U., Durner, W., von Unold, G., Mueller, L., Wieland, R., 2010. The evaporation method: Extending the measurement range of soil hydraulic properties using the air-entry pressure of the ceramic cup. J. Plant Nutr. Soil Sci. 173, 563–572. https://doi.org/10.1002/jpln.200900201

Schlüter, S., Albrecht, L., Schwärzel, K., Kreiselmeier, J., in press. Long-term effects of conventional tillage and no-tillage on saturated and near-saturated hydraulic conductivity – Can their prediction be improved by pore metrics obtained with X-ray CT? Geoderma Spec. Issue Recent Adv. Pore-Scale Imaging Soil Syst.

Schlüter, S., Großmann, C., Diel, J., Wu, G.-M., Tischer, S., Deubel, A., Rücknagel, J., 2018. Long-term effects of conventional and reduced tillage on soil structure, soil ecological and soil hydraulic properties. Geoderma 332, 10–19. https://doi.org/10.1016/j.geoderma.2018.07.001

Schwärzel, K., Bohl, H.P., 2003. An easily installable groundwater lysimeter to determine waterbalance components and hydraulic properties of peat soils. Hydrol. Earth Syst. Sci. 7, 23–32. https://doi.org/10.5194/hess-7-23-2003

Schwärzel, K., Carrick, S., Wahren, A., Feger, K.-H., Bodner, G., Buchan, G., 2011. Soil hydraulic properties of recently tilled soil under cropping rotation compared with two-year pasture. Vadose Zone J. 10, 354-366. https://doi.org/10.2136/vzj2010.0035

Schwärzel, K., Punzel, J., 2007. Hood infiltrometer—A new type of tension infiltrometer. Soil Sci. Soc. Am. J. 71, 1438-1447. https://doi.org/10.2136/sssaj2006.0104

Schwärzel, K., Šimůnek, J., Stoffregen, H., Wessolek, G., van Genuchten, M.Th., 2006. Estimation of the unsaturated hydraulic conductivity of peat soils. Vadose Zone J. 5, 628-640. https://doi.org/10.2136/vzj2005.0061

Schwen, A., Bodner, G., Loiskandl, W., 2011a. Time-variable soil hydraulic properties in near-surface soil water simulations for different tillage methods. Agric. Water Manag. 99, 42–50. https://doi.org/10.1016/j.agwat.2011.07.020

Schwen, A., Bodner, G., Scholl, P., Buchan, G.D., Loiskandl, W., 2011b. Temporal dynamics of soil hydraulic properties and the water-conducting porosity under different tillage. Soil Tillage Res. 113, 89–98. https://doi.org/10.1016/j.still.2011.02.005

Skaalsveen, K., Ingram, J., Clarke, L.E., 2019. The effect of no-till farming on the soil functions of water purification and retention in north-western Europe: A literature review. Soil Tillage Res. 189, 98–109. https://doi.org/10.1016/j.still.2019.01.004

Soracco, C.G., Lozano, L.A., Sarli, G.O., Gelati, P.R., Filgueira, R.R., 2010. Anisotropy of saturated hydraulic conductivity in a soil under conservation and no-till treatments. Soil Tillage Res. 109, 18–22.

Soracco, C.G., Lozano, L.A., Villarreal, R., Melani, E., Sarli, G.O., 2018. Temporal variation of soil physical quality under conventional and no-till systems. Rev. Bras. Ciênc. Solo 42. https://doi.org/10.1590/18069657rbcs20170408

Soracco, C.G., Villarreal, R., Melani, E.M., Oderiz, J.A., Salazar, M.P., Otero, M.F., Irizar, A.B., Lozano, L.A., 2019. Hydraulic conductivity and pore connectivity. Effects of conventional and no-till systems determined using a simple laboratory device. Geoderma 337, 1236–1244. https://doi.org/10.1016/j.geoderma.2018.10.045

Špongrová, K., Kechavarzi, C., Dresser, M., Matula, S., Godwin, R.J., 2009. Development of an automated tension infiltrometer for field use. Vadose Zone J. 8, 810-817. https://doi.org/10.2136/vzj2008.0135

Strudley, M., Green, T., Ascoughii, J., 2008. Tillage effects on soil hydraulic properties in space and time: State of the science. Soil Tillage Res. 99, 4–48. https://doi.org/10.1016/j.still.2008.01.007

Südzucker AG, 2002. Innovative Bodenbearbeitung - Pflug - Locker - Mulch - Direktsaat. Mannheim/Ochsenfurt [WWW Document]. URL https://bisz.suedzucker.de/wp-content/uploads/2016/05/SZ_Ruebenbroschuere13RZ.pdf (accessed 7.23.2019).

Swinnen, J., Van Veen, J.A., Merckx, R., 1995. Root decay and turnover of rhizodeposits in field-grown winter wheat and spring barley estimated by 14C pulse-labelling. Soil Biol. Biochem. 27, 211–217. https://doi.org/10.1016/0038-0717(94)00161-S

Tilman, D., Balzer, C., Hill, J., Befort, B.L., 2011. Global food demand and the sustainable intensification of agriculture. Proc. Natl. Acad. Sci. 108, 20260–20264. https://doi.org/10.1073/pnas.1116437108

Tisdall, J.M., Oades, J.M., 1982. Organic matter and water-stable aggregates in soils. J. Soil Sci. 33, 141–163. https://doi.org/10.1111/j.1365-2389.1982.tb01755.x

Tóth, B., Weynants, M., Nemes, A., Makó, A., Bilas, G., Tóth, G., 2015. New generation of hydraulic pedotransfer functions for Europe: New hydraulic pedotransfer functions for Europe. Eur. J. Soil Sci. 66, 226–238. https://doi.org/10.1111/ejss.12192

Ugarte Nano, C.C., Nicolardot, B., Ubertosi, M., 2015. Near-saturated hydraulic conductivity measured on a swelling silty clay loam for three integrated weed management based cropping systems. Soil Tillage Res. 150, 192–200. https://doi.org/10.1016/j.still.2015.02.003

UGT, 2019. Hood infiltrometer IL-2700. Umwelt-Geräte-Technik GmbH, Müncheberg. https://www.ugt-online.de/fileadmin/Public/downloads/Produkte/Bodenkunde/Leitfaehigkeit/Hood-Infiltrometer_-_IL_2700.pdf (accessed 22.7.2019).

Ulrich, S., Hofmann, B., Christen, O., 2006. Influence of tillage on soil quality in a long-term trial in Germany, in: Soil Management for Sustainabilty. CATENA Verlag, Reiskirchen.

United Nations, 2019. Goal 2: Zero Hunger [WWW Document]. U. N. Sustain. Dev. URL https://www.un.org/sustainabledevelopment/hunger/ (accessed 13.8.2019).

United Nations, Department of Economic and Social Affairs, Population Division, 2019. World population prospects 2019 - Highlights. https://population.un.org/wpp/Publications/Files/WPP2019_Highlights.pdf (accessed 20.11.2019)

United Nations General Assembly, 2015. Resolution 70/1. - Transforming our world: the 2030 agenda for sustainable development. United Nations General Assembly.

van den Putte, A., Govers, G., Diels, J., Gillijns, K., Demuzere, M., 2010. Assessing the effect of soil tillage on crop growth: A meta-regression analysis on European crop yields under conservation agriculture. Eur. J. Agron. 33, 231–241. https://doi.org/10.1016/j.eja.2010.05.008

Vereecken, H., Schnepf, A., Hopmans, J.W., Javaux, M., Or, D., Roose, T., Vanderborght, J., Young, M.H., Amelung, W., Aitkenhead, M., Allison, S.D., Assouline, S., Baveye, P., Berli, M., Brüggemann, N., Finke, P., Flury, M., Gaiser, T., Govers, G., Ghezzehei, T., Hallett, P., Hendricks Franssen, H.J., Heppell, J., Horn, R., Huisman, J.A., Jacques, D., Jonard, F., Kollet, S., Lafolie, F., Lamorski, K., Leitner, D., McBratney, A., Minasny, B., Montzka, C., Nowak, W., Pachepsky, Y., Padarian, J., Romano, N., Roth, K., Rothfuss, Y., Rowe, E.C., Schwen, A., Šimůnek, J., Tiktak, A., Van Dam, J., van der Zee, S.E.A.T.M., Vogel, H.J., Vrugt, J.A., Wöhling, T., Young, I.M., 2016. Modeling soil processes: Review, key challenges, and new perspectives. Vadose Zone J. 15. https://doi.org/10.2136/vzj2015.09.0131

Vereecken, H., Weynants, M., Javaux, M., Pachepsky, Y., Schaap, M.G., Genuchten, M.Th. van, 2010. Using pedotransfer functions to estimate the van Genuchten–Mualem soil hydraulic properties: A review. Vadose Zone J. 9, 795-820. https://doi.org/10.2136/vzj2010.0045

Villarreal, R., Soracco, C.G., Lozano, L.A., Melani, E.M., Sarli, G.O., 2017. Temporal variation of soil sorptivity under conventional and no-till systems determined by a simple laboratory method. Soil Tillage Res. 168, 92–98. https://doi.org/10.1016/j.still.2016.12.013

Webster, R., 2007. Analysis of variance, inference, multiple comparisons and sampling effects in soil research. Eur. J. Soil Sci. 58, 74–82. https://doi.org/10.1111/j.1365-2389.2006.00801.x

Weninger, T., Bodner, G., Kreiselmeier, J., Chandrasekhar, P., Julich, S., Feger, K.-H., Schwärzel, K., Schwen, A., 2018. Combination of measurement methods for a wide-range description of hydraulic soil properties. Water 10, 1021. https://doi.org/10.3390/w10081021

Weninger, T., Kreiselmeier, J., Chandrasekhar, P., Julich, S., Feger, K.-H., Schwärzel, K., Bodner, G., Schwen, A., 2019. Effects of tillage intensity on pore system and physical quality of silt-textured soils detected by multiple methods. Soil Res. 57. https://doi.org/10.1071/SR18347

Williams, A., Jordan, N.R., Smith, R.G., Hunter, M.C., Kammerer, M., Kane, D.A., Koide, R.T., Davis, A.S., 2018. A regionally-adapted implementation of conservation agriculture delivers rapid improvements to soil properties associated with crop yield stability. Sci. Rep. 8, 8467. https://doi.org/10.1038/s41598-018-26896-2

Wind, G.P., 1969. Capillary conductivity data estimated by a simple method, in: Proceedings of the Wageningen Symposium - June 1966 - Water in the unsaturated zone. Presented at the UNESCO/IASH, International Association of Scientific Hydrology.

Wolf, D., Faust, D., 2013. Holocene sediment fluxes in a fragile loess landscape (Saxony, Germany). CATENA 103, 87–102. https://doi.org/10.1016/j.catena.2011.05.011

Xiao, H., Liu, G., Zhang, Q., Fenli, Z., Zhang, X., Liu, P., Zhang, J., Hu, F., Elbasit, M.A.M.A., 2018. Quantifying contributions of slaking and mechanical breakdown of soil aggregates to splash erosion for different soils from the Loess plateau of China. Soil Tillage Res. 178, 150–158. https://doi.org/10.1016/j.still.2017.12.026

Zumr, D., Jeřábek, J., Klípa, V., Dohnal, M., Sněhota, M., 2019. Estimates of tillage and rainfall effects on unsaturated hydraulic conductivity in a small Central European agricultural catchment. Water 11, 740. https://doi.org/10.3390/w11040740

Appendix

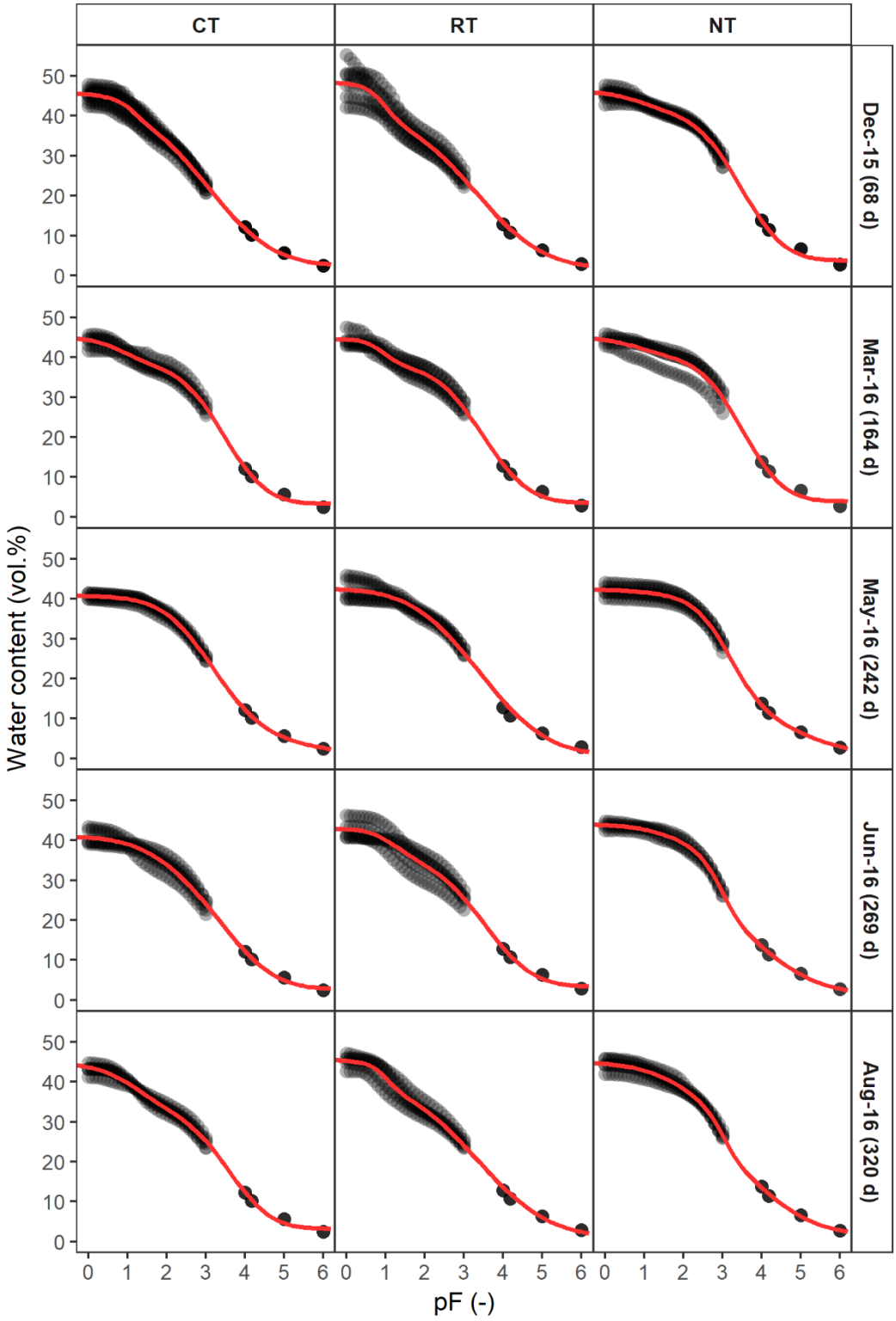

Figure A1 Water retention data points from HYPROP® measurements (pF 0 to 3) at 0.1-pF-intervals and averaged dewpoint hygrometer (pF 4 to 6). Gray dots show measured retention data as point density with darker areas representing more dots. Red lines show fitted reference curves. Grid columns represent tillage treatments where CT = conventional tillage, RT = reduced mulch tillage and NT = no tillage. Grid rows represent dates with time passed since last sowing in brackets.

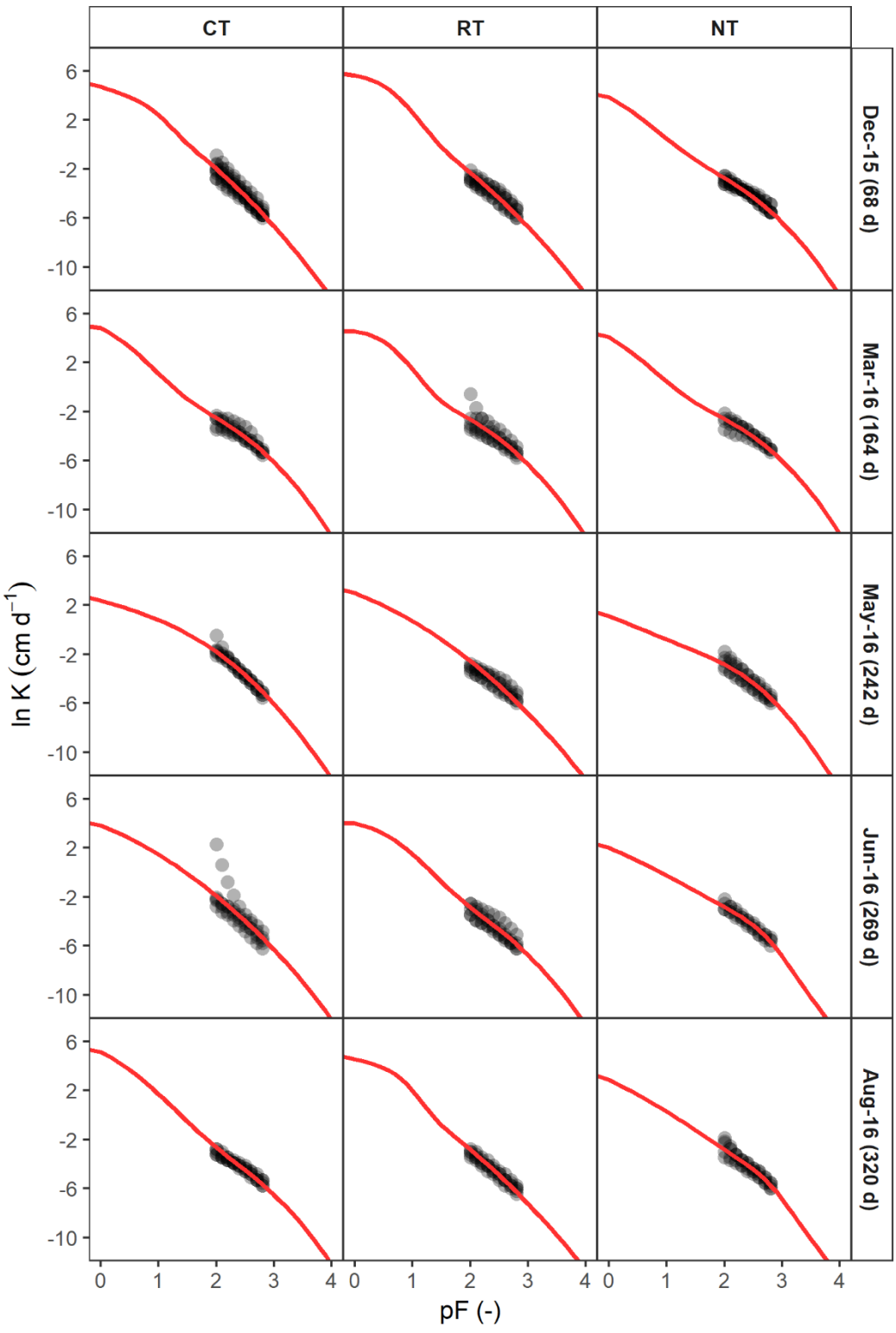

Figure A2 Hydraulic conductivity data points from HYPROP® measurements (pF 2 to 3) at 0.1-pF-intervals. Gray dots show measured hydraulic conductivity data as point density with darker areas representing more dots. Red lines show fitted reference curves. Grid columns represent tillage treatments where CT = conventional tillage, RT = reduced mulch tillage and NT = no tillage. Grid rows represent dates with time passed since last sowing in brackets.

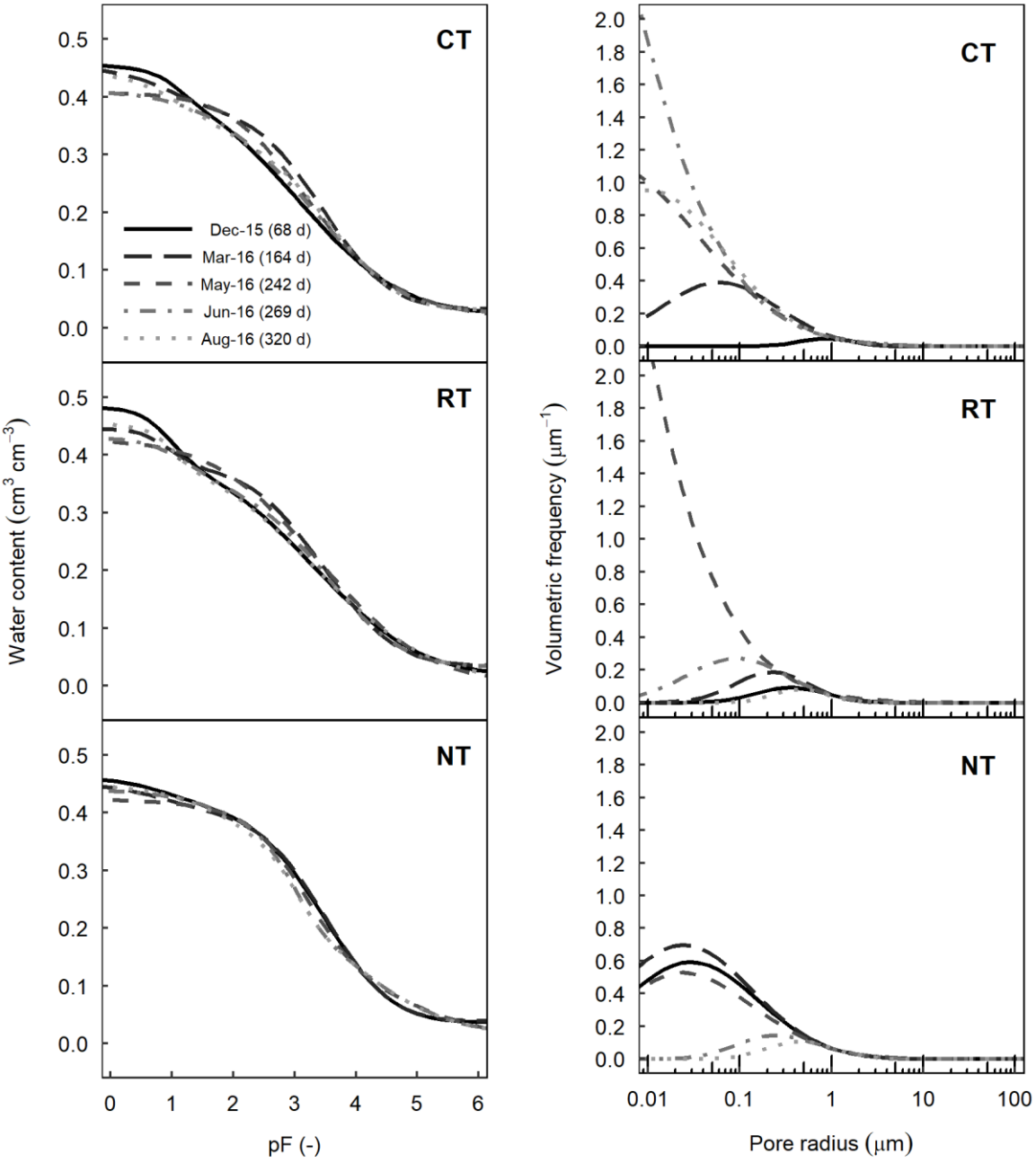

Figure A3 Temporal variation of the reference water retention curves and their corresponding soil pore size distribution (Eq. 8) for the treatments conventional tillage (CT), reduced mulch tillage (RT) and no tillage (NT). Line shapes represent different dates with days passed since last sowing in brackets.